NUREG/CR-1312
UCRL-52738

Methods for Evaluating the Leak Tightness of Spent Fuel Container Closures

Manuscript Completed: February 1980
Date Published: March 1980

Prepared by

B. J. Benda, R. T. Langland

Lawrence Livermore Laboratory
7000 East Avenue
Livermore, CA 94550

Prepared for
Office of Nuclear Regulatory Research
U. S. Nuclear Regulatory Commission
Washington, D. C. 20555
NRC FIN No. A-0117

NRC FORM 335 (7-77) U.S. NUCLEAR REGULATORY COMMISSION

BIBLIOGRAPHIC DATA SHEET

1. REPORT NUMBER *(Assigned by DDC)*
NUREG/CR-1312
UCRL-52738

4. TITLE AND SUBTITLE *(Add Volume No., if appropriate)*
Methods for Evaluating the Leak Tightness of Spent Fuel Container Closures

2. *(Leave blank)*

3. RECIPIENT'S ACCESSION NO.

7. AUTHOR(S)
B. J. Benda, R. T. Langland

5. DATE REPORT COMPLETED
MONTH February YEAR 80

9. PERFORMING ORGANIZATION NAME AND MAILING ADDRESS *(Include Zip Code)*
LLL/NRC
P.O. Box 808
Livermore, California

DATE REPORT ISSUED
MONTH March YEAR 1980

6. *(Leave blank)*

8. *(Leave blank)*

12. SPONSORING ORGANIZATION NAME AND MAILING ADDRESS *(Include Zip Code)*
U.S. Nuclear Regulatory Commission
Division of Safeguards, Fuel Cycle & Environmental Research
Office of Nuclear Regulatory Research

10. PROJECT/TASK/WORK UNIT NO.

11. CONTRACT NO.
FIN A0117

13. TYPE OF REPORT
Technical Report

PERIOD COVERED *(Inclusive dates)*

15. SUPPLEMENTARY NOTES

14. *(Leave blank)*

16. ABSTRACT *(200 words or less)*

For the Nuclear Regulatory Commission, Lawrence Livermore Laboratory undertook a project to develop and improve methods for assessing the leak tightness of general seal designs for nuclear waste shipping casks. Our objective was to develop and verify analytical tools for predicting leak rates of spent fuel cask closures. We built quarter- and half-scale configurations of five different seal-flange hardware configurations, including: polymer O-rings, silver-coated hollow-metal O-rings, Conoseals, Grayloc seals, and Batzer seals. Using helium as a tracer gas, we conducted leak-rate tests under conditions simulating normal use of spent fuel containers. Leak rates were then correlated with such measured and calculated parameters as temperature, bolt load, seal-flange interface stress, and the differential pressure across the seal. Computer codes were developed, and analyses of the seal-flange configuration related bolt closure force to both seal-flange interface contact stress and surface area.

17. KEY WORDS AND DOCUMENT ANALYSIS

17a. DESCRIPTORS

17b. IDENTIFIERS/OPEN-ENDED TERMS

18. AVAILABILITY STATEMENT
Unlimited

19. SECURITY CLASS *(This report)*
UNCLASSIFIED

21. NO. OF PAGES

20. SECURITY CLASS *(This page)*
UNCLASSIFIED

22. PRICE
$

NRC FORM 335 (7-77)

*U.S. GOVERNMENT PRINTING OFFICE : 1980 O-620-269/9

FOREWORD

The work reported here began as part of a program at Lawrence Livermore Laboratory (LLL) to develop and improve structural analysis methods for shipping container components. This program was funded by the Nuclear Regulatory Commission (NRC), Office of Nuclear Regulatory Research, Division of Safeguards, Fuel Cycle, and Environmental Research, Fuel Cycle Research Branch. Contract monitor is William Lahs.

The original program attacked two key areas--cask puncture and sealing of cask closures. The program was split into two parts (puncture and seals) in April, 1978, so the two efforts could be conducted independently. Total funding for both programs was $800,000. Separation of the programs, however, resulted in a shortfall in funding for the closure and sealing part. Consequently, not all of the closures that were fabricated were analyzed and tested. All hardware and the associated seals are the property of NRC. They are in storage at LLL, awaiting NRC's decision on their disposal.

This final report represents only the work done on the cask closure and sealing. (Separate final reports were submitted to the NRC on the puncture research.[1,2]) LLL believes that the work presented here is incomplete in terms of meeting the original objective of the study. Nevertheless, an excellent analytical tool in the form of the finite element code NIKE2D was developed to predict seal displacement, contact area, and contact stress. In addition, hardware was produced that, when tested, could provide valuable information on leak rates. There is every evidence that our original goal would be met if research were continued; that is, a comprehensive predictive tool could be developed for the NRC to use in evaluating seal designs for nuclear waste shipping casks. Were the funding issue to be resolved and the program continued, improved communications between LLL and NRC and a clearer mutual understanding on the approach to and progress of the project would benefit the renewed effort.

The authors wish to extend their appreciation to all who contributed to the work presented in this report. In particular, we thank R. A. Larder and G. J. Leake for their analyses of the hollow metal O-rings and J. O. Hallquist for his effort in developing NIKE2D.

CONTENTS

Foreword iii

Abstract ix

Summary xi

Introduction 1

Leak Rates and Seal Design 2

Technical Approach 6

Code Development and Verification 8

Seal Testing Program 13

Results 16

Testing and Analysis of Inconel X-750 O-Rings 16

Experimental Program 16

Analytical Program 23

Correlation Between Experiment and Analysis 28

Other Seal Configurations 32

Polymer O-rings 32

Type-321 Stainless Steel O-rings 33

Batzer Flange 33

Conoseal and Grayloc Gasket 34

Conclusion 35

References 36

Appendix A: Polymer O-rings 39

Appendix B: 321 Stainless Steel O-rings 55

Appendix C: Inconel X-750 O-rings 67

Appendix D: Batzer Flange 111

Appendix E: Test Hardware 117

LIST OF ILLUSTRATIONS

1. Leak rate Q vs seal-flange contact stress F/LW 5
2. Cross section of a Batzer seal 7
3. A Wheeler wire gasket seal 8
4. A Conoseal 9
5. Finite element model of a hollow O-ring seal 10
6. Effective stress in an O-ring element in Fig. 5 11
7. Nonlinear truss elements 12
8. The assembly fabricated to test the Grayloc seal 15
9. Schematic of the metallic O-ring flange 18
10. The two pairs of O-rings exhibited major flaws 22
11. Detailed model of an O-ring for developing load-deflection curve 24
12. O-ring load-deflection curve 25
13. A model of the seal-flange assembly 25
14. Experimentally recorded bolt force and pressure loadings 26
15. Deflection history curve for the O-ring 26
16. O-ring displacement from Fig. 15 on an expanded vertical scale 27
17. Deformed flange model 28
18. Contact area and pressure for Test 9 29
19. Contour lines of constant strain 30
20. An inverse relationship between leak rate and contact force 31
21. Total compressive interface force between seal and flange . . . 32

LIST OF TABLES

1. Leak rates vs volume and bubble equivalents, from Ref. 4 2
2. Leak rates and relationships between mass flow rate Q and upstream and downstream pressures 3
3. Test matrix for seal leak rate tests 14
4. Hardware for testing 10-in.-diam O-ring 19
5. Bolt force data 20
6. Leak rate data 21

ABSTRACT

For the Nuclear Regulatory Commission, Lawrence Livermore Laboratory undertook a project to develop and improve methods for assessing the leak tightness of general seal designs for nuclear waste shipping casks. Our objective was to develop and verify analytical tools for predicting leak rates of spent fuel cask closures. We built quarter- and half-scale configurations of five different seal-flange hardware configurations, including: polymer O-rings, silver-coated hollow-metal O-rings, Conoseals, Grayloc seals, and Batzer seals. Using helium as a tracer gas, we conducted leak-rate tests under conditions simulating normal use of spent fuel containers. Leak rates were then correlated with such measured and calculated parameters as temperature, bolt load, seal-flange interface stress, and the differential pressure across the seal. Computer codes were developed, and analyses of the seal-flange configuration related bolt closure force to both seal-flange interface contact stress and surface area.

SUMMARY

A combined experimental and analytical program designed to develop an analytical tool to predict leak rates of cask closures was conducted at Lawrence Livermore Laboratory. Five different closure configurations were considered for leak rate testing.

Two sizes of each closure were built (nominal 10-in. and 20-in. diam) representing 1/4- and 1/2-scale configurations. The seal-closure configuration represented existing designs that had a high level of performance in their current application. Some were already being used for spent fuel shipping containers. The five seals designs were the Conoseal and the Grayloc seal, polymer O-rings, hollow metal O-rings, and Batzer seals. Each flange represented a different design approach to achieve leak rates less than 10^{-6} std. cc/s.

Key parameters that influence the performance of the seals were identified. These parameters are surface finish, material hardness, pressure differential across the seal, temperature, and seal-flange interface contact area and stress. Most parameters can be measured during testing, but two of the most significant parameters, the interface contact area and stress, must be determined analytically.

A finite element code, NIKE2D, was developed to calculate the contact area and stress for arbitrary seal geometries. The contact-impact algorithm developed for this implicit finite element code can efficiently solve both static and dynamic contact stress problems.

A combined analysis and test program was begun. The testing program measured leak rates for given combinations of bolt load, pressure differential across the seals, and temperature. Although not considered a test variable, the surface finish of each test flange was determined. To establish corresponding values of contact area and stress, a supporting analysis of the test conditions was performed.

The program was not funded to completion, and not all hardware was tested or analyzed. Analyses were performed on two types of hollow metal O-rings

(silver-coated Type-321 stainless steel and silver-coated Inconel X-750) and the Batzer flange. Tests were conducted on the polymer and metal O-rings. Tests were not performed on all sizes of seals, and no tests were done on the Batzer seal, Conoseal, and Grayloc gasket.

Testing was conducted on two types of polymer O-rings, silicone and Viton. Both performed well. Their leak rates were governed by the permeation of the leak detection fluid through the polymer. The Viton seal leak rate was an order of magnitude less than that of the silicone seal. Leak rates for both were directly proportional to the pressure differential across the seal and varied from 10^{-7} to 10^{-5} std. cc/s. At the request of the sponsor, testing and analysis was stopped on these O-rings. No tests were done at elevated temperatures.

During analysis of the hollow metal O-rings, a design flaw in the flanges used to test these seals became evident. The analyses showed that the hollow metal O-rings unloaded because of the location of the seals relative to the bolt circle in conjunction with internal pressurization. This was confirmed in the leak rate tests and resulted in a flange design modification. The analysis of the hollow metal O-rings showed they had little springback and were, therefore, very sensitive to unloading. Analysis of the Inconel X-750 O-rings showed plastic strain levels that exceeded the strain limit of the material. This was experimentally confirmed by post-test examination of these seals. The 321 stainless steel hollow metal O-rings were more ductile and did not experience failure. Both types of metal O-rings had either small or large leak rates. These were less than 2.8×10^{-10} std. cc/s or greater than 1×10^{-3} std. cc/s, respectively.

The Batzer flange was analyzed to verify the substructuring finite element method and not to complement any test loads or conditions.

Although incomplete, this program resulted in an excellent structural analysis code to predict the behavior of cask closures under a variety of loading conditions. Limited test data corroborated analytical results. The analyses accurately predicted both severe unloading of the hollow metal O-rings during tests and the lack of significant rebound or springback of these seals. Large plastic strains were seen in the analysis of the Inconel X-750 O-rings, and

post-test inspection found the seals had been stressed to failure. There were insufficient data from the testing and analysis to verify or develop any general leak rate models. Qualitatively, the seals performed in a manner consistent with the hypothesized leak rate models.

INTRODUCTION

The U.S. Code of Federal Regulations[3] specifies the performance of spent nuclear fuel casks under accident and normal operating conditions. One requirement governs the leakage of radioactive material. Because the evaluation of cask performance using these specifications is difficult at best, the American National Standards Institute (ANSI) proposed a more practical standard for packages of radioactive material--ANSI Standard N14.5. The standard calls for leak rate testing, using a tracer fluid such as helium, and computational techniques that would relate a leak rate measured under certain conditions to that at different conditions, such as higher temperature and pressure.

The ANSI standard necessitates testing of full-scale hardware, which is a practical way to monitor the integrity of existing shipping casks. However, many cask designs have yet to be licensed by the NRC. Building each proposed cask closure for leak tightness testing can be very expensive, whether done by the licensee or the NRC. Without independent assessment tools, the NRC must rely on information provided by those firms seeking a license. Such data may not be comprehensive or objectively presented.

The requirement for independent tools to assess the leak tightness of proposed cask designs was a major reason for this research. We planned to develop the analytical tools--computer codes--by both testing and analyzing different seal flange configurations, then comparing key test and analysis parameters, including:

- Bolt load,
- Temperature,
- Seal-flange interface stress,
- Seal contact surface area,
- Differential pressure across the seals.

We hoped to discern or verify relationships between these parameters and leak rates, which we measured on 1/4- and 1/2-scale cask closures. If the relationships could be verified in the laboratory and predicted by the codes that we developed, the NRC would be able to use these analytical codes instead of the more costly test programs to evaluate proposed seal designs.

LEAK RATES AND SEAL DESIGN

Leak rate testing is a well established technology. Several companies build test equipment and offer courses and workshops in leak rate testing. Their services are needed because all containers leak. Hence, the question becomes: How much?

Leak rates are specified in standard cubic centimeters per second (std. cc/s). Table 1 shows the relationships between leak rate and volume and bubble equivalents. Bubble equivalents reflect the frequency of bubbles emitted by the leak when submerged under water.

The laws of fluid mechanics govern the escape of the tracer fluid used in leak testing. Different flow mechanisms occur at different leak rates, as can be seen in Table 2. The leak rate region of interest for casks is from 10^{-2} to 10^{-12} std. cc/s. In this region, the leaks may be described as orifice, molecular, or permeation leaks. Leaks from orifices have a mass flow rate Q proportional to $(P_1^2 - P_2^2)$--the difference between the squares of the upstream and downstream pressures P_1 and P_2, respectively. Molecular and

TABLE 1. Leak rates vs volume and bubble equivalents, from Ref. 4.

Leak rate, std. cc/s	Volume equivalent	Bubble equivalent
10^{-1}	1cc/10 s	Steady stream
10^{-2}	1cc/100 s	10/s
10^{-3}	3cc/h	1/s
10^{-4}	1cc/3 h	1/10 s
10^{-5}	1cc/24 h	No bubble equivalent
10^{-6}	1cc/2 wk	No bubble equivalent
10^{-7}	3cc/yr	No bubble equivalent
10^{-8}	1cc/3 yr	No bubble equivalent
10^{-9}	1cc/30 yr	No bubble equivalent

TABLE 2. Leak rates and relationships between mass flow rate Q and upstream and downstream pressures, P_1 and P_2, respectively, for different flow regions.

	Mass flow region			
	Turbulent	Laminar	Molecular	Permeation
Leak rate, std. cc/s	$>10^{-2}$	10^{-1} to 10^{-6}	$<10^{-5}$	Depends upon material thickness
Mass flow rate, Q	$\propto(P_1^2 - P_2^2)^{1/2}$	$\propto(P_1^2 - P_2^2)$	$\propto(P_1 - P_2)$	$\propto(P_1 - P_2)$

permeation leaks have flow rates proportional to the difference between the upstream and downstream pressures. These different relationships to pressure give us a way to identify the type of leaks we encounter during testing. That is, changing the pressure differentials and plotting them against the flow rate can verify the kind of leak being monitored.

The techniques for testing leak rates are well established. Usually, a tracer fluid such as helium is used, and its presence is detected by a mass spectrometer. Different detectors are used for other tracer fluids, for instance, a radioactive tracer. Each detection technique is usually good over a limited range of leak rates. All tests done at LLL used helium as a tracer fluid and helium leak rate detectors. Done under the conditions of anticipated use, leak rate testing is a good way to evaluate the integrity and performance of existing hardware.

Assessment of a seal design before it is built is difficult, particularly if a leak rate less than 10^{-6} std. cc/s is desired. The design of seals with this performance is an art, especially for high-pressure systems. However, there are general design principles that characterize every successful seal design with this level of performance. For seal designs that have metal-to-metal contact, these principles are

- Put a soft metal seal against a hard metal closure.
- Obtain as high a contact stress as possible.
- Retain some springback in the seal to account for unloading.

The exact geometries may differ. Examples of seals that have the necessary performance in their current applications are hollow metal O-rings, Conoseals, Gamah, Grayloc, Batzer, and Wheeler seals. Each design differs in material and geometry, but all embody one or more of the underlying design principles. In vacuum applications, these seals commonly achieve leak rates less than 10^{-11} std. cc/s.

Designs that use polymer seals and metal closures have slightly different principles than metal-to-metal seals. Polymers are inherently soft and have good springback. Other design requirements include:

- Good seal deformation (as high as 30% strain).
- Good surface finish--32 to 64 AA.
- Resistance to dirt and scratching. (A piece of dirt or a hair creates a 10^{-6} std. cc/s leak.)

However, polymers are not well suited to applications at elevated temperatures. The practical limit of polymers in vacuum applications is approximately 10^{-8} std. cc/s per inch of seal. The limit is governed by the permeability of the polymer to the tracer fluid.

The above general principles do not offer a method for predicting how a seal configuration will perform, nor do they permit a relative comparison between two proposed designs. Pioneering work by Roth[5] on vacuum technology has provided what few techniques we do have for seal assessment. Roth developed a model for leak rates that is represented by the following equation for helium at 25°C:

$$Q = C \times \Delta P = 34\ A^2\ \frac{L}{W}\ \exp\ (-3\ F/LWR) \times \Delta P \qquad (1)$$

where

Q = flow rate

ΔP = pressure differential

R = a measure of material hardness

L = length of a seal

W = contact surface width

F = contact surface force

A = measure of sealing surface irregularity.

The model assumes a simple geometry in which F is uniform and L and W are known. The other factors such as A, R, and ΔP can be measured. Although the model needs experimental verification, other investigators report success in applying the simple model.[6,7,8] Most seal designs do not fit these assumptions. While L may be known, the force F and contact width W are very difficult to determine, especially for complicated geometries. Only recently have new computer modeling techniques held some hope for determining F and W for complicated geometries.

Leak rates for Roth's model, shown in Fig. 1, clearly demonstrate that the seal flange interface contact area and force significantly affect the predicted leak rate.

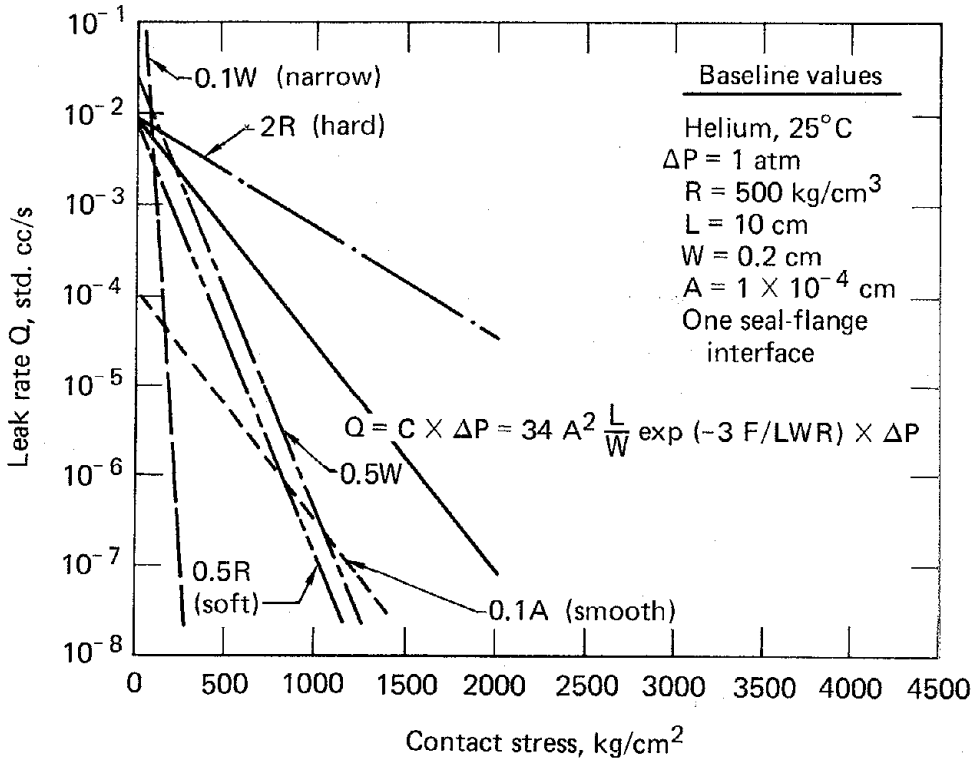

FIG. 1. Leak rate Q vs seal-flange contact stress F/LW according to Roth's model--in which ΔP is the pressure differential, R is a measure of material hardness, L is the seal length, W is the contact width, F is the contact surface force, and A is a measure of sealing surface irregularity--for the baseline values and variations of R, W, and A.

TECHNICAL APPROACH

Roth's model, Eq. (1), was the starting point for our effort to develop a method for predicting leak rates for cask closures. By designing, building, testing, and analyzing typical cask closure hardware, we planned to both verify his model and to use it in developing a code that accurately predicts test results. Five different kinds of seals were selected for examination: polymer O-rings, hollow metal O-rings, Conoseals, Grayloc seals, and Batzer seals. Quarter- and half-scale closures were built with seals that are nominally 10 and 20 in. in diameter. Though significantly different, each seal design is a possible candidate for use on future spent fuel casks. The Appendixes contain drawings and documentation of each design except the Conoseal and Grayloc, which are proprietary and unavailable.

Our test program called for either measuring or calculating the key parameters in Roth's leak rate model under conditions that simulate actual use. Measured variables are temperature, surface finish, pressure differential across the seal, material hardness, and bolt loads. Calculated quantities are the seal-flange interface stress and the seal contact area for a given bolt load or displacement. The measured leak rate is then correlated with these variables. This approach provides a method to examine the validity of Roth's model as well as other proposed leak rate models. It establishes key parameters that influence the leak rate of a given seal design. For example, certain seal designs are known to be more sensitive to temperature or unloading than others.

Perhaps the key to obtaining a good seal design and the most important variable in any model is the stress at the seal-flange interface (Fig. 1). It is also the variable most influenced by the geometry of each seal design. There are many different ways of obtaining a high value of this stress:

- The Batzer seal applies a large force to a small surface area (Fig. 2).
- The Wheeler seal (not examined in this study) forces the seal into a confined space by a ramp or angle on the flange (Fig. 3).
- The Conoseal (Fig. 4) wedges a flat-rectangular-cross-section ring into a confined space.

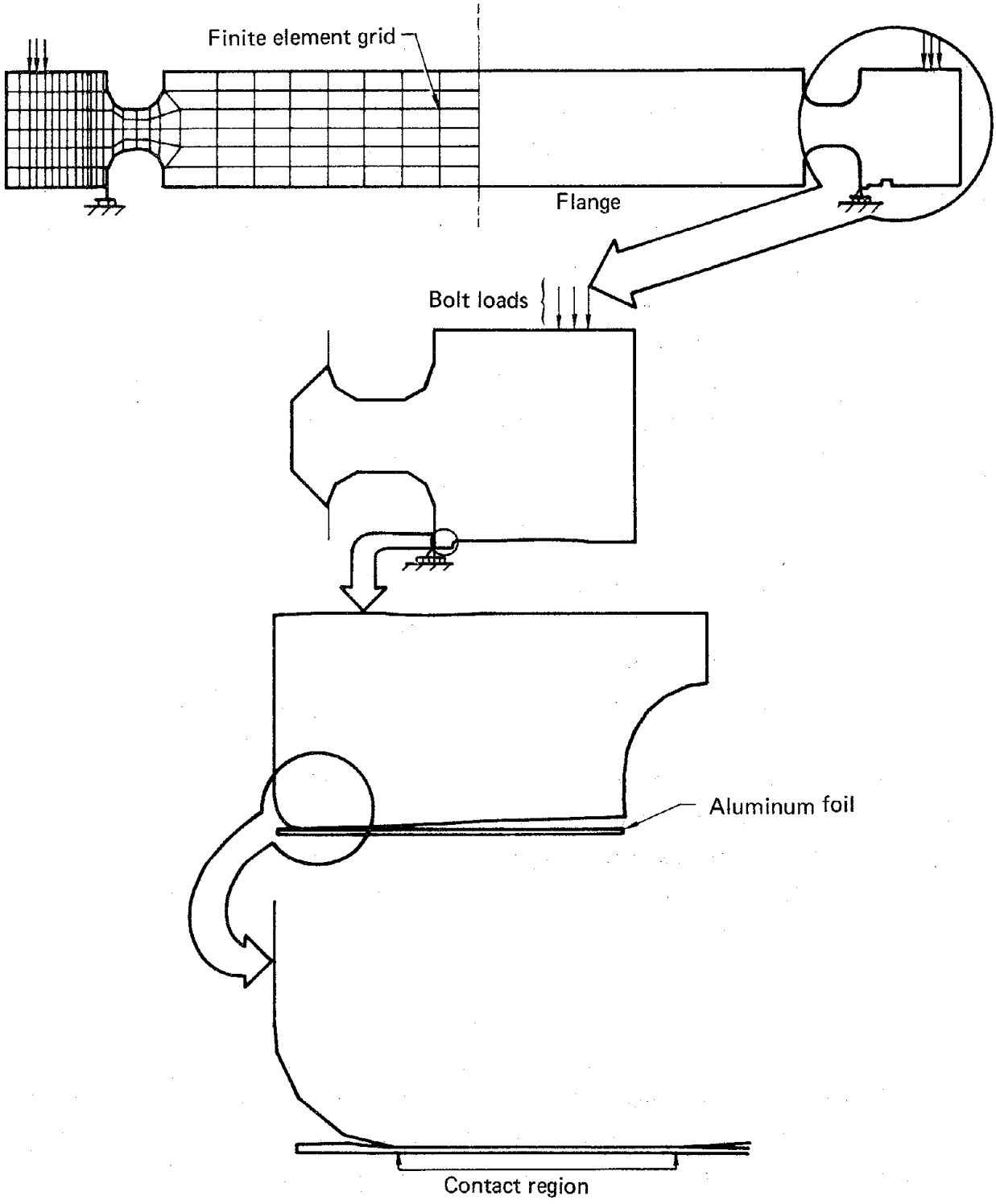

FIG. 2. Cross section of a Batzer seal, top, in which a large force, applied to a small surface area, compresses an aluminum-foil gasket. These seals are often called knife-edge seals, though the contact area is rounded as the series of close-up views shows. Grid lines represent finite elements.

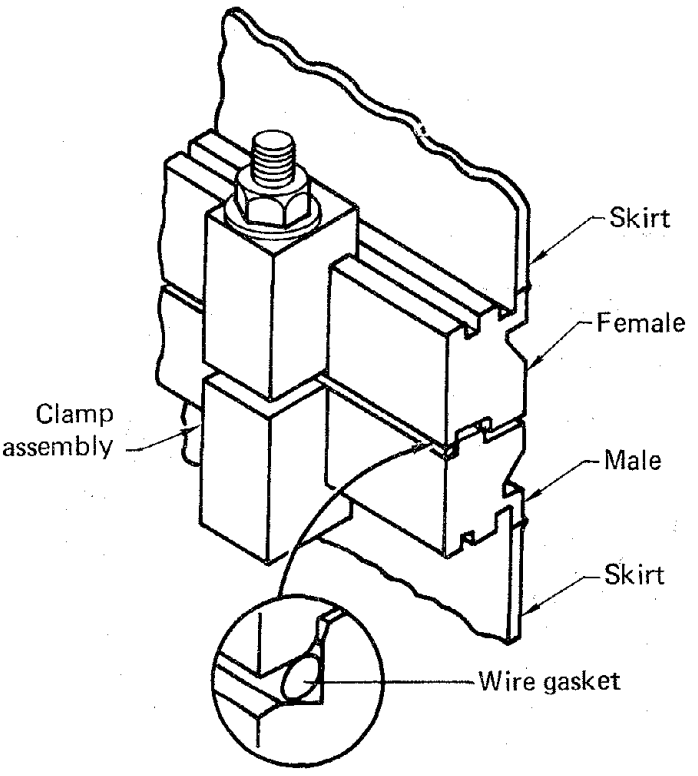

FIG. 3. A Wheeler wire gasket seal achieves high seal-flange interface stress by forcing the seal into a confined space, thus creating a nearly hydrostatic stress state in the seal.

The only way to evaluate the high contact stresses generated by all these designs is to calculate them. Predicting the contact stresses accurately was a major requirement for our program, as was relating them to such measurable quantities as bolt loads, torques, or displacements.

CODE DEVELOPMENT AND VERIFICATION

To model the seal-flange interaction, a calculational technique was needed. Not only did the technique have to represent the impact-contact of two bodies, it had to:

- Accommodate complex geometries,
- Describe large deformation and strain,
- Account for nonlinear material behavior.

When the seal research program began, a first version of a time-dependent stress analysis code called DYNA2D (Ref. 9) had been developed at LLL. The

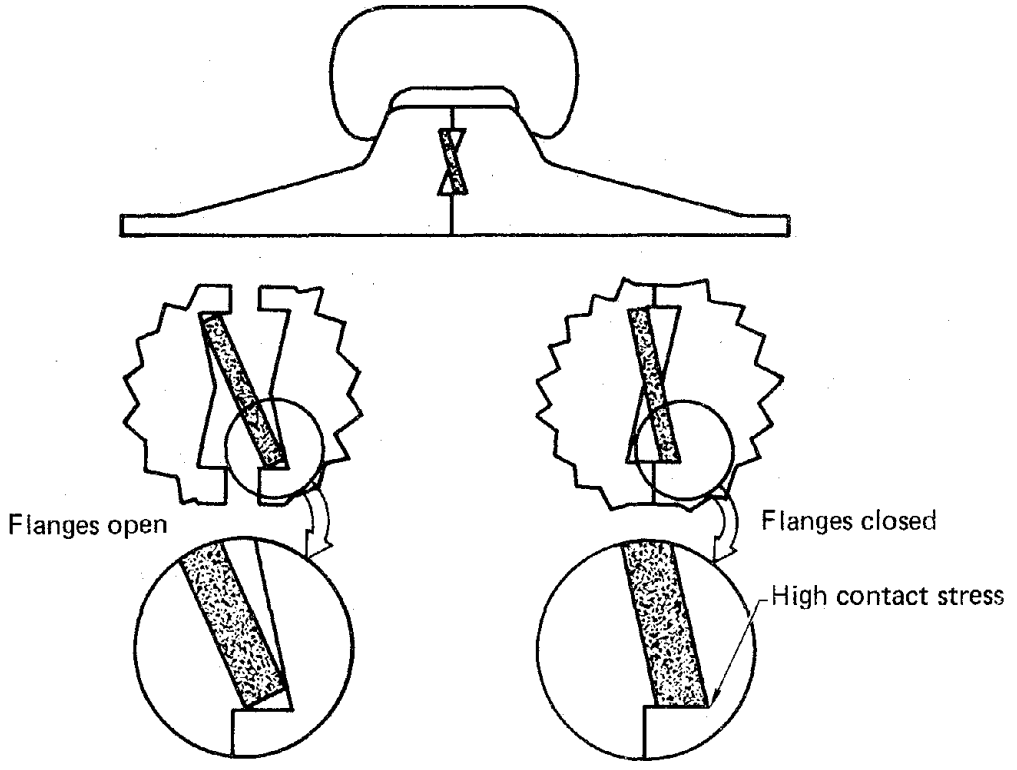

FIG. 4. A Conoseal generates high contact stress at the seal corners by jamming the seal into a confined space and causing it to buckle. This action also produces good springback.

code has a special feature that allows two surfaces to progressively interact as they come together.

We used DYNA2D to establish the feasibility of computer calculations for seals by successfully modeling the interaction between a hollow metal O-ring and its flat sealing surface. The computer simulation was run until a steady-state response was achieved. Figure 5 shows the model and displaced solutions, while Fig. 6 shows the effective stress in one element of the O-ring. Figure 6 reveals the shortcomings of DYNA2D and any explicit code when used to solve a quasistatic problem--the small size and, thus, large number of calculational steps required for "ringing" to subside in order to reach the steady-state solution. The large number of steps required made such solutions prohibitively expensive and time consuming, but DYNA2D provided a reference solution for further modeling efforts.

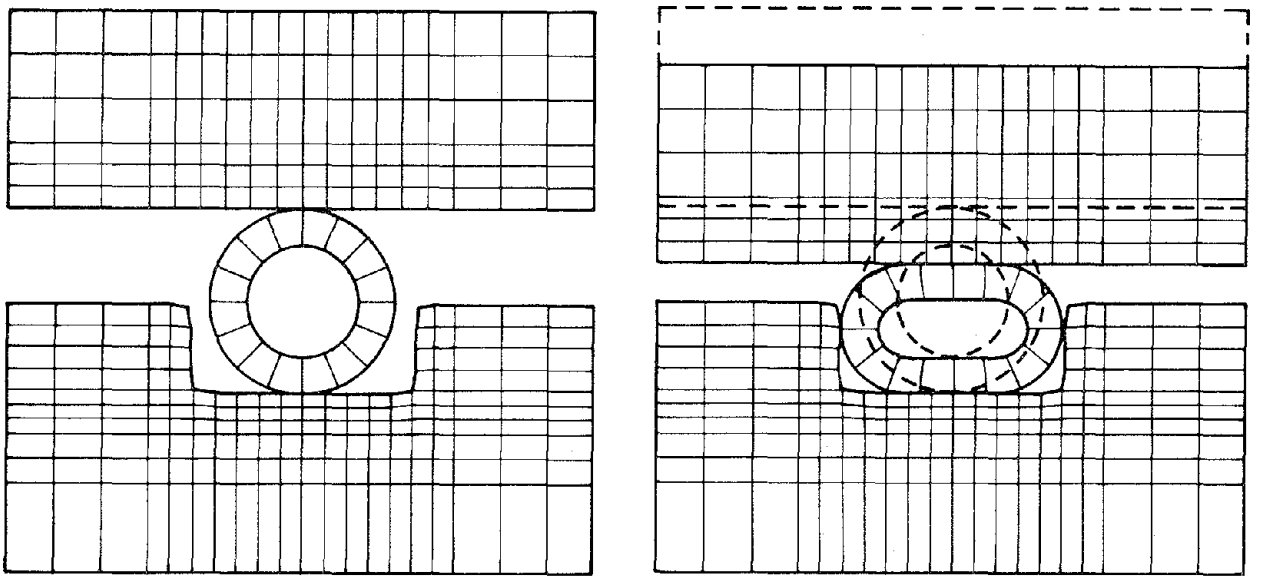

FIG. 5. Finite element model of a hollow O-ring seal, left, for analysis by DYNA2D. Displaced configuration, right, illustrates how pressure flattens the O-ring and forces it into the groove.

A better analysis tool was needed--an implicit finite element code that could do for quasistatic problems in perhaps 100 times fewer calculational steps what DYNA2D could do for time-dependent problems. Unfortunately, differences between implicit and explicit code formulations made it impossible to simply substitute the contact-impact algorithms from DYNA2D into an implicit code. Two finite element codes that employ implicit solution schemes were selected as possible alternatives, ADINA and MARC.[10,11] Both codes had a "gap" element, a nonlinear truss placed between two surfaces that might interact during problem solution. The truss elements would act as rigid links when the two surfaces come into contact. This technique had been used for a limited class of contact problems, and we decided to try it.

We selected ADINA to run feasibility studies. The formulation of the truss in ADINA was modified and, after a very long trial-and-error effort, ADINA successfully calculated a solution that agreed with that from DYNA2D. Figure 7a illustrates the O-ring model with the nonlinear truss elements in place. We concluded, however, that this gap element would never be the appropriate way to model arbitrary problems requiring contact-impact capabilities for the following reasons[12]:

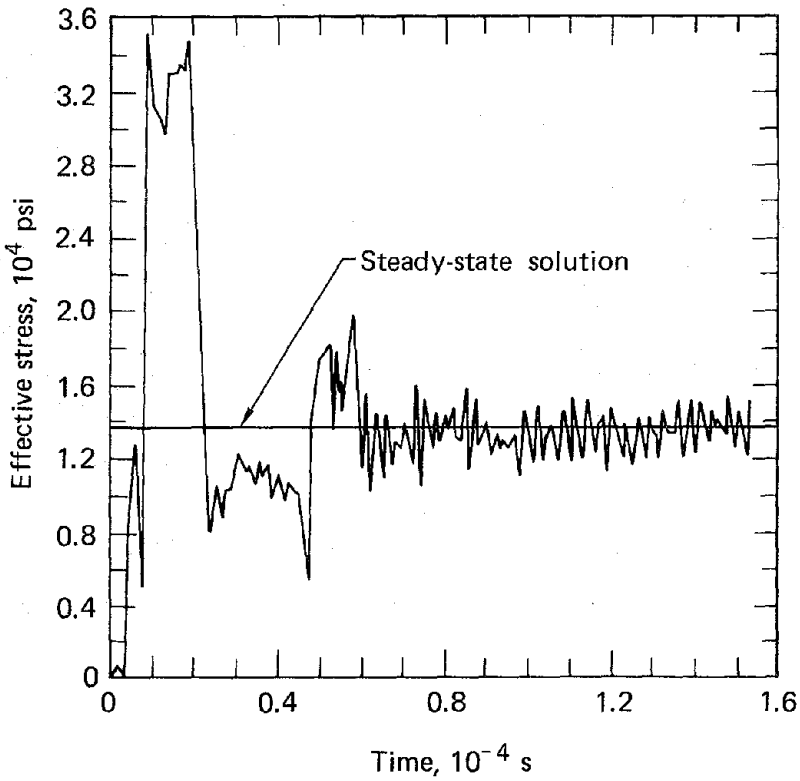

FIG. 6. Effective stress in an O-ring element in Fig. 5 next to a flat surface is a function of time because DYNA2D is a dynamic code. The spike caused by initial contact and the "ringing" both result from the time-dependent nature of DYNA2D; the steady-state solution is interpreted as the static solution.

- The truss formulation required a special modification that only applied to the O-ring.
- No friction exists in this formulation.
- Equilibrium iteration could not be used.
- Truss reaction forces were applied at the wrong points.
- The stress vs strain curve that defines truss stiffness (Fig. 7b) had to be determined by trial and error to obtain a numerically stable solution.

LLL's Code Development Group in the Mechanical Engineering Department then took over the effort to develop a contact-impact algorithm in an implicit finite element code. The puncture program, which was originally part of this seals program, also needed the same code capability. This contact-impact capability, sometimes called a "slide line," was put into NSAP2D.[13] In

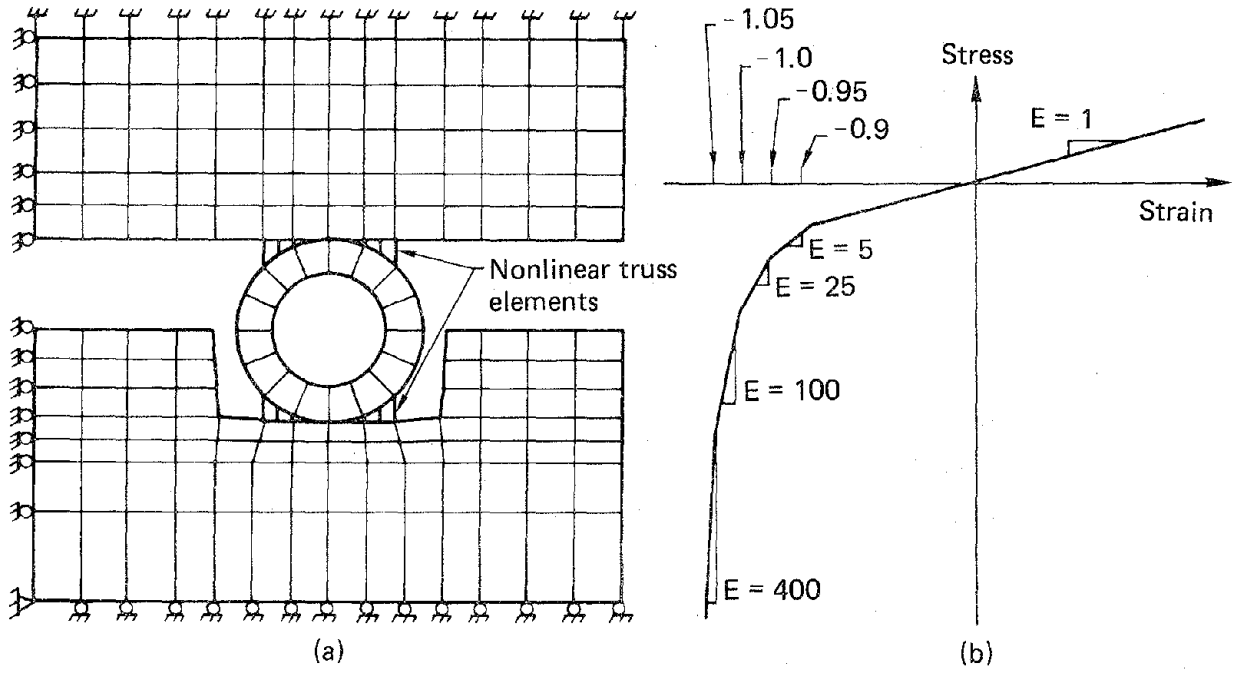

FIG. 7. Nonlinear truss elements are part of the finite element model of the hollow O-ring (a) developed for solution by the ADINA code. A nonlinear stress-strain curve (b) had to be developed by trial and error to get a numerically stable solution using ADINA.

general, slide-line capability means that surfaces that are not in contact at the start of a calculation can come in contact and interact later in the computation. The sophisticated penalty-function GAP algorithm in NSAP2D incorporates sliding with separation, closure, friction, and tied interfaces along arbitrary nodal surfaces. One side of the contact surface is referred to as the master node segment, while the other side is referred to as the slave node segment. The relative displacements of these surfaces are monitored. Any slave node that penetrates through its respective master contact surface causes a linear interface spring to be inserted into the stiffness matrix that couples the penetrating node to two adjacent nodes on the contact surface. The spring acts normal to the contact surface and develops an interface force proportional to the penetration of the slave node.

NSAP2D has been refined and renamed NIKE2D.[14] The code represents the first, and up to now, only successful development of an implicit slide-line capability. As such, it represents a major breakthrough in finite element

code development. With NIKE2D, we can calculate the contact stress between the seal and flange and the contact area. Results of such analyses are discussed in the subsequent section of this report that presents analysis and test results and in detail in the Appendixes.

SEAL TESTING PROGRAM

An experimental program was developed to complement the seal analysis by defining a mechanism for testing quarter- and half-scale seal fixtures in various cask operating environments. The experimental data would be combined with analytical results to establish design relationships for seal leak rates.

The significant experimental parameters chosen for the tests and their range of values, which were determined from both normal and accident cask operating conditions, are as follows:

Bolt force	50 to 110% of recommended clamping force
Internal pressure	14.7 to 1000 psi
Temperature	75 to 500°F
Scale	1/4 and 1/2 scale

A test matrix (Table 3) was developed to identify the parameter combinations for each seal-flange configuration. The matrix was designed to simplify the experimental procedure by allowing for successive testing of a given seal assembly. We believed that the tests defined in the matrix would provide a sufficient range of data and allow us to formulate the desired design curves.

Test hardware were designed and selected based on simplicity and commonality. All seals were tested in bolted circular flanges. The detailed designs of the test flanges varied to accommodate each seal configuration; however, all designs called for a volume within the test seal circle that connected to a pressure source and a volume outside of the test seal that connected to leak detection equipment. Whenever possible, nuts, bolts, washers, load transducers, and adapters were designed to allow for common use with all test configurations. Figure 8, which shows the assembly fabricated to test the Grayloc seal, illustrates the general aspects of the flange design, including bolted flanges, the seal, the pressure port, and the leak sensing port.

TABLE 3. Test matrix for seal leak rate tests.

Test number	Seal load					Internal pressure, psi					Temperature, °F						Seal diam, in.	
	0.5 F*	0.75 F	1.0 F	1.1 F	14.7	200	400	600	800	1000	-10	70	100	240	400	540	10	20
1	X				X							X					X	X
2		X			X							X					X	X
3			X		X							X					X	X
4				X	X							X					X	X
5	X					X						X					X	X
6		X				X						X					X	X
7			X			X						X					X	X
8				X		X						X					X	X
9	X						X					X					X	X
10		X					X					X					X	X
11			X				X					X					X	X
12				X			X					X					X	X
13	X							X				X					X	X
14		X						X				X					X	X
15			X					X				X					X	X
16				X				X				X					X	X
17	X								X			X					X	X
18		X							X			X					X	X
19			X						X			X					X	X
20				X					X			X					X	X
21	X									X		X					X	X
22		X								X		X					X	X
23			X							X		X					X	X
24				X						X		X					X	X
25			X		X						X						X	X
26			X		X								X				X	X
27			X		X									X			X	X
28			X		X										X		X	X
29			X		X											X	X	X

*F = specification load.

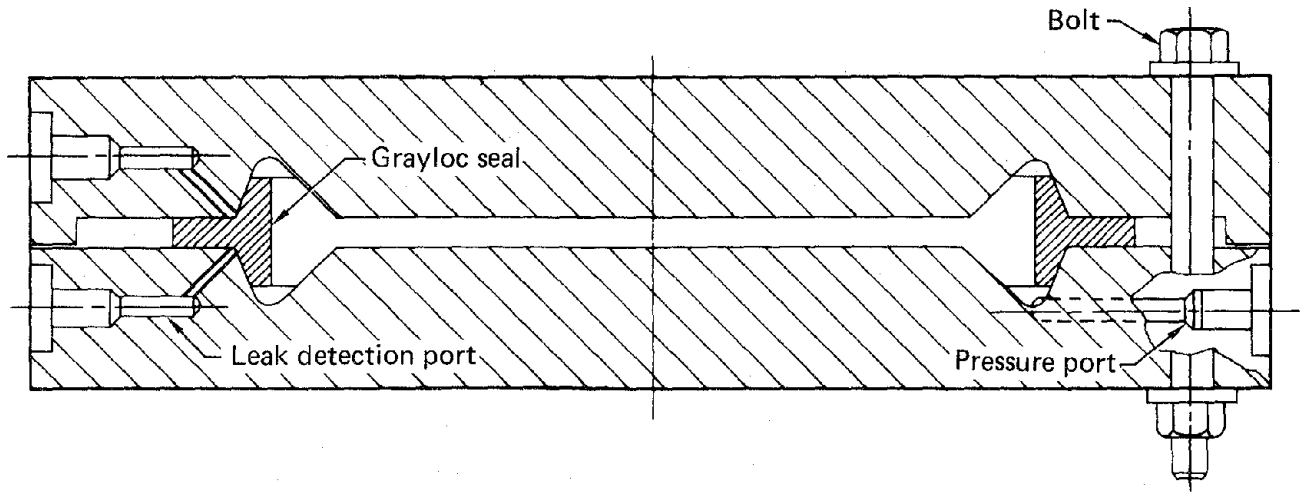

FIG. 8. The assembly fabricated to test the Grayloc seal illustrates the general aspects of the flange design.

The general procedure for each test point can be summarized as follows:

- Apply desired bolt force as measured by instrumented load washers.
- Achieve desired steady-state temperature.
- Apply internal pressure.
- Monitor leak rate until a steady-state value is identified.

We intended the test matrix and procedure to be flexible. Results could dictate different parameter values or call for a revised test method.

RESULTS

Delayed delivery of hardware, damage to test flanges, direction from the NRC and, finally, cutback in available funding, prevented analysis and testing of all seal configurations. To illustrate the test procedure followed during the program and to demonstrate the capability of the analysis method, this section gives a detailed description of the work completed with the Inconel X-750 O-rings. Following this discussion, brief summaries of results obtained with the other seal configurations are given. For detailed discussion of all results, the reader is referred to the Appendixes, which are copies of progress reports documenting all of the test and analysis efforts.

TESTING AND ANALYSIS OF INCONEL X-750 O-RINGS

The combined experimental and analytical study of the Inconel X-750 O-rings was conducted to develop design curves relating the leak rate of the seal to such parameters as contact pressure, contact area, pressure differential across the seal, applied bolt force, temperature, and seal circumference.

Experimental Program

The purpose of the experimental program was to obtain leak rate data for the Inconel X-750 O-rings as a function of applied bolt force, internal pressure, temperature, and seal circumference. The general test matrix (Table 3) served as the basis for our experimental program, but it had to be revised when testing began. Our first tests of 321 stainless steel O-rings indicated that closure could not be maintained and that a leak rate which saturated detection equipment resulted when a clamping force equal to only 50% of the manufacturer's recommended force is applied to the flange (See Appendix B). To ensure enough data points during Inconel X-750 testing, the test matrix was modified by adding a seal load equal to 125% of the recommended clamping force at each pressure level.

Test Hardware. The primary hardware used to test the Inconel X-750 O-rings consisted of a pair of bolted circular flanges. Details of the flange design were all within seal manufacturer's tolerances, including the inner diameter,

width and depth of the O-ring groove, and the machine finish of the flange contact surface. Figure 9, a schematic of the flange design, shows several significant features, including the primary and secondary O-ring grooves, the pressure inlet port, the leak sensing port, lower contact surface, and bolt circle diameter. When assembled, the flanges mate in a back-to-front configuration. A part drawing of the design is given in Appendix C.

Each assembly requires two metallic O-rings. The smaller, inner seal is the primary seal being evaluated for leak tightness. The larger, outer seal provides the boundary for a small volume between the two O-rings. This volume is connected to the mass spectrometer detection equipment via the sensing port. The mass spectrometer accurately detects the presence of the trace gas, helium, and converts the helium data into a flow or leak rate for the primary O-ring. The detection equipment can sense leaks as small as 2.8×10^{-10} std. cc/s. Leak rates greater than 1.0×10^{-3} std. cc/s would exceed measurement tolerances and saturate the equipment.

Internal pressure is applied to the flange assembly via the pressure port. A pressure fitting welded to the port outlet connects the flange to the pressure source. The pressure level is controlled by the appropriate use of regulators and valves.

The magnitude of the bolt force applied to the assembly is measured by load collars fabricated at LLL. To limit expense, only 4 of the 18 bolts used to secure the flanges were equipped with instrumented load collars. To provide a uniform clamping load, the value of torque that gave the desired force in the instrumented bolts was applied to all other bolts for each test step.

A list of all hardware associated with each seal-flange assembly is given in Table 4.

Test Procedure. Prior to assembly, the O-ring grooves and contact surfaces on each flange were thoroughly cleaned with alcohol. The O-rings were inspected and placed in the flange without lubricant or other treatment. Although the groove dimensions met design tolerances, insertion of the O-rings required some effort because all seals fit very snug against the outer diameter of the grooves. The upper flange was then lowered over the bolts and onto the

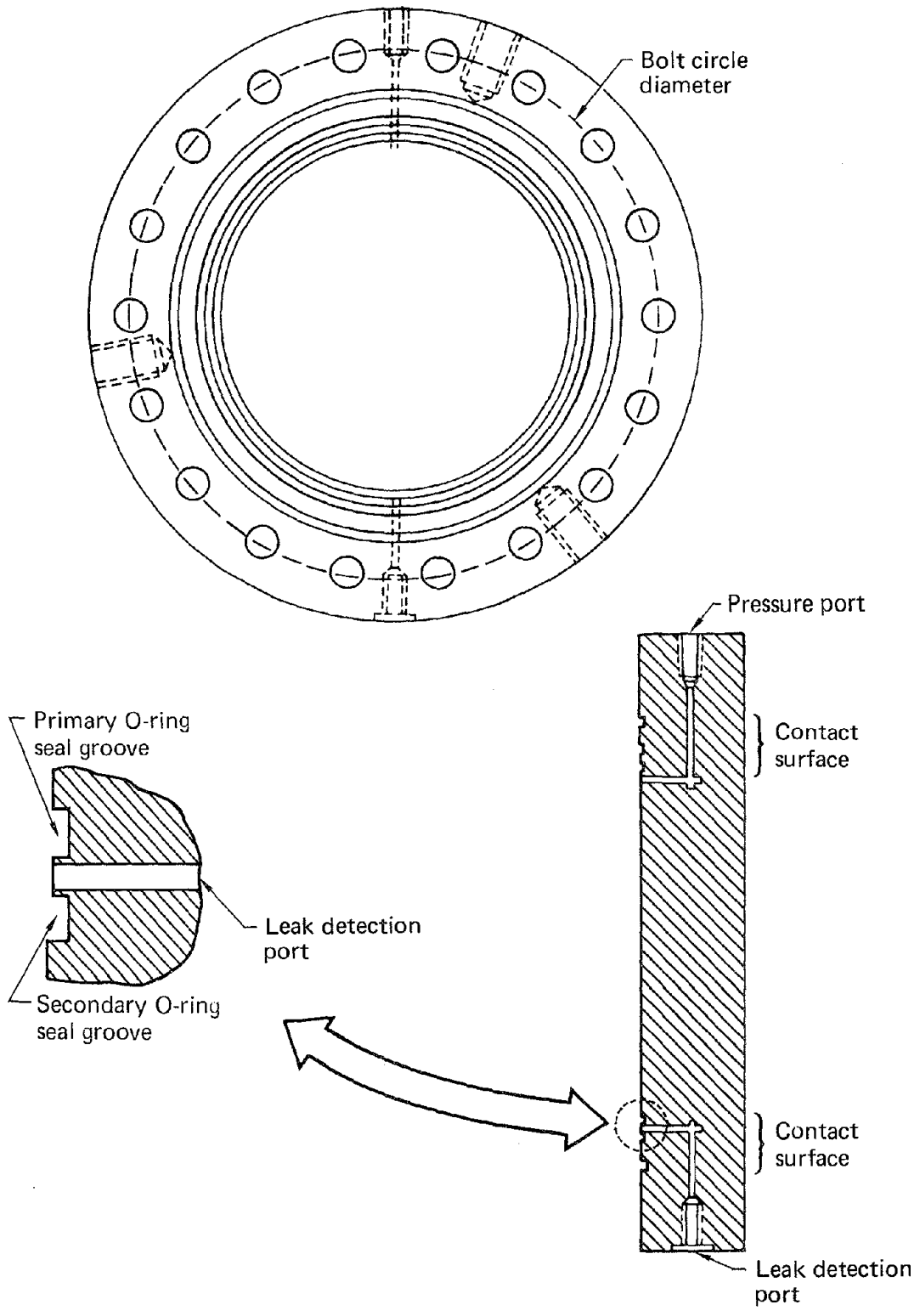

FIG. 9. Schematic of the metallic O-ring flange. See Appendix C for a detailed parts drawing.

TABLE 4. Hardware for testing 10-in.-diam O-ring.

Item	Description	Quantity
Test flanges	Circular, stainless steel (LLL drawing AA-119481-00)	2
Primary O-rings	Silver-coated, Inconel X-750 UAP* components U6312-10250SEB	3
Secondary O-rings	Silver-coated, Inconel X-750 UAP components U6312-10750SEB	3
Bolts	UNF 1 - 12 stainless steel with nuts	18
Washers	1 in., stainless steel	36
Instrumented load collars		4
Dummy load collars		14
Mass Spectrometer Leak Detection Equipment DuPont model 24-120B		1

*UAP Components, Inc., Columbia, SC.

seals. The pressure and leak detection lines were connected and the assembly was ready for testing.

The experimental procedure was the same for each test and consisted of the following steps:

1. Apply and record the appropriate bolt force.
2. Evacuate the volume between the O-rings and bring the leak detection equipment on line.
3. Apply the appropriate pressure to the flange assembly.
4. Record seal leak rate, internal pressure, and bolt force.
5. Release pressure by venting the flange assembly.

All data were recorded in a test log book. In addition, the bolt loads given by the load collars were recorded on both paper and magnetic tape. The pressure was recorded on a strip chart.

Test Results. Thirteen tests were performed using two sets of 10-in.-diam Inconel X-750 O-rings. The pressure differential across the primary seal varied from 14.7 to 400 psi. All tests were conducted at ambient temperature.

Nine tests were performed on the first pair of seals. These tests generally followed the sequence outlined in the modified test matrix. Table 5 lists the actual bolt force recorded from the four instrumented load collars for each test. Also given are the average applied bolt force, the desired calculated force, and the error between actual and calculated loads. Table 6 shows the leak rates that were obtained for each of the nine tests. The experiments were stopped after the seal leak rate remained both large and constant over a wide range of applied bolt forces and internal pressures. To determine whether these data were being affected by faulty hardware, the flanges were disassembled and visually inspected with a magnifying glass for possible damage to the contact surface. There were no apparent flaws on either O-ring grooves or upper contact surface. The O-rings were set aside for inspection.

TABLE 5. Bolt force data.

Test number	Desired force/bolt, lb	Measured force in instrumented bolts, lb					Error, %
		1	2	3	4	Average	
1	1058	1009	958	1137	1080	1046	-1.1
2	1587	1513	1723	1559	1656	1613	+1.6
3	2116	2089	2413	2202	2183	2222	+5.0
4	2328	2461	2482	2178	2338	2367	+1.7
5	2504	2445	2657	2405	2524	2507	+0.1
6	3303	3063	2911	3012	2981	2992	-1.4
7	3244	3253	3164	3095	3213	3180	-2.0
8	3562	3569	3606	3564	3518	3564	0.1
9	3950	3937	3864	3865	3912	3894	-1.4

TABLE 6. Leak rate data.

Test number	Seal load*	Internal pressure, psi	Leak rate, std. cc/s
1	0.50 F	14.7	---
2	0.75 F	14.7	4.2×10^{-6}
3	1.00 F	14.7	2.8×10^{-10}
4	1.10 F	14.7	2.8×10^{-10}
5	0.75 F	200	3.6×10^{-2}
6	1.00 F	200	3.6×10^{-2}
7	1.10 F	200	3.6×10^{-2}
8	1.25 F	200	3.6×10^{-2}
9	1.00 F	400	3.6×10^{-2}

*F = recommended clamping force.

The flanges were cleaned as before, and a second pair of O-rings was installed. Results with the first set of Inconel X-750 seals indicated that the leak rate remained constant for all tests when the pressure was 200 psi or more. To obtain additional data, four tests were attempted with internal pressure varying between 14.7 and 200 psi. However, a sufficient vacuum between the O-rings could not be maintained at any level of bolt force. Consequently, no tests could be run with the second set of seals. The flanges were again disassembled and inspected. No anomalies were found. The O-rings were removed for inspection. Further testing was discontinued until an explanation of these data could be made through inspection of the seals or analysis of the flange assemblies.

Inspection of the two pairs of O-rings revealed major flaws on or near the contact surface. Figure 10a is a magnified view of a section of the smaller seal from the first pair tested. A hole penetrating the seal wall is evident on the border between the portion of the O-ring surface that made contact with the flange (darkened area) and the portion that did not (light area). Although many of the scratches shown in the silver coating resulted from handling after the tests had been conducted, we believe that the hole was a

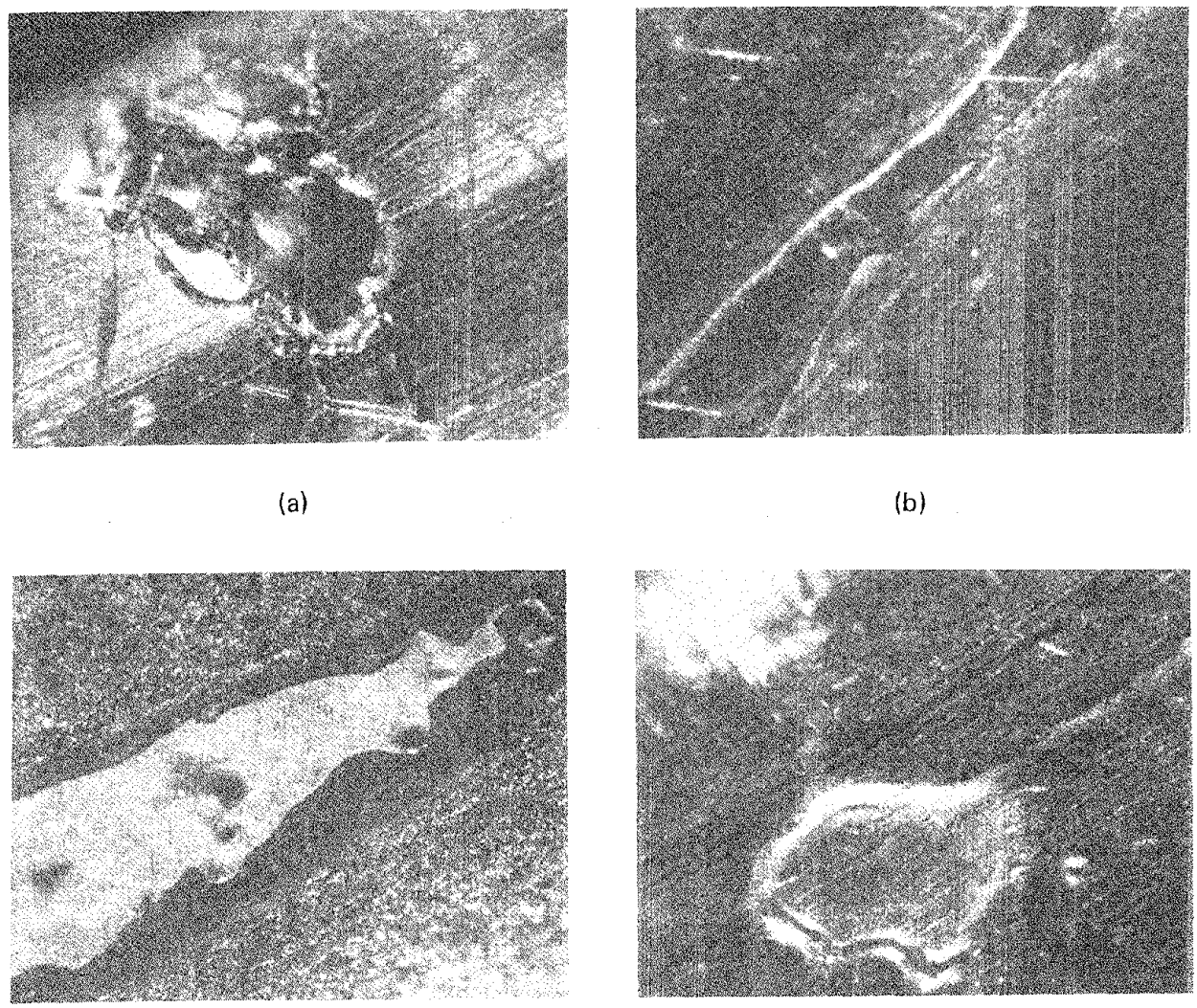

FIG. 10. The two pairs of O-rings exhibited major flaws on or near the contact surface, including: (a) a hole in the seal wall on the border between the contact portion (darkened area) and the noncontact portion (light area) of the smaller O-ring in the first pair tested; (b) a pair of cracks that run circumferentially in the larger O-ring of the first pair and that are still evident after the silver coating had been removed (c); lesser flaws in the second pair (d). Such flaws (a) reduce seal area, (b) reduce contact pressure, (c) indicate that ultimate strain was exceeded, and (d) provide leak paths.

manufacturing flaw. This hole would reduce the local contact area of the seal and potentially increase the leak rate. Figure 10b shows a pair of cracks running circumferentially in the larger O-ring used during the first set of tests. The cracks are still evident after the silver coating had been removed (Fig. 10c), indicating that the Inconel X-750 was deformed beyond its ultimate capacity. Such failure would reduce the local contact pressure between seal and flange and tend to increase the leak rate. Springback of the seal during unloading would be greatly reduced. No holes or cracks were found in the second set of O-rings tested; however, lesser flaws seen in the contact surface could easily provide a leak path (Fig. 10d). Although it is impossible to determine their exact impact on the experimental data, such flaws can only tend to compromise the leak tightness of the seal. No further testing of the Inconel X-750 O-ring was conducted.

Analytical Program

The analytical program was designed to accurately model the experimental procedure. We planned to determine the contact pressure and contact area for the O-ring under conditions that corresponded to the actual levels of bolt force and internal pressure used during the test sequence. These analytical results would then be combined with measured leak rate data to develop the performance curves for the Inconel X-750 O-rings.

The O-ring analysis followed a three-phase substructuring technique. First, a detailed model of the O-ring was developed (Fig. 11). The seal was compressed to the maximum displacement dictated by O-ring groove geometry and then unloaded. The reaction force was determined and used to develop a force-deflection curve for the O-ring. This curve (Fig. 12) gave the effective stiffness of the seal.

A model of the seal-flange assembly was then developed (Fig. 13). Material properties of Type-321 stainless steel were input for the flange elements, while the behavior of elements modeling the O-rings was given by the force-deflection curve of Fig. 12. Figure 14 shows bolt forces and pressure loadings recorded during the nine tests of the first set of Inconel X-750 O-rings. These measured values were simultaneously input to the assembly model.

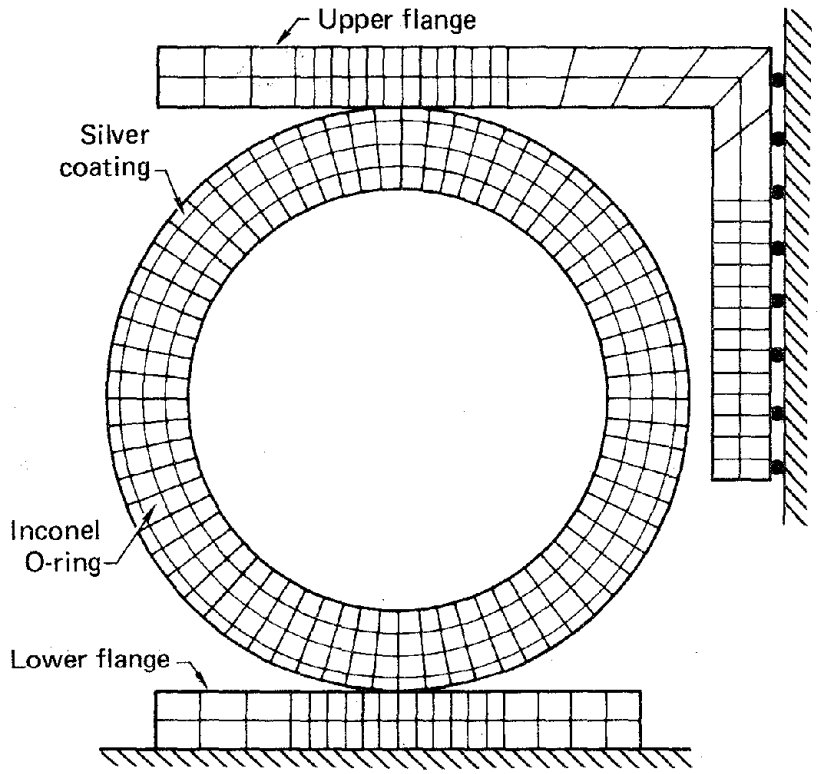

FIG. 11. Detailed model of an O-ring for developing a load-deflection curve using the finite element code NIKE2D.

The results of the flange assembly analysis are given by the deflection history curve for the O-ring (Fig. 15). Figure 16 shows the O-ring displacement on an expanded vertical scale after the internal pressure was added. The effects of increased bolt force and internal pressure are evident in the fluctuations in O-ring compression.

Figure 17 shows the deformed flange model under loads corresponding to Test 4 in the load history curve. The stress contour lines reveal that the upper and lower flanges make contact at their outer perimeter before the seal is completely compressed. Consequently, not all of the force applied by the bolts was reacted at the seals. This implies that loads developed in the seal during testing were less than the applied bolt force would have dictated.

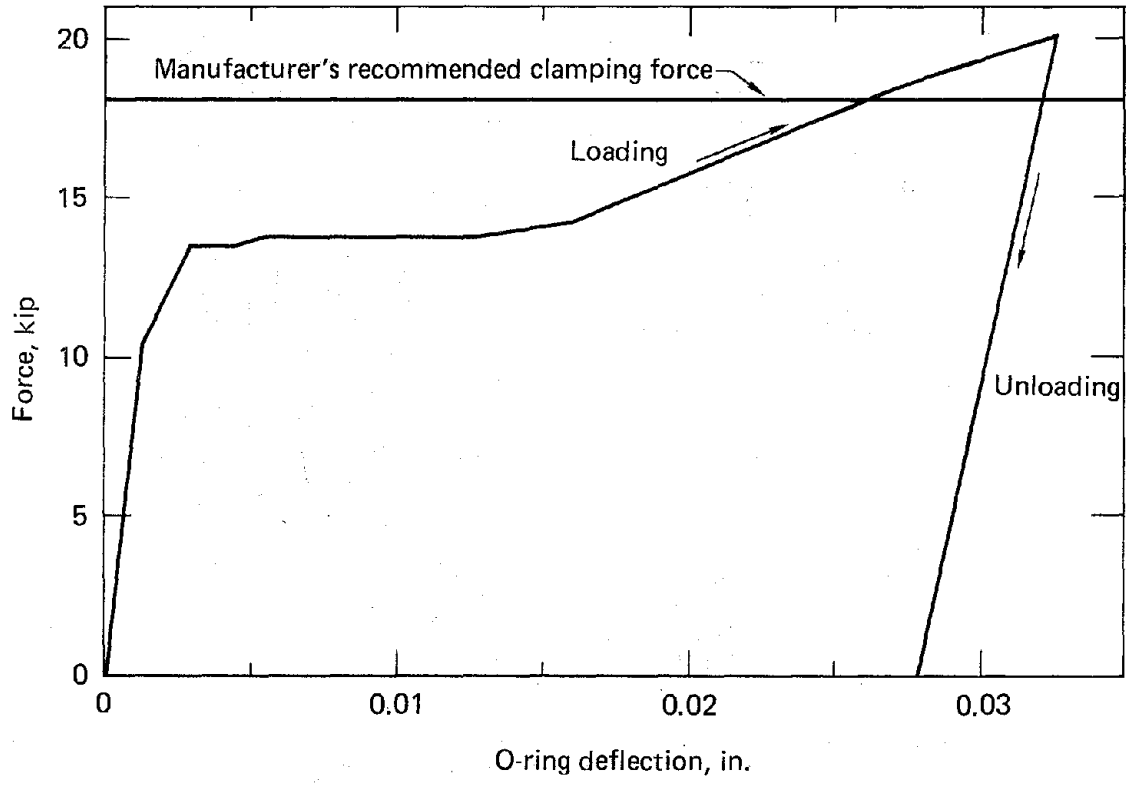

FIG. 12. O-ring load-deflection curve shows amount of deflection needed to reach manufacturer's recommmended clamping force and sensitivity to unloading.

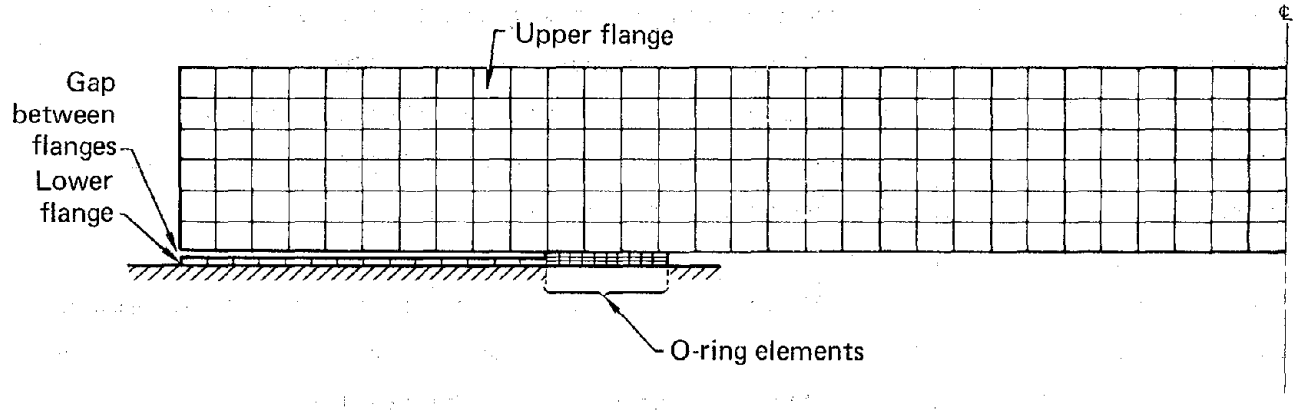

FIG. 13. A model of the seal-flange assembly. Behavior of the flange elements is based on material properties of Type-321 stainless steel. O-ring elements behave according to the load-deflection curve of Fig. 12.

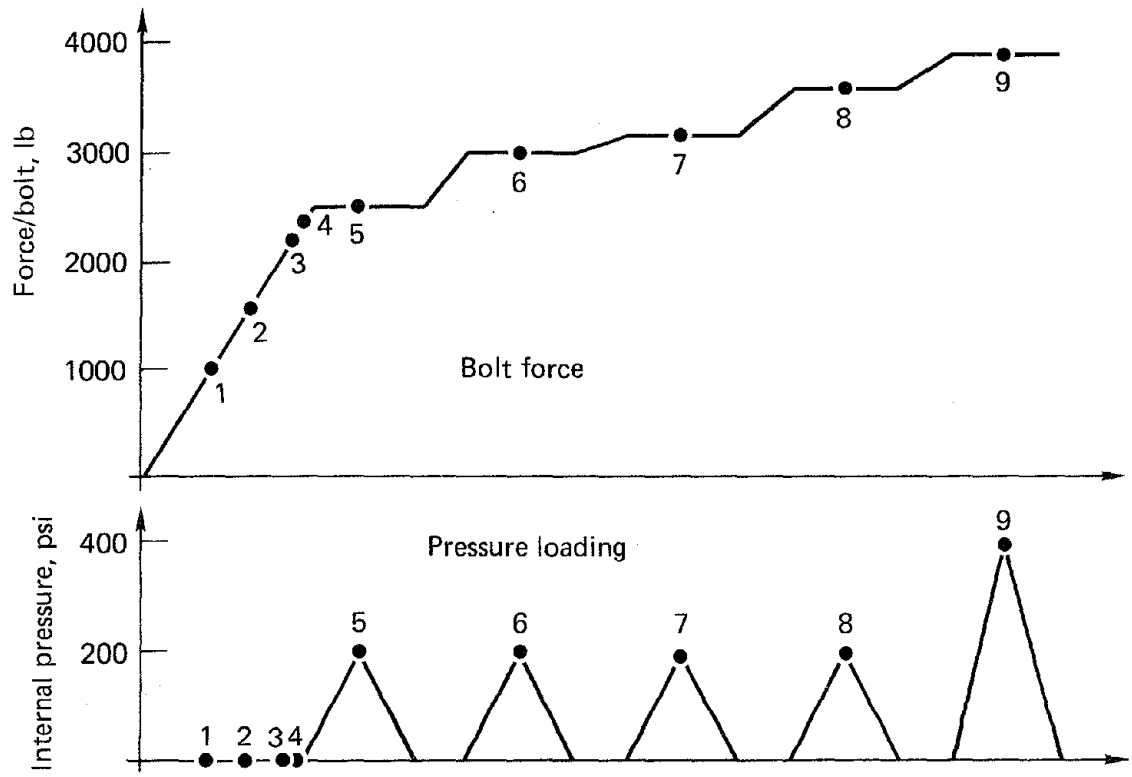

FIG. 14. Experimentally recorded bolt force and pressure loadings were simultaneously input to the model. Numbers refer to the nine data points obtained with the first set of Inconel X-750 O-rings.

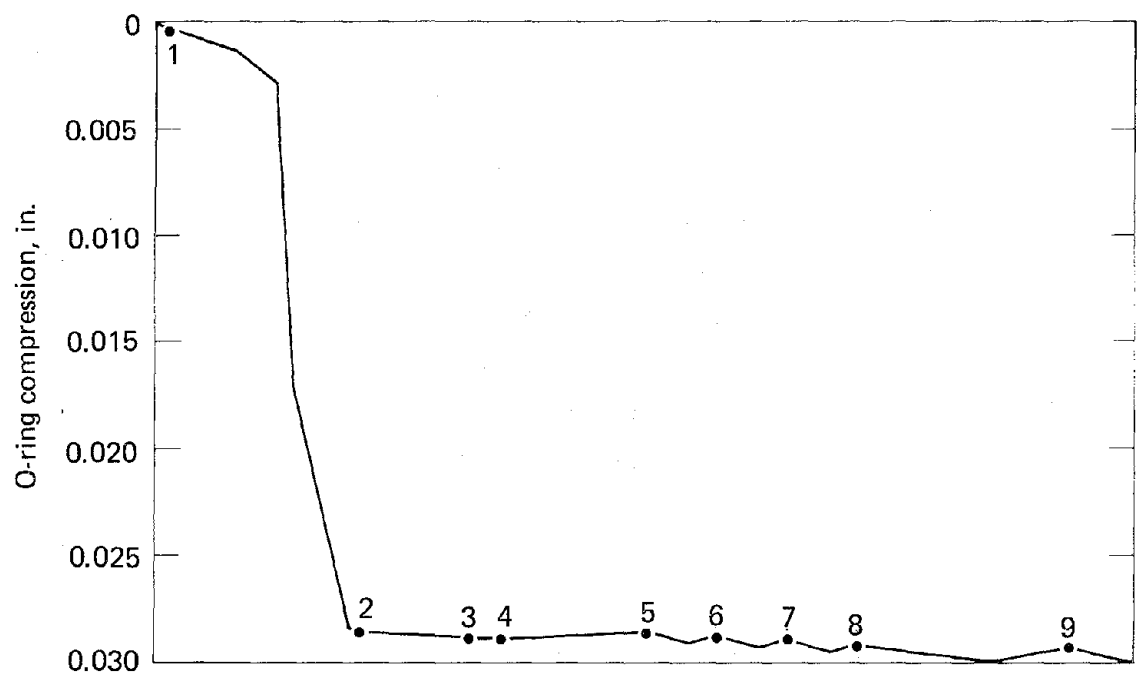

FIG. 15. Deflection history curve for the O-ring is the result of the flange assembly analysis. Numbers correspond to tests.

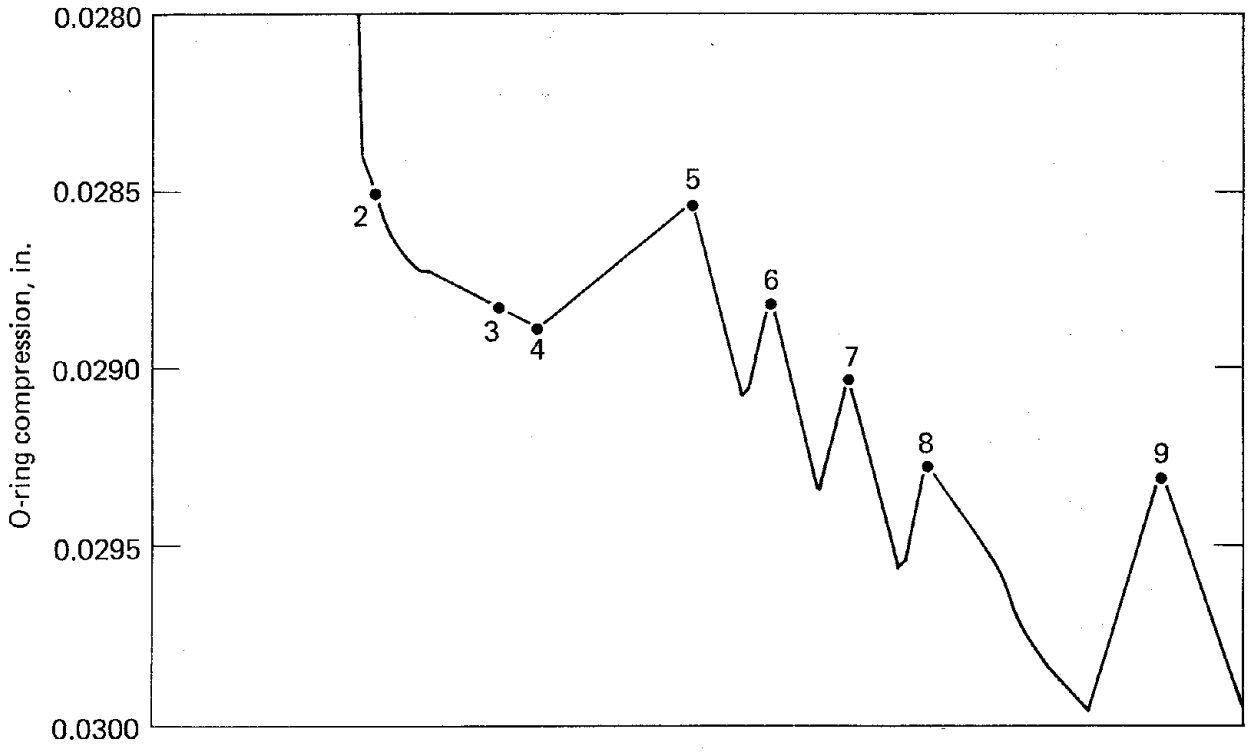

FIG. 16. O-ring displacement from Fig. 15 on an expanded vertical scale after the internal pressure was added. The effects of increased bolt force and internal pressure are evident in the fluctuations in O-ring compression. Numbers correspond to tests.

The deflection history curve obtained from the assembly analysis was then used as input to the detailed O-ring model (Fig. 11). Contact area and pressure were determined for displacements corresponding to each test. A typical deformed configuration corresponding to Test 9 is shown in Fig. 18. Data for the other tests are given in Table 6. As the deformation of the seal increases during the analysis, the curvature of the model O-ring surface reverses and the region of initial contact completely unloads (See Appendix C). The accuracy of this shape was verified by comparison with the actual deformed shape of the O-rings tested.

Figure 19 shows regions of effective plastic strain for the fully compressed O-ring. Contour lines of constant strain indicate areas with as much as 30% plastic strain, which exceeds the ultimate strain capacity for Inconel X-750 and further supports the possibility of local O-ring failure.

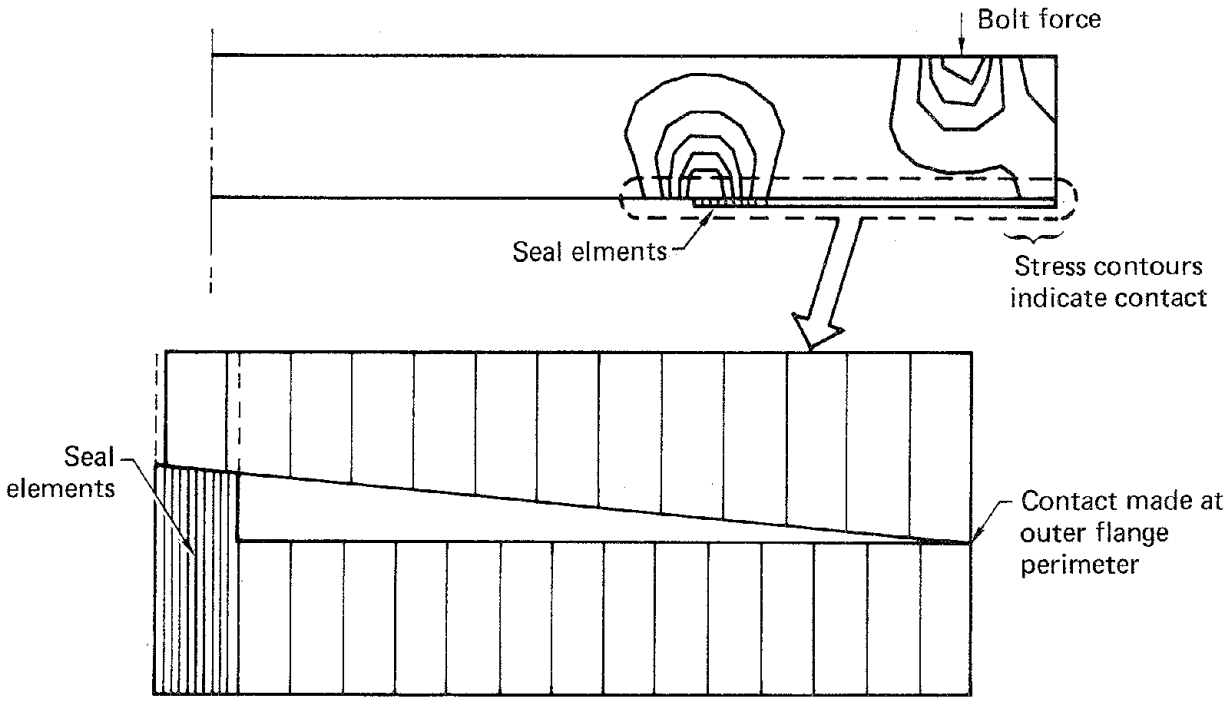

FIG. 17. Deformed flange model under loads corresponding to Test 4. Stress contour lines indicate that the upper and lower flanges touch at their outer perimeter before the seal is completely compressed, suggesting that loads developed in the seal during testing were less than the applied bolt force would have dictated.

Correlation Between Experiment and Analysis

Both testing and analysis found the leak tightness of the Inconel X-750 O-rings to be extremely sensitive to the displacement of the compression flange. Analyses showed that a 30-mil compression of the O-ring was required to develop the manufacturer's recommended clamping force between the seal and flange. However, a 2-mil unloading of the flange would decrease the contact force in the seal by 50% (Fig. 12) as a result of plastic deformation in the seal and its lack of adequate springback. Insufficient contact pressure between the O-ring and flange would result, and seal integrity would be lost. These results suggest that great care be taken in the design and use of O-ring closures to ensure that the seals do not unload under any operating condition.

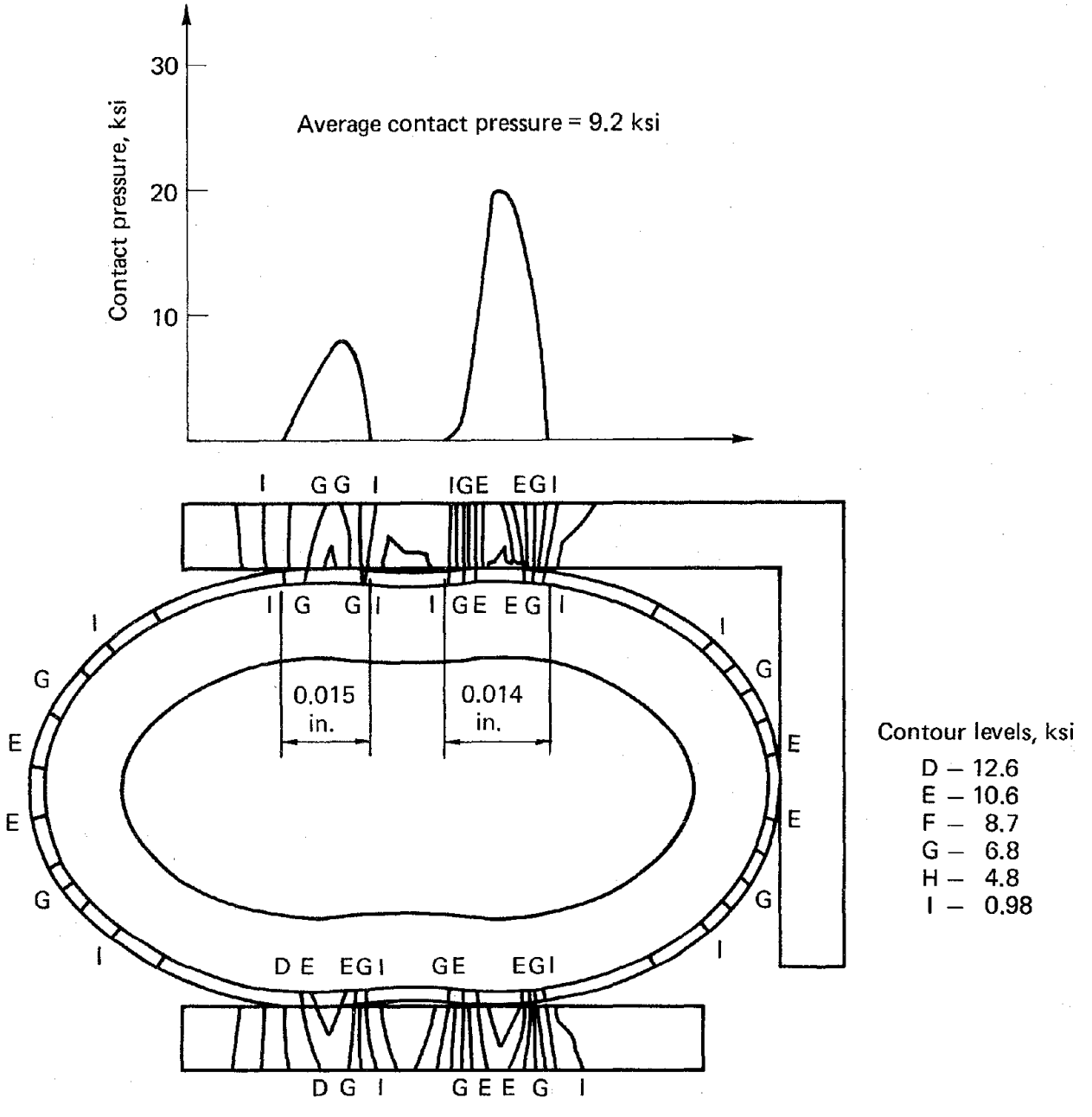

FIG. 18. Contact area and pressure for Test 9 show regions of expanding contact between the O-ring and flange. Such curves were determined by using displacements of flange nodes near the seal (obtained from the assembly analysis) as input to the detailed O-ring model, the same model used to develop the load-deflection curve for the seal.

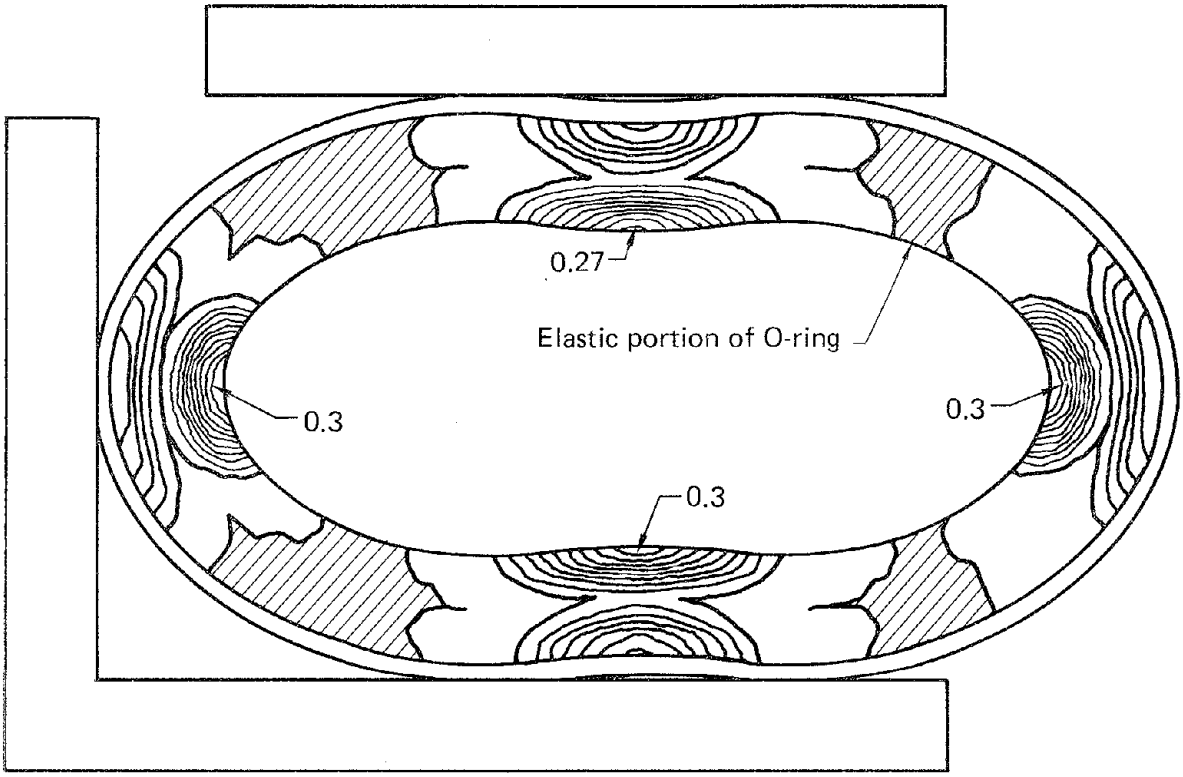

FIG. 19. Drawn at increments of 3% plastic strain, contour lines of constant strain indicate areas with as much as 30% plastic strain in the fully compressed O-ring. These large values exceed the ultimate strain capacity for Inconel X-750 and further support the possibility of local O-ring failure. Shaded areas depict elastic portions of the O-ring.

The sensitivity of the O-rings to unloading limited the amount of data obtained during testing. We found that the Inconel X-750 O-rings gave either very small or very large leak rates under most test conditions. Little data were obtained between these two extremes, especially when testing the effect of pressure on O-ring performance. As pressure was applied to the test assembly, the flanges bent under the load. Although the bending was small, it was enough in most cases to unload the O-ring and compromise the seal. The large plastic deformation and lack of springback in the O-rings were primarily responsible for this problem, but the design of the test flanges was also a factor. The 2-in. difference between the O-ring radius and the bolt circle radius allowed for a greater displacement of the flanges near the seals. Had the O-rings been placed adjacent to the bolt circle, the unloading effect of

the pressure would have been lessened. These results indicate that placement of the seals near the location of applied clamping force be a primary design consideration.

Although limited data were obtained, results showed an inverse relationship between leak rate and contact force in those tests for which no internal pressure was applied (Fig. 20). Figure 21, which shows the total compressive interface force between seal and flange throughout the analysis history, demonstrates the effect of pressure on the leak rate of the seal assembly. As pressure is applied, the test flange bends elastically. The contact force drops significantly below the recommended clamping load, and the seal is compromised. When the pressure is released, the flanges return to their

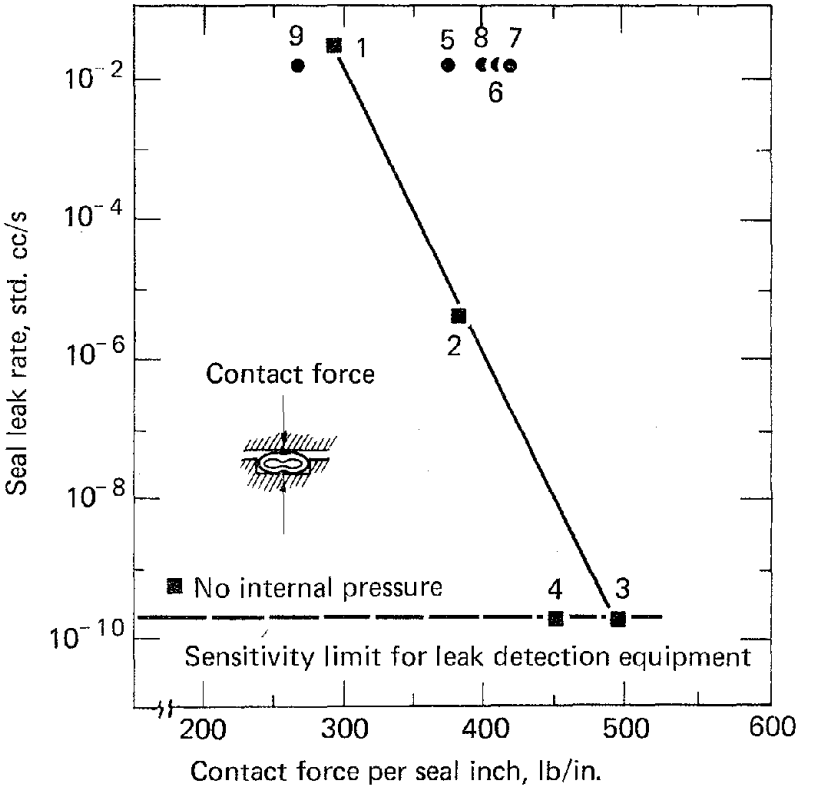

FIG. 20. An inverse relationship between leak rate and contact force was shown for those tests in which no internal pressure was applied. The other test points reveal a significant increase in leak rate that resulted partly from rotation of the flange and partly from probable O-ring failure under load cycling.

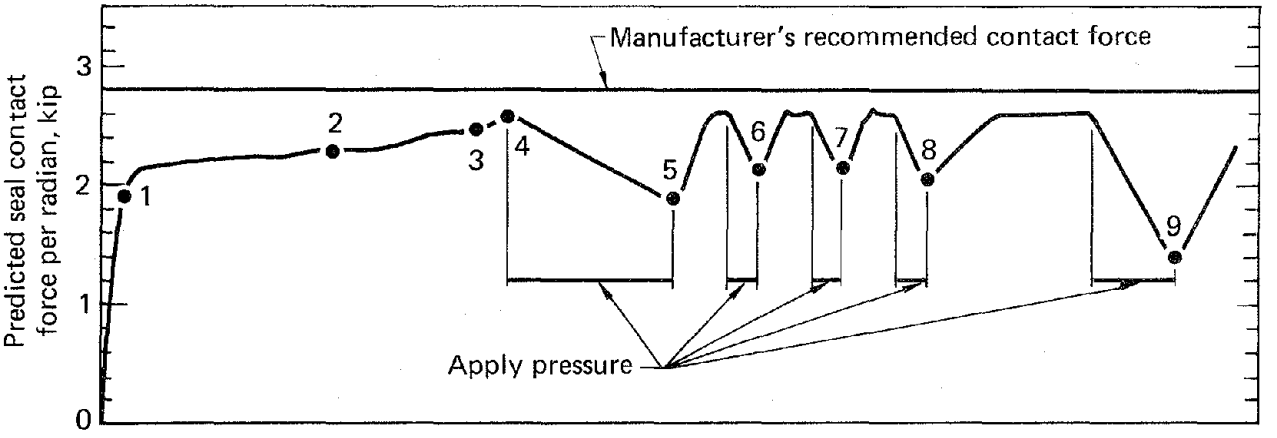

FIG. 21. Total compressive interface force between seal and flange throughout the analysis history. As pressure is applied, the contact force drops significantly below the recommended clamping load. When the pressure is released, the contact force increases, and a positive seal is again attained.

undeformed shape, the contact force increases, and a positive seal is again attained.

Plastic deformation of the seal caused the relationship between leak rate and average contact pressure and contact area to be less apparent. Once the seal plastically deforms and is seated in the groove, the contact area remains relatively constant despite changes in applied force. Only when the compression flange begins to lift off of the O-ring does the contact area significantly change. Then, of course, the leak tightness of the seal has been lost.

OTHER SEAL CONFIGURATIONS

This section briefly summarizes the experimental and analytical results obtained with all seal configurations in this study other than Inconel X-750. For more details, the reader is referred to the Appendixes.

Polymer O-rings

Tests were conducted with two types of 10-in.-nominal-diam polymer O-rings (silicone and Viton) at ambient temperature and with internal pressures

ranging from approximately 1 to 14.7 psi. The leak rate obtained during those experiments varied from 10^{-7} to 10^{-5} std. cc/s. The leak-rate data gave evidence that the leak resulted from permeation rather than flow through an orifice. This was supported both by the linear relationship between leak rate and internal pressure and the time lag between when the pressure was applied and when the leak was measured. The permeation rate of helium through the Viton seals was less than that for the silicone seals at all pressures. Further testing of the polymer O-rings at higher pressures was discontinued at the request of the NRC. No analysis of this seal configuration was performed.

Type-321 Stainless Steel O-rings

Both testing and analyses were conducted with the 10-in.-diam 321 stainless steel O-rings. As with the Inconel X-750 seals, the leak rates recorded for these tests were either very small ($<2.8\ 10^{-10}$ std. cc/s) or very large ($>10^{-3}$ std. cc/s). Analysis of the test configuration attributed the lack of good test data to a poor flange design. Lack of metal-to-metal contact outside of the flange bolt circle caused large bending stresses near the seal grooves as bolt forces were applied. These stresses caused displacements of the flange that subsequently unloaded the seals and compromised their leak tightness. To correct this problem, the design was modified to give metal-to-metal contact at the perimeter of the test flanges and thereby reduce the bending stresses near the seal locations. No further testing or analysis of the 321 stainless steel O-ring configuration were conducted.

Batzer Flange

To verify our substructuring method of finite element analysis, two models of the Batzer flange were generated. The first model approximated the entire test flange. Analysis of this model gave nodal displacements and rotations near the contact area. These values were then used as input to a second, detailed model for analysis of the Batzer flange contact surface. Resulting data provided the values of contact stress and contact area corresponding to the given applied loadings.

Preliminary analysis of the Batzer flange helped to verify both the modeling approach and the capability of the NSAP2D computer code. However, since no

testing of this seal configuration was conducted, no additional analyses were performed.

Conoseal and Grayloc Gasket

No tests or analyses were conducted with either the Conoseal or the Grayloc seal.

CONCLUSION

An excellent analytical tool--the finite element code NIKE2D--was developed that can predict seal displacement, contact area, and contact stress for a variety of seal closures in nuclear waste shipping casks. Limited test data qualitatively verified the code's predictive capability. Hardware exists for further testing to establish quantitative relationships between code predictions and test results. In particular, eight pieces of flange hardware were produced in 1/4- and 1/2-scale sizes of rail cask configurations. They are specially configured for leak-rate testing and, if tested, could provide useful practical data. Used with NIKE2D, the additional test data could then form the basis for a comprehensive predictive tool that the NRC would use to evaluate proposed seal designs for nuclear waste shipping casks.

REFERENCES

1. R. A. Larder and D. F. Arthur, Puncture of Shielded Radioactive Material Shipping Containers Part I--Analysis and Results, Lawrence Livermore Laboratory, Livermore, CA, UCRL 52638 and NUREG/CR-0930, PT. I (1978).
2. R. A. Larder and D. F. Arthur, Puncture of Shielded Radioactive Material Shipping Containers, Part II--Static and Dynamic Tests of Laminated Plates, Lawrence Livermore Laboratory, Livermore, CA, UCRL 52638 and NUREG/CR-0930, PT. II (1978).
3. "Packaging of Radioactive Material for Transport and Transportation of Radioactive Material Under Certain Conditions," Part 71 of Title 10 of the U.S. Code of Federal Regulations (10 CFR 71) (U.S. Government Printing Office, Washington, D.C.).
4. Proceedings of Leak Detection Seminar/Workshop, Varian Associates, Lexington Vacuum Division (June 1976).
5. A. Roth, Vacuum Technology (North-Holland Publishing Company, 1976) p. 384-409.
6. G. J. Armand, J. Lapujoulade, and I. Paigne, "Corrections Between Leak Rate and Some Phenomena Observed in Metal to Metal Contact," Trans. 2nd International Vacuum Congress (Permagon Press, 1962).
7. A. Roth and A. Amilani, "Sealing Factors, Their Measurement and Use in the Design of Vacuum Gasket Seals," Trans. 3rd International Vacuum Congress (Permagon Press, 1965).
8. L. G. Gitzendanner and F. O. Rathbun, Statistical Interface--Leakage Analysis, General Electric Co., Report 65-GL-73.
9. J. O. Hallquist, DYNA2D: An Explicit Finite Element and Finite Difference Code for Axisymmetric and Plane Strain Calculations, Lawrence Livermore Laboratory, Livermore, CA, UCRL 52429 (1978).
10. Klaus-Jurgen Bathe, ADINA: A Finite Element Program for Automatic Dynamic Incremental Nonlinear Analysis, Massachusetts Institute of Technology, Cambridge, MA, Report 82448-1 (Rev. 1978).
11. MARC, MARC Analysis Corporation, Palo Alto, CA.
12. B. J. Benda and R. C. Greenlaw, Application of ADINA to Nonlinear Contact Problems, ADINA Conference, Massachusetts Institute of Technology, Cambridge, MA, Aug. 4-5, 1977.
13. J. O. Hallquist, NSAP2D: An Implicit, Finite Deformation, Finite-Element Code for Analyzing the Static and Dynamic Response of 2-D Solids, Lawrence Livermore Laboratory, Livermore, CA, Internal publication (May 1977).

14. J. O. Hallquist, NIKE2D: An Implicit, Finite Deformation, Finite-Element Code for Analyzing the Static and Dynamic Response of Two Dimensional Solids, Lawrence Livermore Laboratory, Livermore, CA, UCRL 52678 (1979).

LLL:1980/2

APPENDIX A: POLYMER O-RINGS

(Note: This appendix reproduces the technical content of the progress report submitted to the NRC for work done between April 1, 1978 through September 1, 1978)

PROGRESS REPORT

April 1, 1978 through September 1, 1978

DEVELOP AND IMPROVE STRUCTURAL ANALYSIS TECHNIQUES FOR CONTAINER COMPONENTS

by

G. J. LEAKE

R. A. LARDER

B. J. BENDA

ENGINEERING MECHANICS SECTION OF

THE NUCLEAR TEST ENGINEERING DIVISION

of

LAWRENCE LIVERMORE LABORATORY

LIVERMORE, CALIFORNIA

Sponsored by

Nuclear Regulatory Commission

Division of Safeguard

Fuel Cycle and Environmental

Research

PROGRESS REPORT ON THE DEVELOPMENT AND IMPROVEMENT OF METHODS FOR ASSESSING THE PERFORMANCE OF CONTAINER CLOSURES FOR MAY THROUGH AUGUST 1978

INTRODUCTION

The work on this project is being done by Lawrence Livermore Laboratory (LLL) under contract with the Nuclear Regulatory Commission (NRC) to develop and improve methods for assessing the performance of container closures. The project includes experimental and analytical studies of five different seal-flange configurations.

SUMMARY

Progress on this program has been proceeding slowly due to delays in manufacturing the test hardware and the time involved in reworking delivered flanges. Rework was necessary to correct manufacturing error and damage to sealing surfaces that occurred during handling and shipping. Even so, significant achievements have been accomplished. Preliminary check-out tests on the polymer O-ring flanges using silicone and Viton O-rings indicate that the leak rate measuring scheme we are using is satisfactory. Also completed during this quarter was a detailed NIKE2D finite element analysis of a hollow metal O-ring. Due to recent developments to the NIKE2D code, excellent results were obtained in the analysis. As soon as the remaining problems with the test hardware are resolved, the experiments and the corresponding analysis can be completed.

PROGRAM STATUS

Experimental

The following hardware has been received:

1) Polymer O-ring flanges
2) Hollow metal O-ring flanges
3) Conoseal flanges
4) Viton and silicone O-rings
5) 321 stainless steel O-rings
6) Conoseals
7) Bolts
8) Load washers

Waiting to be received are:

1) Batzer flanges
2) Grayloc flanges
3) Grayloc seals
4) Inconel X O-rings

All parts should be in-house early in October. Necessary rework should be completed by the last week in September. The main problem to be solved before testing can continue is with the load washers. These washers do not have the required sensitivity to control and record the clamping force. Our test personnel are working on an alternate scheme to solve this problem.

Analytical

The NIKE2D finite element code has been chosen as the analytical method to be used in assessing the various seal types. A complete detailed static analysis of a hollow metal O-ring has been successfully completed. Further analysis is halted until the problems with the test hardware have been solved.

PROGRAM RESULTS

Experimental

The object of the experimental program is to obtain data on five different seal types for leak rate vs. internal pressure, seal load, and temperature. Size effect will also be studied by having nominally 10.0 and 20.0 inch diameter seals for each seal type. The five seal types in this study are polymer O-rings, hollow metal O-rings, Conoseal, Batzer seal, and the Grayloc seal. Figure 1 shows a sketch of the experimental set up and the seal types.

Our test engineers have approved the proposed test procedures. These procedures call for each seal type and size to be tested in two parts. In the first part, a seal will be placed in its flanges and leak tested in 24 steps to obtain data for leak rate vs. pressure and seal load. The seal load will be adjusted by increasing the bolt clamping force in calculated fractions of the manufacturers specified value. In the second part, a new seal will be placed in the flanges and leak tested at atmospheric pressure and the manufacturers specified seal load in five temperature steps. These 29 steps are shown in the comprehensive test matrix in Table 1.

The only major problem to solve before starting the proposed test series is how to adjust and monitor the bolt clamping force. The load washers originally intended for this job are not giving consistent readings in the range of loading to be applied in the tests. As soon as this problem is solved, the proposed testing can begin.

Successful preliminary check-out tests on silicone and Viton O-rings have shown that the proposed leak testing scheme will work. Leak rate data were obtained using a helium mass spectrometer. The differential pressure was varied in the preliminary tests from 0.3 psi to 14.5 psi. These tests confirmed that very low leak rates (less than 10^{-6} std. cc/sec) are obtainable with the Viton O-rings. The curves obtained in the preliminary

tests shown in Figure 2 clearly display that the Viton O-rings have a much lower leak rate at these pressures than do the silicone O-rings. The difference in these leak rates is very close to the difference predicted using the Parker O-ring material handbook. Also recorded in the preliminary check-out test was a definite time lag between the instant the helium was introduced until the moment the detector first sensed the helium. This time (lag shown in Figure 3) is a good indicator that the leak is due to molecular permeation through the silicone and Viton rather than a direct leak path.

Analytical

Since the yearly summary ending April 1, 1978, a detailed analysis of a seal closure area was completed. The NIKE2D finite element code was used to perform this analysis. The results of this analysis look very good. To achieve these results the NIKE2D code had to have the capability of analyzing sliding surfaces, opening and closing of gaps, and friction between the contact surfaces. Another important feature that was recently added to the NIKE2D code is the unloading modulus option. This option allows the code to overcome potential numerical problems while calculating the unloading of a part.

The detailed analysis that was done was of a 10.25 inch diameter 321 stainless steel hollow O-ring. The O-ring analyzed had a tubing outside diameter of .093 inch and .002 inch of silver plating. The load case analyzed was for 1000 psi of internal pressure at room temperature. First, an overall model of the flange was generated to do a stress analysis and to calculate the deflections at the inner seal groove. This model (shown in Figure 4) predicted acceptable stresses, but the calculated deflections at the inner seal groove would have excessively unloaded the seal. A design change ws initiated to correct this situation. Next, a detailed axisymmetric analysis of the hollow metal O-ring was done. Figure 5 shows the model with the

applied displacement function and boundary conditions indicated. Since the hollow metal O-ring is displacement-limited by the seal groove, the displacement function is calculated from the closing of the flanges and any unloading calculated with the flange analysis. From this detailed analysis it is possible to obtain the contact stress and the contact area. The contact area can be obtained from the deformed shape as shown in Figure 6. This deformed shape agrees very well with observed 321 stainless steel O-ring behavior. The contact stress is given in curves of contact stress vs. the displacement function as shown in Figures 7 and 8. The maximum calculated seal load in this analysis is 720 lbs/in.

NIKE2D meets the objectives of giving a way to predict the contact stress and the contact area in a static case. Also, since unloading of the seal is possible, the amount of allowable unloading can be estimated. NIKE2D is capable of analyzing dynamic cases, so it is possible to predict movement and gaps under accident conditions. The analysis effort has been stopped until the problems in the experimental portion of this study have been resolved.

Table 1 Test matrix for seal leak rate tests.

Test number	Seal Load (F=specification force)				Internal pressure (psi)						Temperature (°F)						Seal diam (in)	
	0.5F	0.75F	1.0F	1.1F	14.7	200	400	600	800	1000	-40	70	100	240	400	540	10.0	20.0
1	X				X							X					X	X
2		X			X							X					X	X
3			X		X							X					X	X
4				X	X							X					X	X
5	X					X						X					X	X
6		X				X						X					X	X
7			X			X						X					X	X
8				X		X						X					X	X
9	X						X					X					X	X
10		X					X					X					X	X
11			X				X					X					X	X
12				X			X					X					X	X
13	X							X				X					X	X
14		X						X				X					X	X
15			X					X				X					X	X
16				X				X				X					X	X
17	X								X			X					X	X
18		X							X			X					X	X
19			X						X			X					X	X
20				X					X			X					X	X
21	X									X		X					X	X
22		X								X		X					X	X
23			X							X		X					X	X
24				X						X		X					X	X
25			X		X						X						X	X
26			X		X								X				X	X
27			X		X									X			X	X
28			X		X										X		X	X
29			X		X											X	X	X

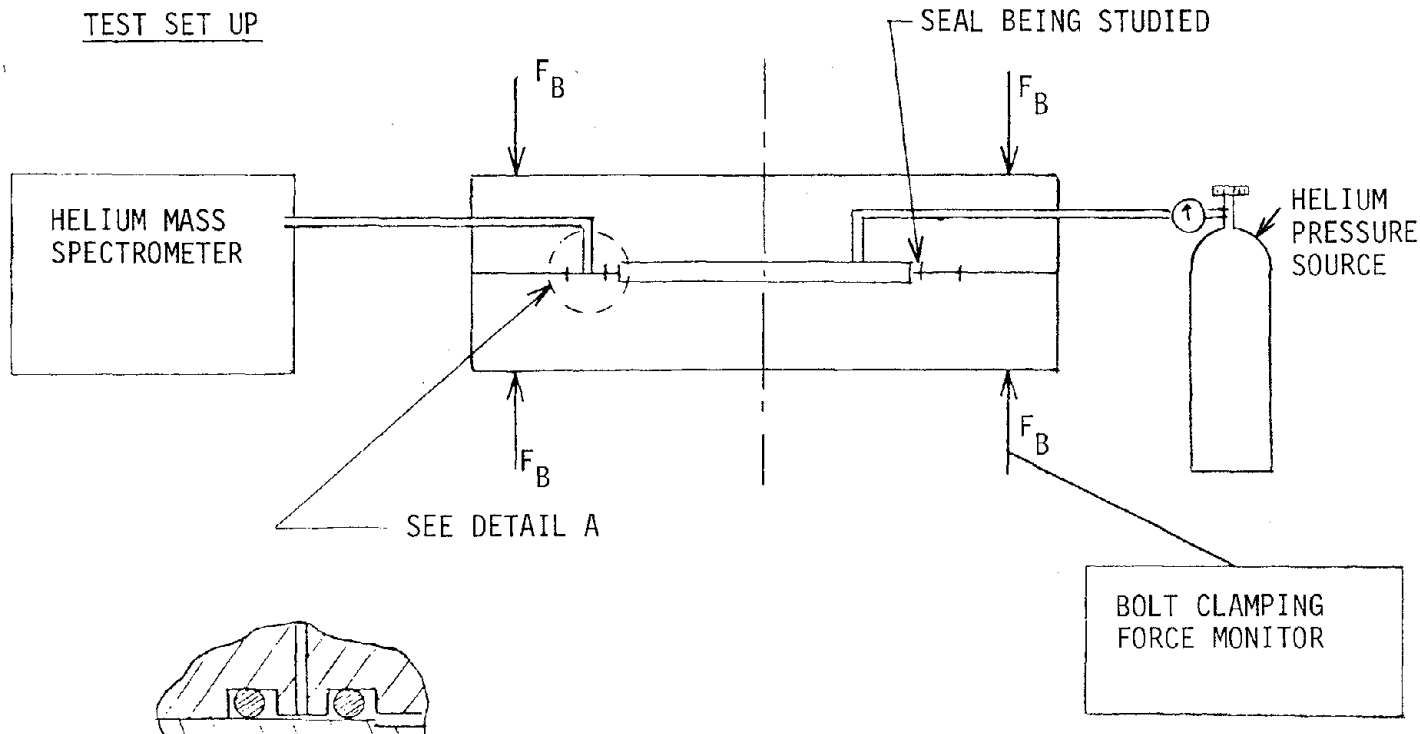

DETAIL A. POLYMER O-RING

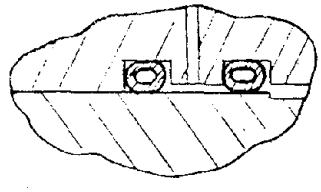

DETAIL A. HOLLOW METAL O-RING

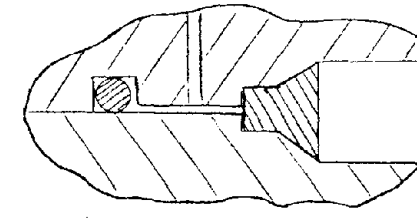

DETAIL A. GRAYLOC SEAL

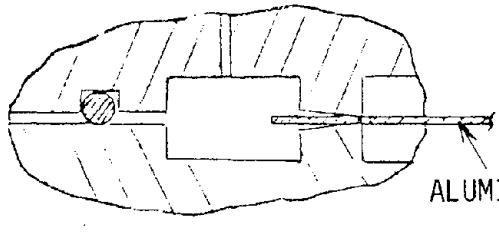

DETAIL A. BATZER SEAL

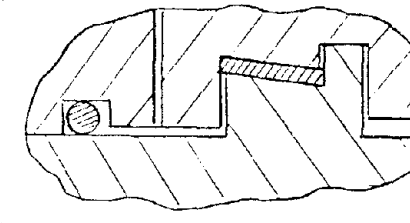

DETAIL A. CONO SEAL

FIGURE 1. TEST SET UP FOR FIVE WIDELY VARYING SEAL TYPES

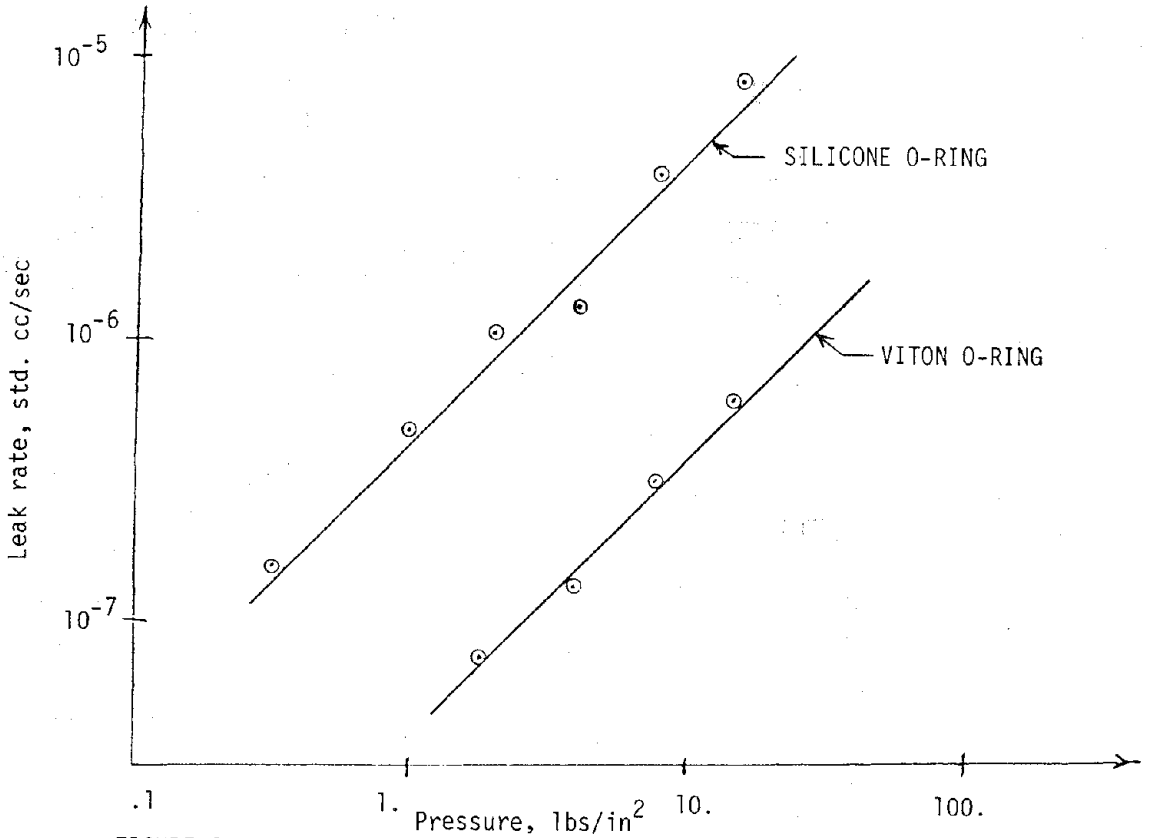

FIGURE 2. VITON HAS A MUCH LOWER LEAK RATE THAN SILICONE AT THESE PRESSURES.

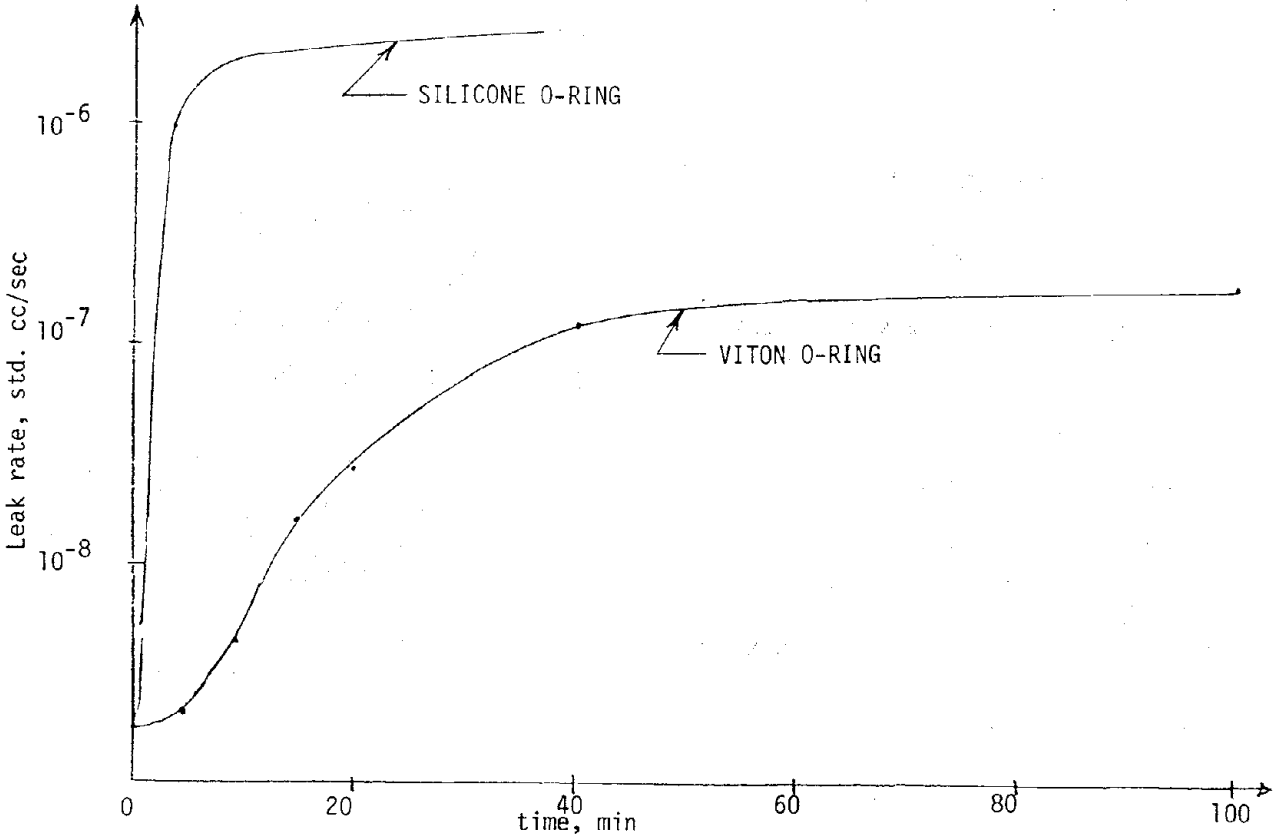

FIGURE 3. RESPONSE TIME SHOWING A TIME LAG INDICITIVE OF MOLECULAR PERMEATION THROUGH THE VITON AND SILICONE

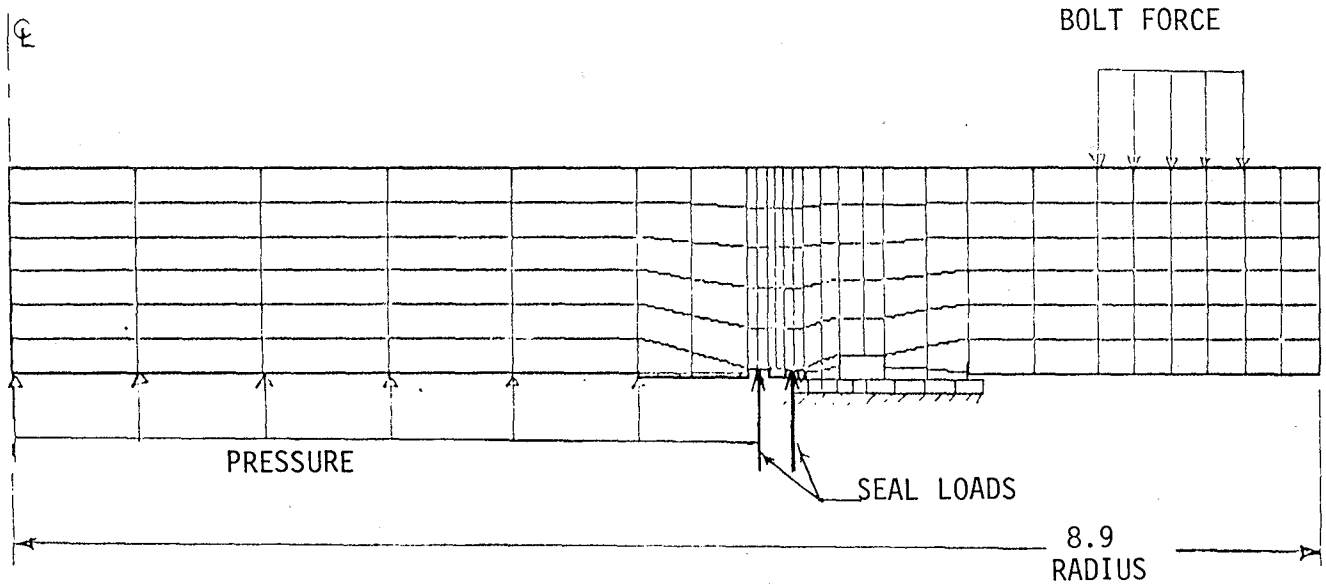

FIGURE 4. FLANGE MODEL USED IN CALCULATING DISPLACEMENT AT INNER SEAL GROVE

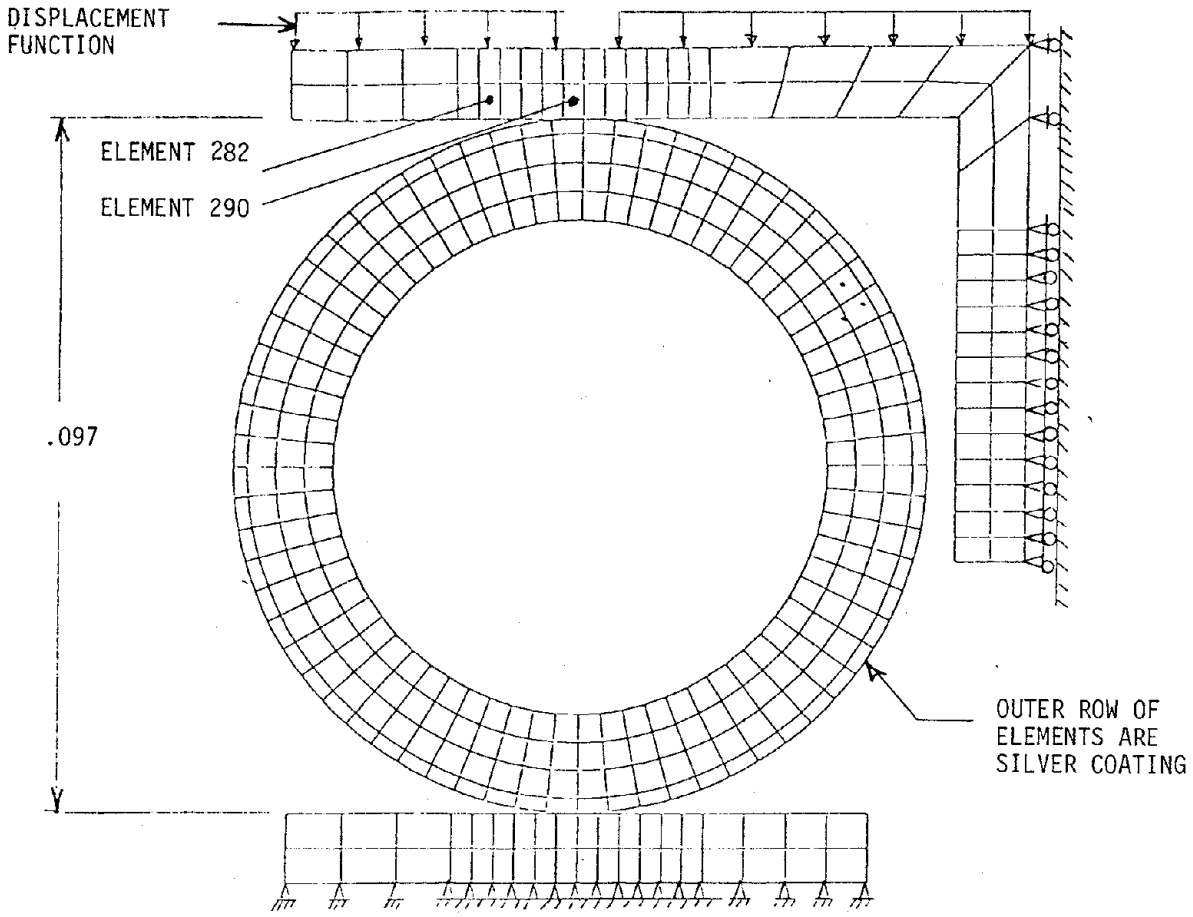

FIGURE 5. AXISYMMETRIC MODEL OF A 10.25 INCH DIAMETER 321 STAINLESS STEEL O-RING

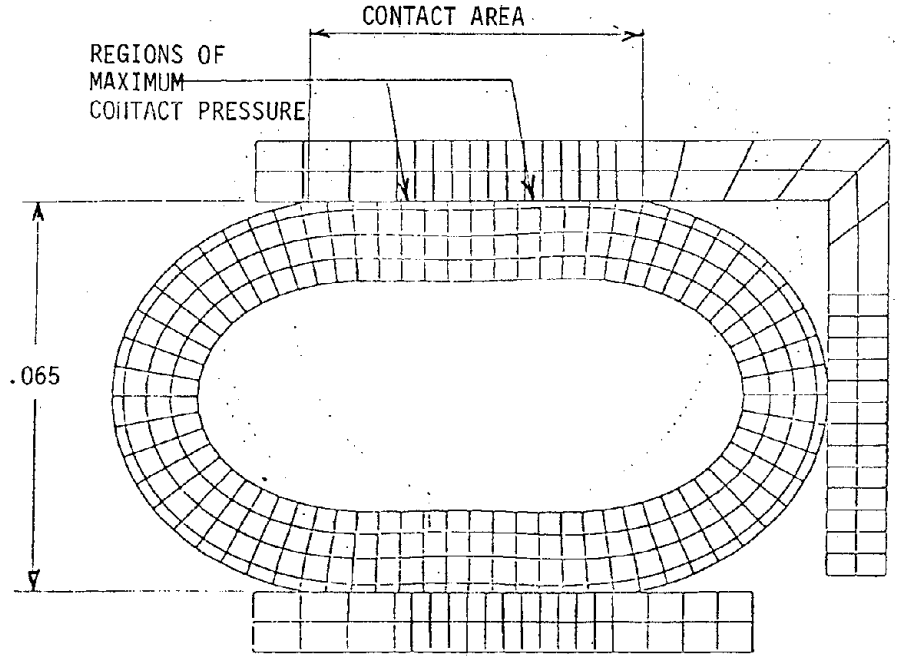

FIGURE 6. DEFORMED SHAPE OF O-RING AGREES WITH ACTUAL OBSERVED CASES.

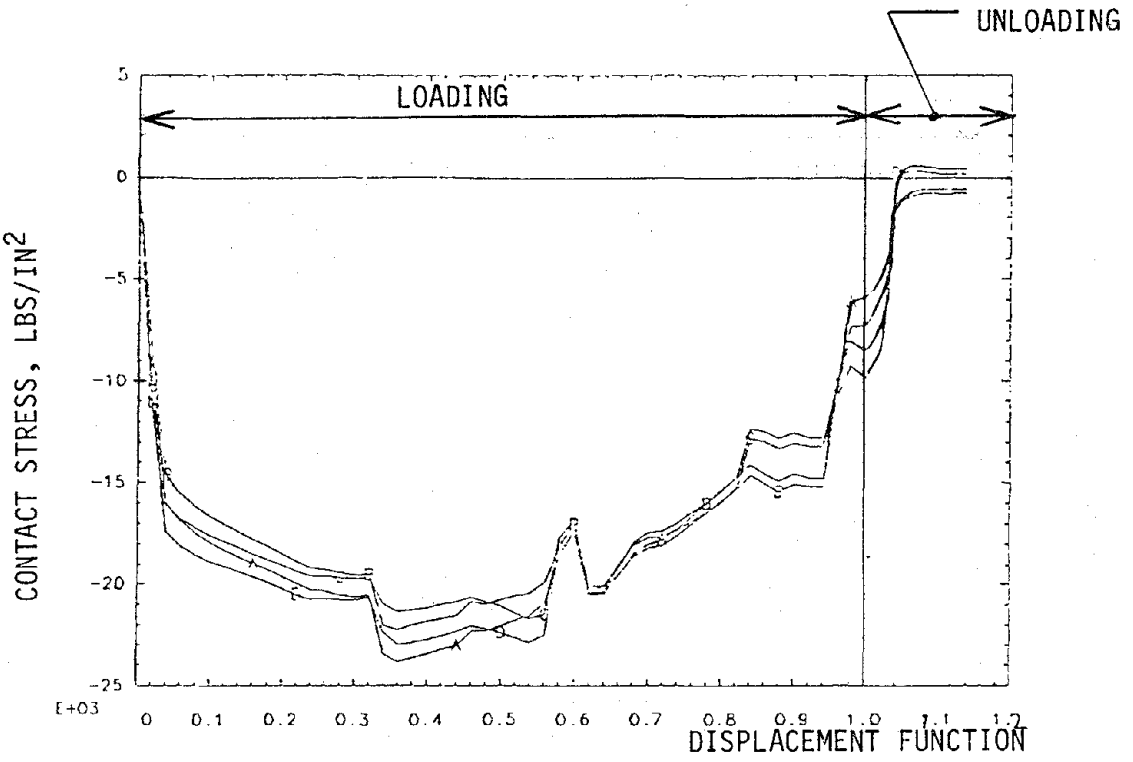

FIGURE 7. CONTACT STRESS AT CENTER OF CONTACT AREA (ELEMENT 290 SEE FIGURE 5 FOR LOCATION.)

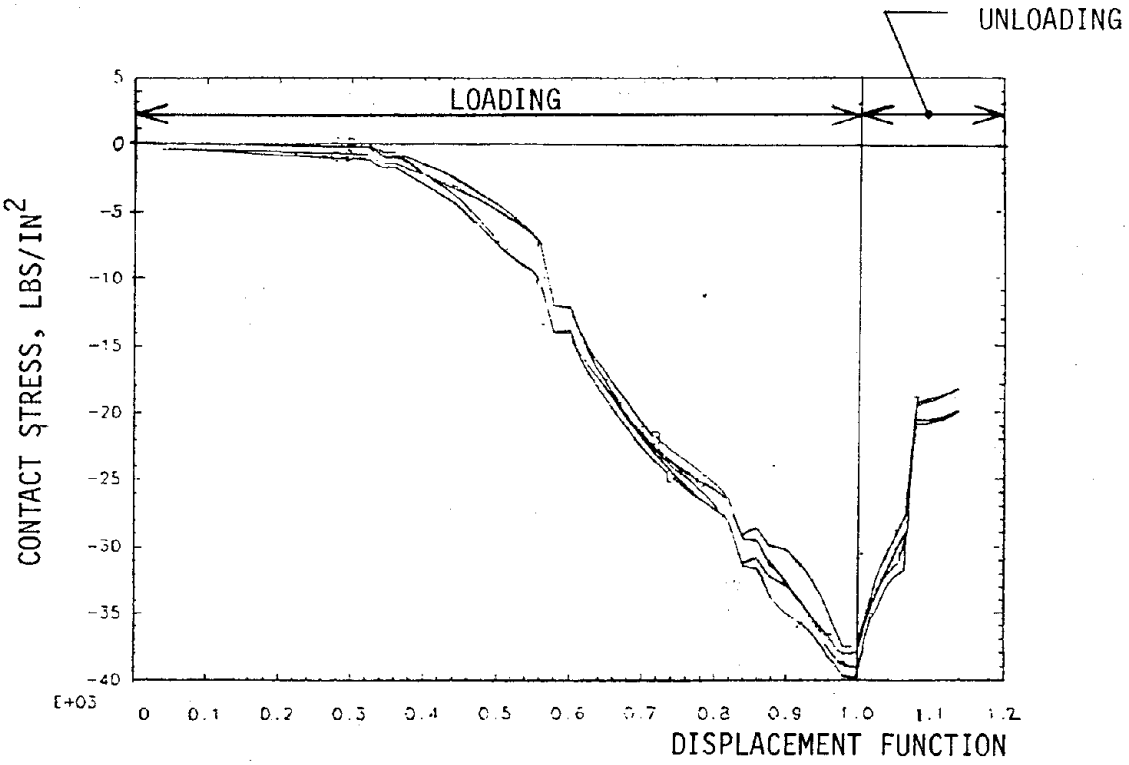

FIGURE 8. MAXIMUM CONTACT STRESS AT DISPLACEMENT FUNCTION = 1.0 OR FULL COMPRESSION OF O-RING (ELEMENT 282 SEE FIG. 5 FOR LOCATION)

APPENDIX B: 321 STAINLESS STEEL O-RINGS

(Note: This appendix reproduces the technical content of a progress report submitted to the NRC dated October 1978)

REPORT ON THE TESTING OF 321 STAINLESS STEEL O-RINGS

OCTOBER 1978

DEVELOP AND IMPROVE STRUCTURAL ANALYSIS

TECHNIQUES FOR CONTAINER COMPONENTS

by

B. J. BENDA

ENGINEERING MECHANICS SECTION OF

THE NUCLEAR TEST ENGINEERING DIVISION

OF

LAWRENCE LIVERMORE LABORATORY

LIVERMORE, CALIFORNIA

Sponsored by

Nuclear Regulatory Commission

Division of Safeguard

Fuel Cycle and Environmental Research

Report on the Testing of 321 Stainless Steel O-rings

Brian J. Benda

October, 1978

Introduction

The work on this project is being done by Lawrence Livermore Laboratory (LLL) under contract with the Nuclear Regulatory Commission (NRC) to develop and improve methods for assessing the performance of container closures. The project includes experimental and analytical studies of five different seal configurations.

Summary

Seven tests were conducted using the 10" nominal diameter, silver coated, 321 stainless steel O-ring. The pressure differential across the seal varied from 14.7 psi to 200 psi. For tests at ambient pressure, leak rates less than 3.5×10^{-10} std. cc/sec were achieved. This low leak rate was maintained for over twenty minutes without change. We concluded that the metal O-rings do not have the high permeation rates demonstrated by the polymer seals and noted in our last progress report. In subsequent tests with the metal O-ring at this pressure level, increasing the bolt force did not affect seal performance.

Tests conducted with an internal pressure of 200 psi verified the need for the design change noted in our previous report. Both the application of the larger bolt force and the introduction of pressure unloaded the seals to the point where the leak rate was too large to be recorded by the detection equipment. The analysis showing the cause of this large leak rate and a description of the design modification that would correct the problem is given later in his report.

Table 1 summarizes all tests of the metallic O-ring completed to date.

Description and Comments

For the most part, the seven tests followed the sequence given by the matrix in Table 2. Only three bolt force levels were considered with a pressure of 14.7 psi, since I felt that the leak rate would not be affected by a still larger clamping force. A brief description of each test is given below.

Test 1 - With no pressure gradient across the seal, a force equal to one-half of the seal manufacturer's recommended clamping load was applied to the flanges. At this load, we could not evacuate the volume between the two O-rings. We concluded that the O-rings had not been seated by this load and an effective seal had not been attained. We therefore went on to the next test step.

Test 2 - A force equal to three-fourths of the manufacturer's recommended clamping load was applied to the flanges. This load was sufficient to seat the seal, and a good vacuum was pulled between the O-rings. Helium at 14.7 psi was introduced to the volume within the primary seal and the mass spectrometer detector was switched on. After twenty minutes of monitoring, no leaks were detected. Since the spectrometer equipment had a sensitivity of 3.5×10^{-10} std. cc/sec, we concluded that the leak rate for the test did not exceed this value.

Test 3 - A force equal to the manufacturer's recommended clamping load was applied to the flanges. After ten minutes of monitoring, no leaks were detected. As in the previous test, we concluded that the leak rate did not exceed 3.5×10^{-10} std. cc/sec. No additional testing was done at this pressure level.

Test 4 - In this test the force applied to the flange equaled one-half the recommended clamping load plus the force required to react the internal pressure. The ability to pull a vacuum between the O-rings indicated that a

good seal had been maintained. However, when we applied an internal pressure equal to 200 psi, the seal unloaded. A leak rate larger than the tolerance of the recording equipment resulted. This was not too surprising. Once the pressure was applied, the contact force on the bearing surfaces was relieved, leaving only half the recommended force on the seal. As seen in test number one, this force will not provide an adequate seal.

Tests 5, 6, 7 - I will jointly comment on these tests which corresponded to applied loads equal to the pressure reaction force plus 75%, 100%, and 110% of the recommended clamping load, respectively. In all three cases, we could not draw an adequate vacuum between the seals prior to applying the internal pressure. When the 200 psi pressure was added to the system, the seals unloaded completely. As the bolt forces were increased in tests 6 and 7, our ability to draw a vacuum between the O-rings decreased. This indicated that the seals actually unloaded as the clamping force was increased. Figure 1 illustrates the test configuration and shows how the seals unloaded. The distance between the bolt circle and the contact bearing surface resulted in a large moment applied to the flanges. This bending moment caused the flanges to rotate into the shape shown schematically in Figure 2. With no bearing surface outside the bolt circle, increased bolt force will increase the bending moment and actually unload the seal. An analysis of this configuration at higher pressure using the finite element code NIKE2D verified that a gap does open between the flanges and the seal (Figure 3).

To correct this problem, a shim that runs circumferentially around the flange must be placed outside the bolt circle. As shown in Figure 4, this shim would limit the bending moment generated by the bolt force and would not allow rotation of the flanges. Increased bolt load would then give the intended result of increasing the bearing pressure between the two flanges.

Conclusions

The low leak rates determined in the tests at ambient pressure for the metallic O-ring (3.5×10^{-10} std. cc/sec) were better than had been anticipated. No significant helium permeation was detected. We were unable to test at higher pressures due to a flaw in the design of the flanges which caused unloading of the seals at increased bolt force. Our analysis showed the effect of this flaw by predicting a leak path between seal and flange. We feel that a flat, circular shim would solve this problem and allow us to continue with the test matrix.

Test Number	Total Clamping Force (lbs.)	Pressure (psi)	% Specified Force	Leak Rate (std cc/sec)
1	13,370	14.7	49	large
2	20,586	14.7	76	3.5×10^{-10}
3	39,016	14.7	107	3.5×10^{-10}
4	30,894	200	53	large
5	37,379	200	77	large
6	44,175	200	107	large
7	47,630	200	115	large

Table 1. Test completed for metallic O-rings

Table 2 Test matrix for seal leak rate tests.

Test number	Seal Load (F=specification force)				Internal pressure (psi)						Temperature (°F)						Seal diam (in)	
	0.5F	0.75F	1.0F	1.1F	14.7	200	400	600	800	1000	-40	70	100	240	400	540	10.0	20.0
1	X				X							X					X	X
2		X			X							X					X	X
3			X		X							X					X	X
4				X	X							X					X	X
5	X					X						X					X	X
6		X				X						X					X	X
7			X			X						X					X	X
8				X		X						X					X	X
9	X						X					X					X	X
10		X					X					X					X	X
11			X				X					X					X	X
12				X			X					X					X	X
13	X							X				X					X	X
14		X						X				X					X	X
15			X					X				X					X	X
16				X				X				X					X	X
17	X								X			X					X	X
18		X							X			X					X	X
19			X						X			X					X	X
20				X					X			X					X	X
21	X									X		X					X	X
22		X								X		X					X	X
23			X							X		X					X	X
24				X						X		X					X	X
25			X		X						X						X	X
26			X		X								X				X	X
27			X		X									X			X	X
28			X		X										X		X	X
29			X		X											X	X	X

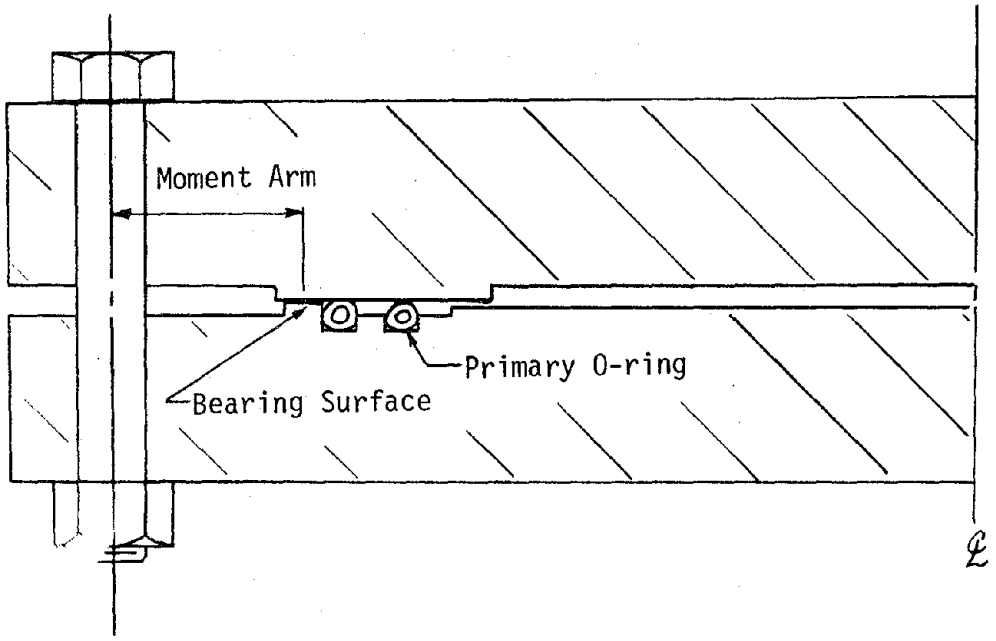

Figure 1. Bearing Surface Between Seals and Bolt Circle Causes Bending Moment in Flange

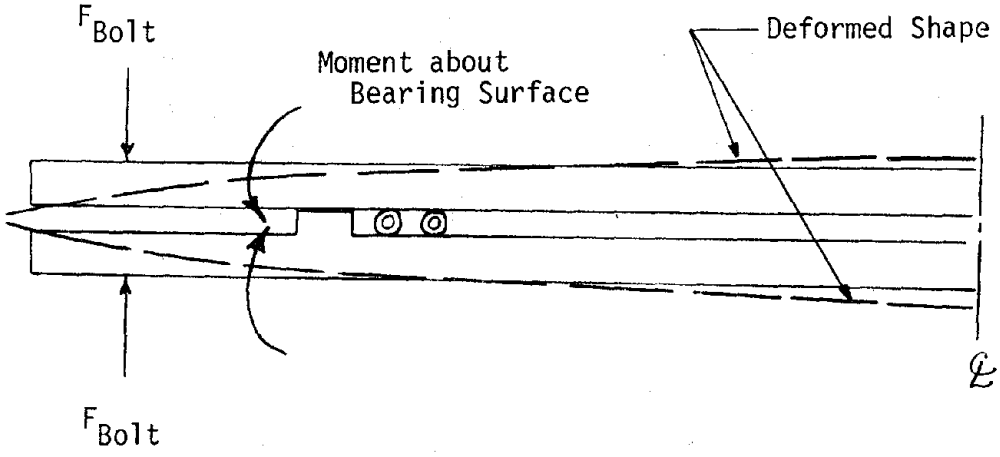

Figure 2. Bending of Plate Unloads Seals

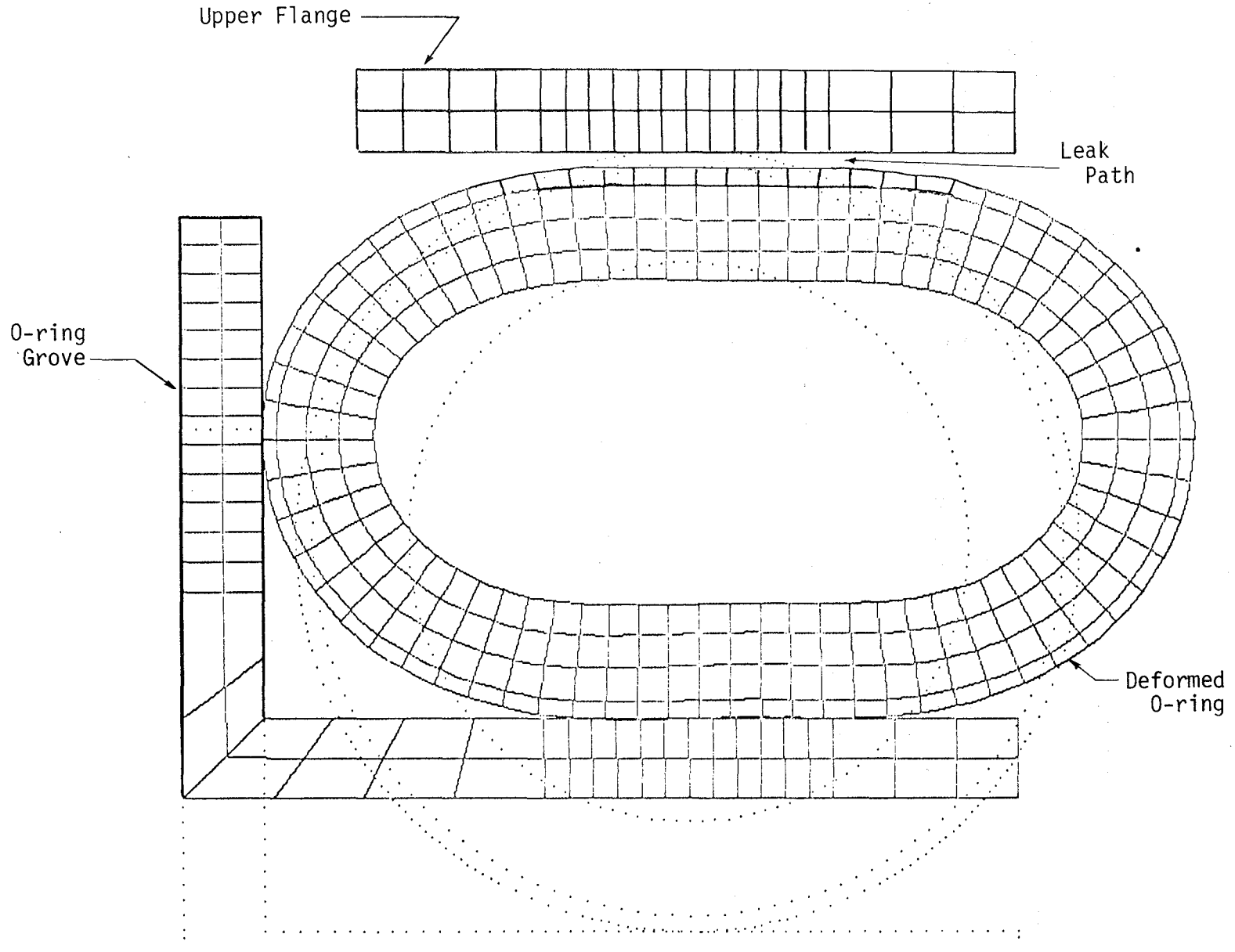

Figure 3. NIKE2D Analysis Showing Leak Path Between Flange and Seal

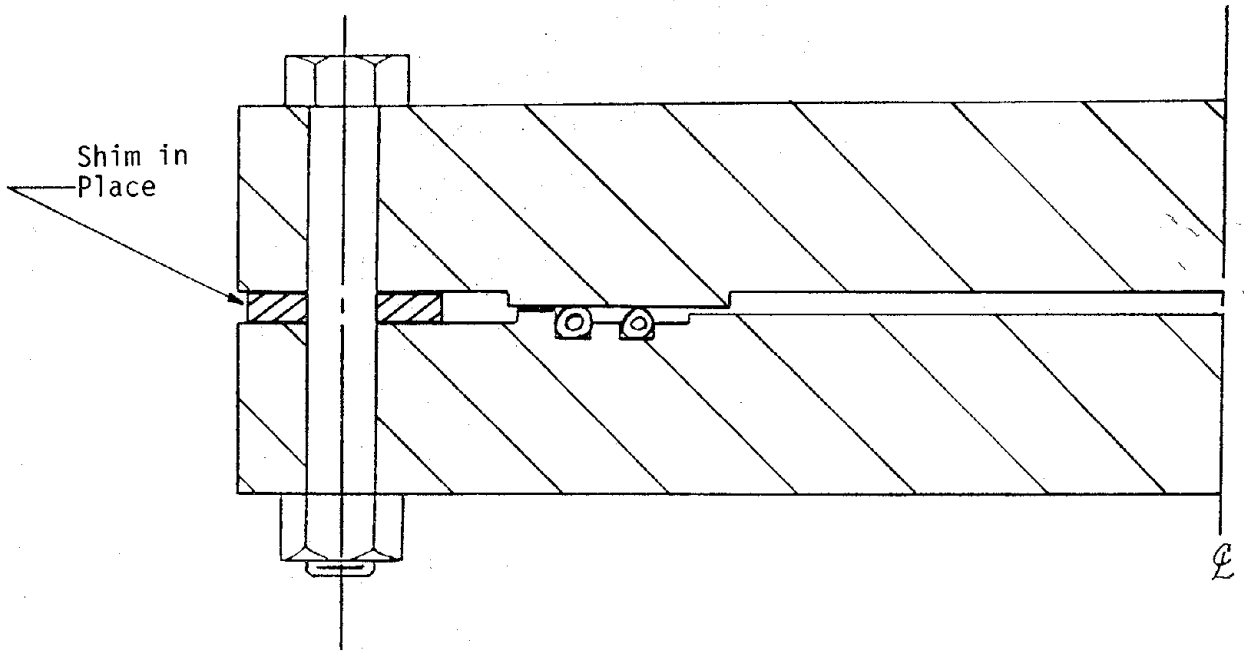

Figure 4. Shim Prevents Rotation of Flanges and Unloading of Seals

APPENDIX C: INCONEL X-750 O-RINGS

(Note: This appendix reproduces the technical content of an informal report titled "Final Report on the Testing and Analysis of Inconel X-750 O-rings" that was previously submitted to the NRC)

Final Report on the Testing and Analysis of Inconel X-750 O-rings

by

Brian J. Benda

Richard A. Larder

Engineering Mechanics Section of

The Nuclear Test Engineering Division

of

Lawrence Livermore Laboratory

Livermore, California

Sponsored by

Nuclear Regulatory Commission

Division of Safeguard

Fuel Cycle and Environmental Research

Introduction

This report documents the testing and analyses of silver-coated Inconel X-750 0-rings. The work on this project was done by Lawrence Livermore Laboratory (LLL) under contract with the Nuclear Regulatory Commission (NRC) to develop and improve methods for assessing the leak tightness of general seal designs that may be used for closure of nuclear waste shipping casks. The combined experimental/analytical program was conducted to develop design curves relating the leak rate of the Inconel X 0-rings to such parameters as contact pressure between seal and flange, contact area of the seal, pressure differential across the seal, applied bolt force, temperature, and seal circumference. These design curves would subsequently allow for an analytical determination of seal leak rates. A detailed description of the program can be found in quarterly reports that have previously been issued.

Conclusions

Both testing and analysis found the leak tightness of the Inconel-X 0-rings to be extremely sensitive to the displacement of the compression

flange. Analyses showed that a thirty mil compression of the O-ring was required to develop the manufacturer's recommended clamping force between the seal and flange. However, due to plastic deformation in the seal and its lack of adequate springback, a two mil unloading of the flange would decrease the contact force in the seal by fifty per cent (Figure 1). Insufficient contact pressure between the O-ring and flange would result, and seal integrity would be lost. These results suggest that great care be taken in the design and use of O-ring closures to ensure that the seals do not unload under any environmental conditions.

The sensitivity of the O-rings to unloading limited the amount of data obtained during testing. We found that the Inconel X O-rings gave either very small or very large leak rates under most test conditions. Little data was obtained between these two extremes. This was especially true when testing the effect of pressure on O-ring performance. As pressure was applied to the test assembly, the flanges would bend under the load. In most cases, although the magnitude of this bending was small, it was sufficient to unload the O-ring and compromise the seal. Although the large plastic deformation and lack of springback in the O-rings was primarily responsible for this problem, the design of the test flanges did aggravate the leak tightness of the seal. The two inch difference between the O-ring radius and the bolt circle radius allowed for a greater displacement of the flanges near the seals themselves. Had the O-rings been placed adjacent to the bolt circle, the unloading effect of the pressure would have been lessened. These results indicate that placement of the seals near the location of applied clamping force be a primary design consideration.

Although limited test data were obtained, results did show an inverse relationship between leak rate and contact force. This correlation was especially shown in those test cases where no internal pressre was applied. The plastic deformation of the seal caused the relationship between leak rate and average contact pressure and contact area to be less apparent. Once the seal was fully compressed and seated in the groove, however, an inverse relationship was seen.

Experimental Program

The purpose of the experimental program was to obtain leak rate data for the Inconel X O-rings as a function of applied bolt force, internal pressure, temperature, and seal circumference. A general test matrix had been developed and is given in Table II. This matrix was also shown in earlier reports.

Previous work with 321 stainless O-rings indicated that closure could not be maintained and a leak rate which saturated detection equipment resulted when a clamping force equal to fifty per cent of the manufacturer's recommended force is applied to the flange [1]. To ensure an adequate number of data points, the test matrix was modified by adding a seal load value equal to 125% of the recommended clamping force at each pressure level.

Test Hardware

The primary hardware used to test the Inconel X O-rings consisted of a pair of bolted, circular flanges. The specific details of the flange design were all within seal manufacturer's tolerances. These details included the inner diameter, width and depth of the O-ring groove, and the machine finish of the flange contact surface. A part drawing illustrating the flange design

is given in Figure 2. Several significant features are labeled on this drawing. They include the primary and secondary O-ring grooves, the pressure inlet port, the leak sensing port, lower contact surface, and bolt circle diameter. When assembled, the flanges mate in a back-to-front configuration as shown in Figure 3.

Each assembly requires two metallic O-rings. The smaller, inner seal is the primary seal whose leak tightness is being evaluated. The larger, outer seal provides the boundary for a small volume between the two O-rings. This volume is connected to the mass spectrommeter detection equipment via the sensing port. The mass spectrometer accurately detects the presence of the trace gas, helium, and converts the helium data into a flow or leak rate for the primary O-ring. The detection equipment can sense leaks as small as 2.8×10^{-10} std cc/sec.

Pressure is applied to the volume within the primary seal via the pressure port. A pressure fitting welded to the port outlet connects the flange assembly to the pressure source. The pressure level is controlled by the appropriate use of regulators and valves.

The magnitude of the bolt force applied to the assembly is measured by load collars fabricated at LLL. These collars are not shown in the assembly drawing of Figure 2. In order to limit expense, only four of the eighteen bolts used to secure the flanges were equipped with instrumented load collars. To provide a uniform clamping load, the value of torque which gave the desired force in the instrumented bolts was applied to all other bolts for each test step.

A list of all hardware associated with each seal/flange assembly is given in Table III. Figure 4 shows a schematic diagram of the test assembly.

Test Procedure

Prior to assembly, the 0-ring grooves and contact surfaces on each flange were thoroughly cleaned with alcohol. The 0-rings wer visually inspected and placed in the flange without lubricant or other treatment. Although the groove dimensions met design tolerances, placement of the 0-rings required some effort as all seals fit very snug against the outer diameter of the grooves. The upper flange was then lowered over the bolts and onto the seals. The pressure and leak detection lines were connected and the assembly was ready for testing.

The experimental procedure was the same for each test point and consisted of the following steps:

1. Apply and record the appropriate bolt force;
2. Evacuate the volume between the 0-rings and bring the leak detection equipment on line;
3. Apply the appropriate pressure to the flange assembly;
4. Record seal leak rate, internal pressure, and bolt force;
5. Release pressure by venting the flange assembly.

All data were recorded in a test log book. In addition, the bolt loads as given by the load collars were recorded on both paper and magnetic tape. The pressure was recorded on a strip chart.

Test Results

A total of thirteen tests were performed using two sets of ten inch diameter, Inconel X 0-rings. The pressure differential across the primary seal varied from 14.7 psi to 400 psi. All tests were conducted at ambient temperature. All support hardware operated properly.

Nine tests were performed on the first pair of 0-rings. These tests generally followed the sequence outlined in the modified test matrix. Table

IV lists the actual bolt force recorded from the four instrumented load collars for each test. Also given are the average applied bolt force, the desired calculated force, and the error between actual and calculated loads. Table V shows the leak rates that were obtained for each of the nine tests. The experiments were stopped after the seal leak rate remained constant over a wide range of applied bolt forces and internal pressures. Work by Roth [2] suggested that the leak rate would be proportional to the pressure loading and inversely proportional to the applied clamping force. To determine whether the test data were being affected by faulty hardware, the flanges were disassembled and visually inspected with a magnifying glass for possible damage to the contact surface. There were no apparent flaws on either O-ring grooves or upper contact surface. The O-rings were set aside for inspection.

The flanges were cleaned as before and a second pair of O-rings was installed. Test results with the first set of Inconel O-rings indicated that the leak rate remained constant for all tests with pressures equal to or greater than 200 psi. To obtain additional data, four tests were attempted with internal pressure varying between 14.7 psi and 200 psi. However, a sufficient vacuum could not be maintained at any level of bolt force. Consequently, no tests could be run with the second set of seals. The flanges were again disassembled and inspected. No anomalies were found. The O-rings were removed for inspection. Further testing was discontinued until an explanation of these data could be made through inspection of the seals or analysis of the flange assemblies.

Inspection of the two pairs of O-rings revealed major flaws on or near the contact surface. Although it is impossible to determine their exact impact on the experimental data, such flaws tend to compromise the leak tightness of the

seal. Figure 5 is a magnified view showing a section of the smaller seal from the first pair tested. A hole penetrating the seal wall is seen on the border between the portion of the O-ring surface that made contact with the flange (darkened area) and the portion that did not (light area). Although many of the scratches shown in the silver coating resulted from handling after the tests had been performed, we feel the hole itself was a manufacturing flaw. This hole would reduce the local contact area of the seal and potentially increase the leak rate. Figure 6 shows a pair of cracks running circumferentially in the larger O-ring used during the first set of tests. The cracks are still evident after the silver coating had been removed (Figure 7). This indicates that the Inconel was deformed beyond its ultimate capacity. Such failure would reduce the local contact pressure between seal and flange and tend to increase the leak rate. Although no holes or cracks were found in the second set of O-rings tested, lesser flaws seen in the contact surface could easily provide a leak path (Figure 8).

Analytical Program

The analytical program was designed to accurately model the experimental procedure. The purpose of the program was to determine the contact pressure and contact area for the O-ring under conditions which corresponded to the actual levels of bolt force and internal pressure used during the test sequence. These analytical results would then be combined with measured leak rate data to develop the performance curves for the Inconel X O-rings.

The finite element program, NIKE2D, was chosen for the analysis. NIKE2D is a two dimensional, implicit, static and dynamic, nonlinear code developed by John Hallquist at LLL [3]. The code contains an elastic-plastic material

model with both kinematic and isotropic hardening. Kinematic relationships include large displacement, large rotation, and large strain effects. A slide line algorithm allows the code to accurately model the expanding contact area as the 0-ring is compressed by the flange.

The procedure used for the 0-ring analysis employed a substructuring technique conducted in three phases. First, a detailed model of the 0-ring was developed (Figure 9). The seal was first compressed to the maximum displacement dictated by 0-ring groove geometry and then unloaded. The reaction force was determined and used to develop a force deflection curve for the 0-ring. This curve, which was shown earlier as Figure 1, gave the effective stiffness of the seal.

A model of the seal-flange assembly was then developed (Figure 10). Material properties of 321 stainless steel were input for the flange elements, while the behavior of elements modeling the 0-rings was given by the load-deflection curve described above. Bolt force and pressure loadings recorded from the experiment were simultaneously input to the model. Figures 11 and 12 show this load history input. The conditions corresponding to the nine experimental data points obtained with the first set of Inconel 0-rings are numbered on the load history.

The results of the flange assembly analysis are given by the deflection history curves for the 0-ring shown in Figure 13. Figure 14 shows the 0-ring displacement on an expanded vertical scale after the internal pressure was added. The effects of increased bolt force and internal pressure is evident in the fluctuations in 0-ring compression. The deflections corresponding to each test state are numbered as before.

Figure 15 shows the deformed flange model under loads corresponding to point 4 in the load history curve. As can be seen from the stress contour lines, the upper and lower flanges make contact at their outer perimeter before the seal is completely compressed. Consequently, not all of the force applied by the bolts was reacted at the seals. This suggests that loads developed in the seal during testing were less than the applied bolt force would have dictated.

The displacements of flange nodes near the seal obtained from the assembly analysis were input to the detailed 0-ring model. This was the same model used to develop the load-deflection curve for the seal. At displacements corresponding to the nine experimental test points, contact area and contact pressure were determined. These data are shown in Figures 16 through 24. The regions of expanding contact between the 0-ring and flange are clearly seen.

As the deformation of the seal increases during the analysis, the curvature of the model 0-ring surface reverses and the region of initial contact completely unloads. The accuracy of this shape was verified by comparison with the actual deformed shape of the 0-rings tested.

Figure 25 shows regions of effective plastic strain for the fully compressed 0-ring. Contour lines of constant strain indicate areas with as much as thirty per cent plastic strain. These large strain values exceed the ultimate strain capacity for Inconel and give further support to the possibility of local 0-ring failure.

Correlation between Experiment and Analysis

Although limited test data was obtained, results did show an inverse relationship between leak rate and contact force (Figure 26). This correlation

was shown in those test cases where no internal pressure was applied. Other data on the same plot demonstrate how pressure reduced the contact force and resulted in a significant increase in leak rate. The pressure effects are further demonstrated by Figure 27. This graph shows the total compressive interface force between seal and flange throughout the analysis history. It is seen that as pressure is applied, the contact force drops significantly below the recommended clamping load. When the pressure is released, the contact force increases, and a positive seal is again attained.

The relationship between seal leak rate and either contact pressure or contact area is not apparent. In test number 1, a small contact force acting over a very small contact area resulted in a large pressure between the seal and flange. However, the total force applied to the seal was much less than the recommended clamping force. The result was a large leak rate. As additional load was applied, the O-ring deformed plasticity. The contact area significantly increased while the contact pressure decreased. At those test points which gave low leak rates, the corresponding contact pressure was actually less than that given by the first test (Figure 28). Once the O-ring had been seated in the groove, an inverse relation between leak rate and contact pressure was seen.

No correlation between leak rate and contact area can be made. Once the seal is deformed, the contact area remains relatively constant despite any change in contact pressure. Only when the compression flange lifts off of the seal does the contact area significantly change. The data plotted in Figure 29 show that a large range of leak rates were obtained for a small variation in contact area.

Closure

The results of both analysis and testing were combined by this program in an attempt to establish basic design relationships for the leak tightness of Inconel X O-rings. The particular behavior of the seals themselves and the design of the test flanges limited the amount of experimental data obtained. For those tests which produced leak rate information, corresponding finite element analysis provided contact area and contact pressure data. These analytical data were consistent with experimental results and helped to explain our inability to obtain additional leak rate information at other test conditions.

Although evidence of an inverse relationship between leak rate and contact force, pressure, and area was seen, insufficient data made the correlation very weak. Additional testing with other seal and flange hardware already on hand will be required before reliable design curves can be developed.

References

1 Benda, B. J., "Report on the Testing of 321 Stainless Steel O-rings," submitted to NRC in October, 1978.

2 Roth, A., Vacuum Technology, North-Holland Publishing Company, 1976, p. 384-409.

3 Hallquist, J. O., "NIKE2D - An Implicit, Finite Deformation, Finite Element Code for Analyzing the Static and Dynamic Response of 2-D Solids," (to be released as an LLL publication).

Table II Test matrix for seal leak rate tests.

Test number	Seal Load (F=specification force) 0.5F	0.75F	1.0F	1.1F	Internal pressure (psi) 14.7	200	400	600	800	1000	Temperature (°F) -40	70	100	240	400	540	Seal diam (in) 10.0	20.0
1	X				X							X					X	X
2		X			X							X					X	X
3			X		X							X					X	X
4				X	X							X					X	X
5	X					X						X					X	X
6		X				X						X					X	X
7			X			X						X					X	X
8				X		X						X					X	X
9	X						X					X					X	X
10		X					X					X					X	X
11			X				X					X					X	X
12				X			X					X					X	X
13	X							X				X					X	X
14		X						X				X					X	X
15			X					X				X					X	X
16				X				X				X					X	X
17	X								X			X					X	X
18		X							X			X					X	X
19			X						X			X					X	X
20				X					X			X					X	X
21	X									X		X					X	X
22		X								X		X					X	X
23			X							X		X					X	X
24				X						X		X					X	X
25			X		X						X						X	X
26			X		X								X				X	X
27			X		X									X			X	X
28			X		X										X		X	X
29			X		X											X	X	X

Table III. Hardware for Testing 10" Diameter O-ring

Item Description	Quantity
Test Flanges - Circular, stainless steel LLL drawing AAA-119481-00	2
Primary O-rings - silver coated, Inconel X-750 UAP Components U6312-10250SEB	3
Secondary O-rings - silver coated, Inconel X-750 UAP Components U6312-10750 SEB	3
ıts - UNF 1 - 12 stainless steel with nuts	18
Washers - 1 inch, stainless steel	36
Instrumented load collars	4
Dummy load collars	14
Mass Spectrometer Leak Detection Equipment - Du Pont model 24-120B	1

Table IV. Bolt Force Data

Test Number	Desired Force/Bolt (lbs)	Measure Force in Instrumented Bolts (lbs) 1	2	3	4	Average	Error (%)
1	1058	1009	958	1137	1080	1046	-1.1
2	1587	1513	1723	1559	1656	1613	+1.6
3	2116	2089	2413	2202	2183	2222	+5.0
4	2328	2461	2482	2178	2338	2367	+1.7
5	2504	2445	2657	2405	2524	2507	+0.1
6	3303	3063	2911	3012	2981	2992	-1.4
7	3244	3253	3164	3095	3213	3180	-2.0
8	3562	3569	3606	3564	3518	3564	0.1
9	3950	3937	3864	3865	3912	3894	-1.4

Table V. Leak Rate Data

Test Number	Seal Load F=recommended clamping force	Internal Pressure (psi)	Leak Rate (std cc/sec)
1	0.50 F	14.7	---
2	0.75 F	14.7	$4.2 \cdot 10^{-6}$
3	1.00 F	14.7	$2.8 \cdot 10^{-10}$
4	1.10 F	14.7	$2.8 \cdot 10^{-10}$
5	0.75 F	200.	$3.6 \cdot 10^{-2}$
6	1.00 F	200.	$3.6 \cdot 10^{-2}$
7	1.10 F	200.	$3.6 \cdot 10^{-2}$
8	1.25 F	200.	$3.6 \cdot 10^{-2}$
9	1.00 F	400.	$3.6 \cdot 10^{-2}$

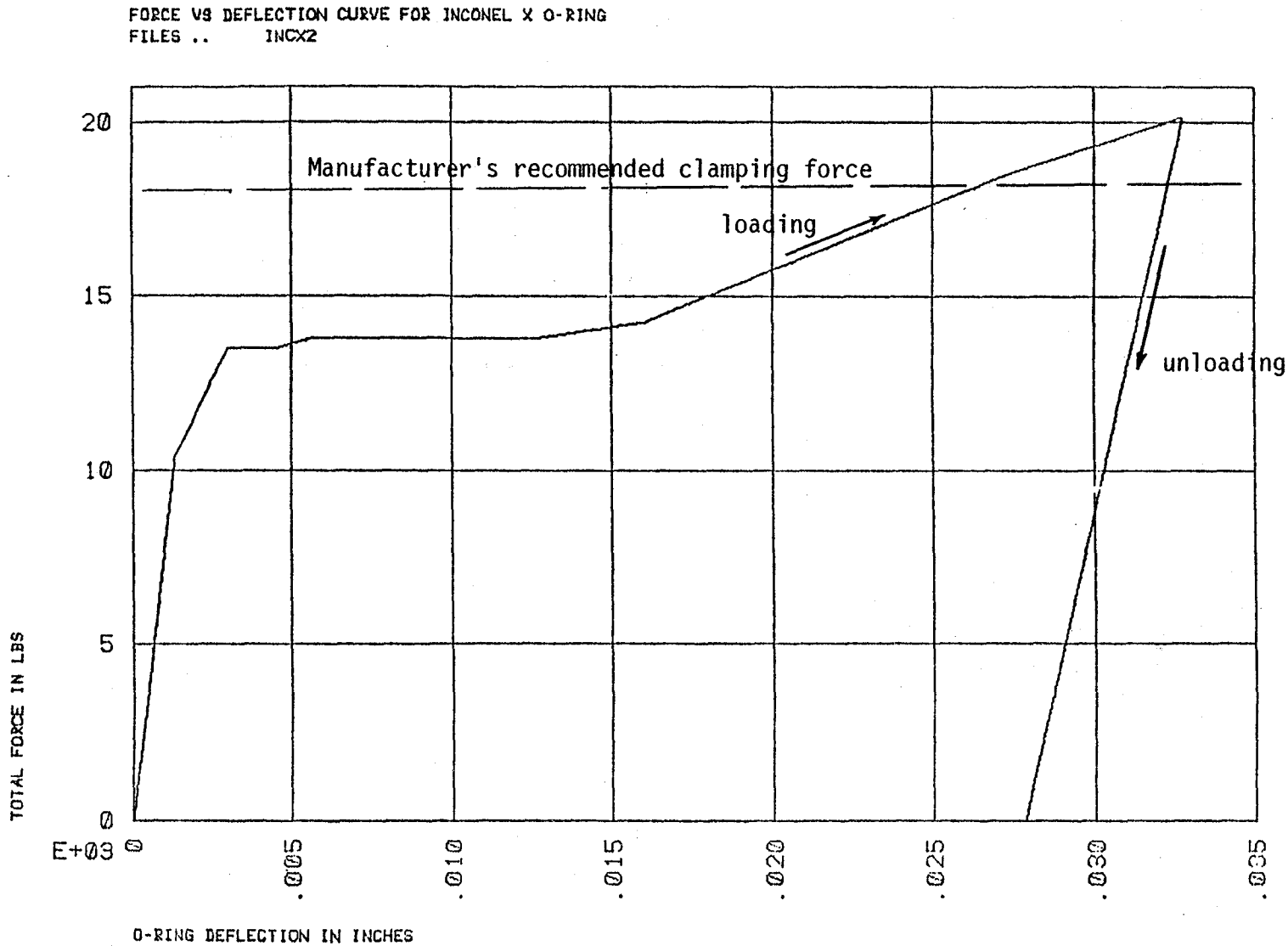

Figure 1. O-ring load deflection curve shows sensitivity to unloading

TAB No.	D ø	E ø	F ø	G ø	J	K	M	N	P	P ø	S	T	U	V	W	X ø	Y ø	Z	CALC WT.
-01	17.76±.03	11.785±.030	10.755 +.004 -.000	10.255 +.004 -.000	4.750	15.184	.065 +.004 -.000	.135 +.002 -.005	1.470 +.000 -.060	1.06±.03	18	15.760	10°	20°	4.25 +.03 -.00	8.50±.03	13.00±.03	3.73 +.03 -.00	99 LBS.
-02	19.65±.03	12.345±.030	11.007 +.005 -.000	10.507 +.005 -.000	9.500	10.293	.090 +.000 -.000	.170 +.002 -.005	2.970 +.000 -.160	1.56±.03	24	28.650	7.5°	15°	4.50 +.03 -.00	18.00±.03	23.50±.03	5.70 +.03 -.00	167 LBS

3. POSITIONAL TOLERANCES APPLY AT MMC UNLESS SPECIFIED.
STAMP PART OF APPROVAL WHERE SHOWN.
PROTECT PART SURFACE FROM DAMAGE

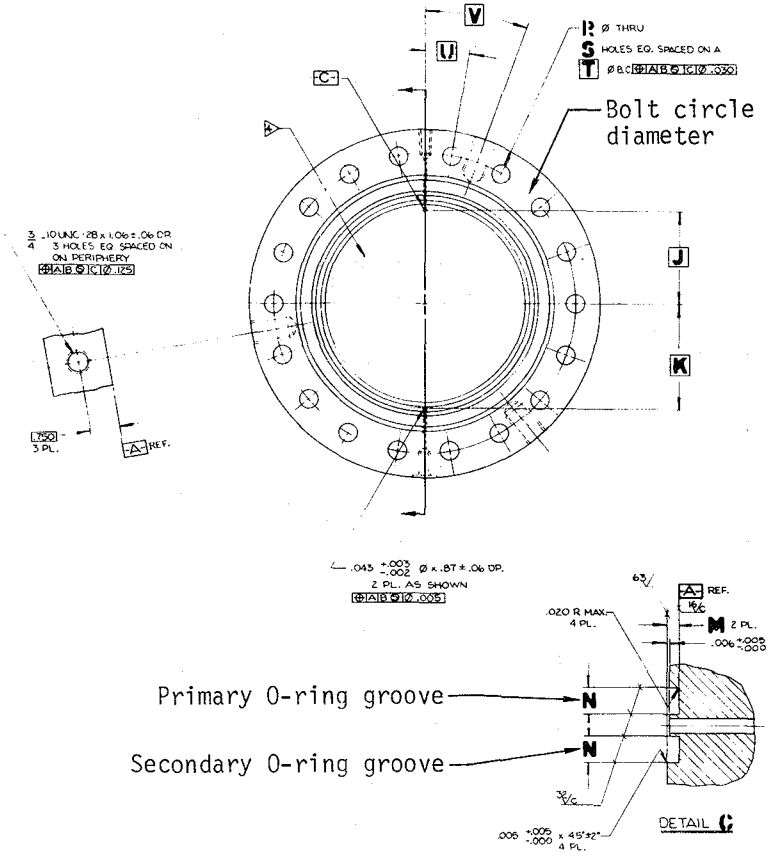

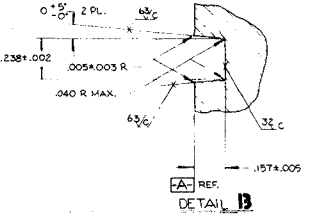

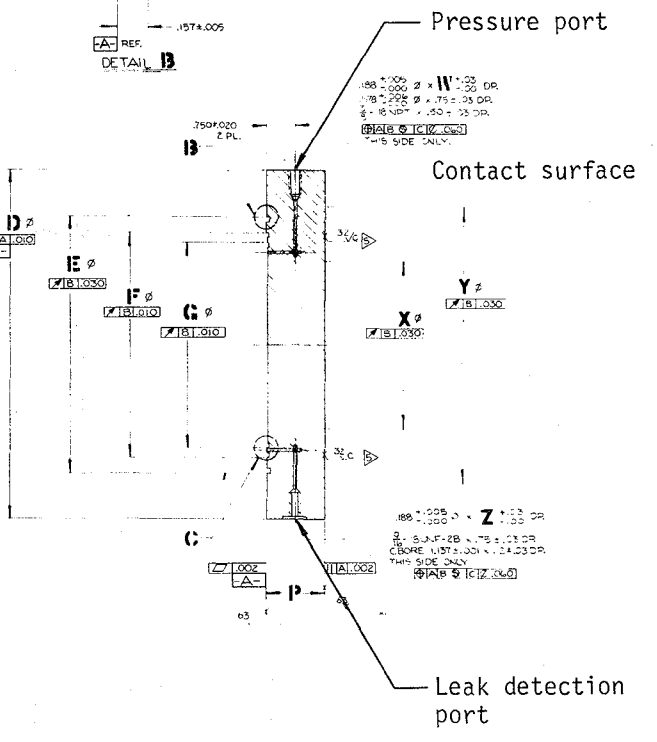

Figure 2. Part drawing showing flange design

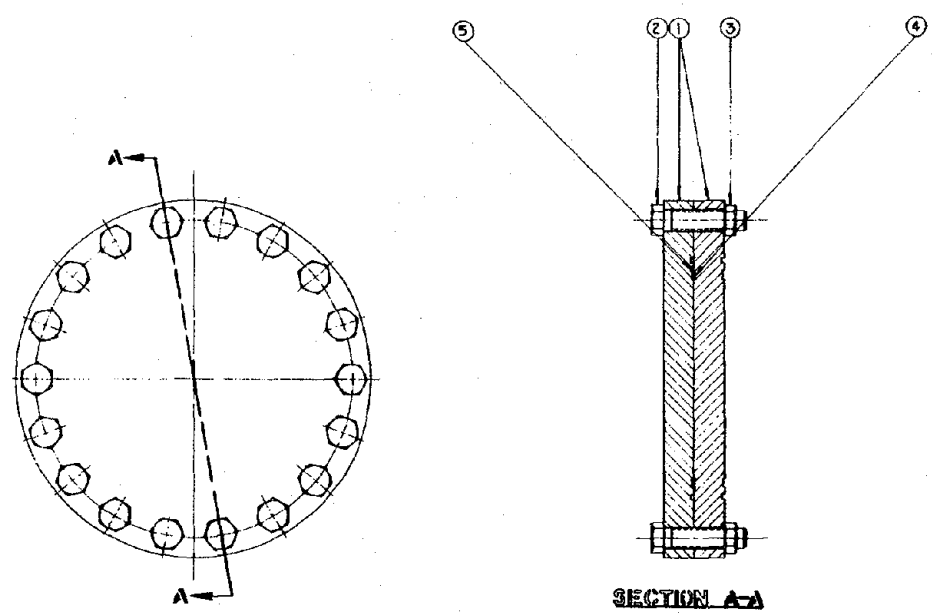

Figure 3. Flange test assembly drawing

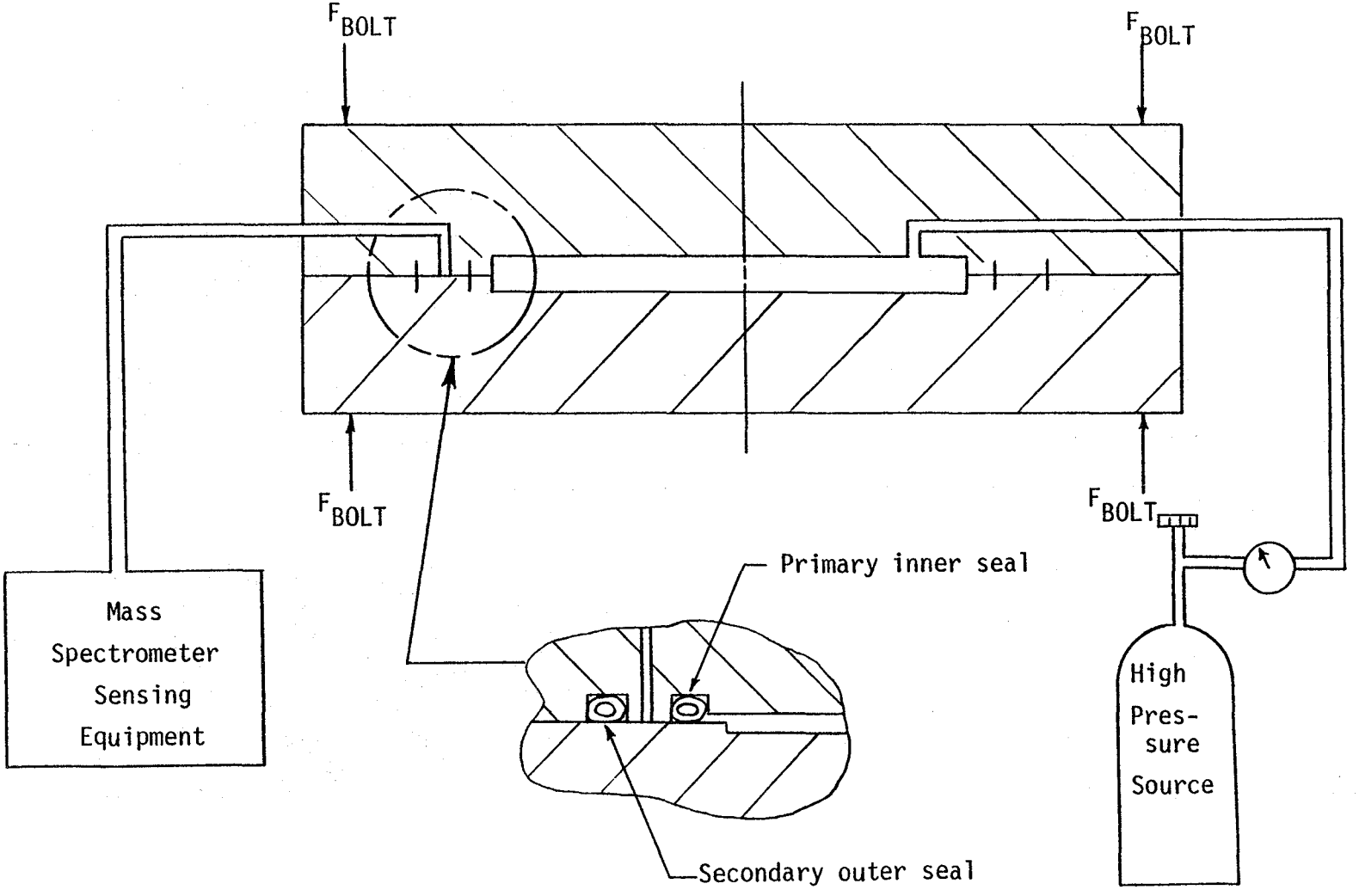

Figure 4. Schematic diagram of test setup

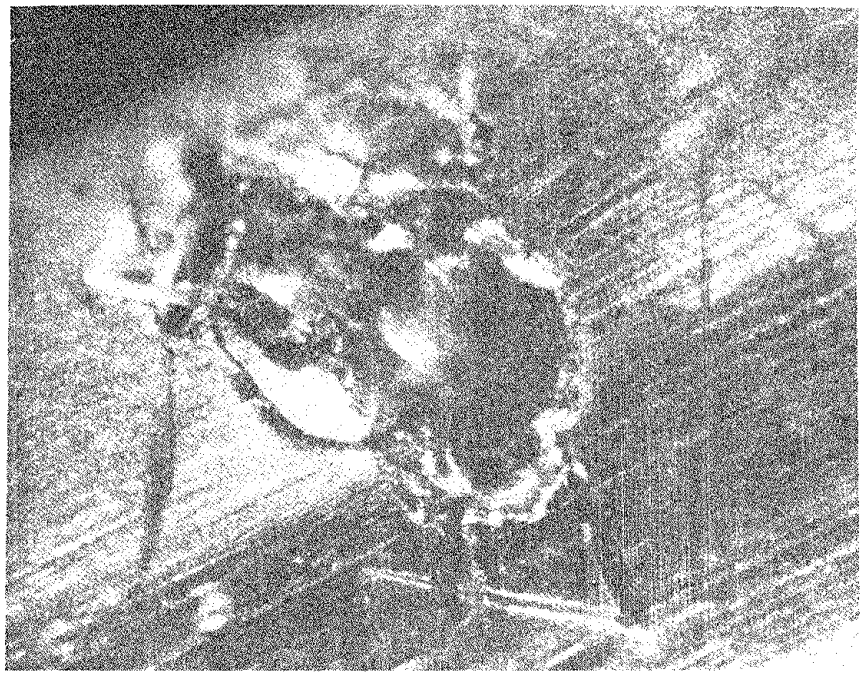

Figure 5. Hole on contact surface reduces seal area

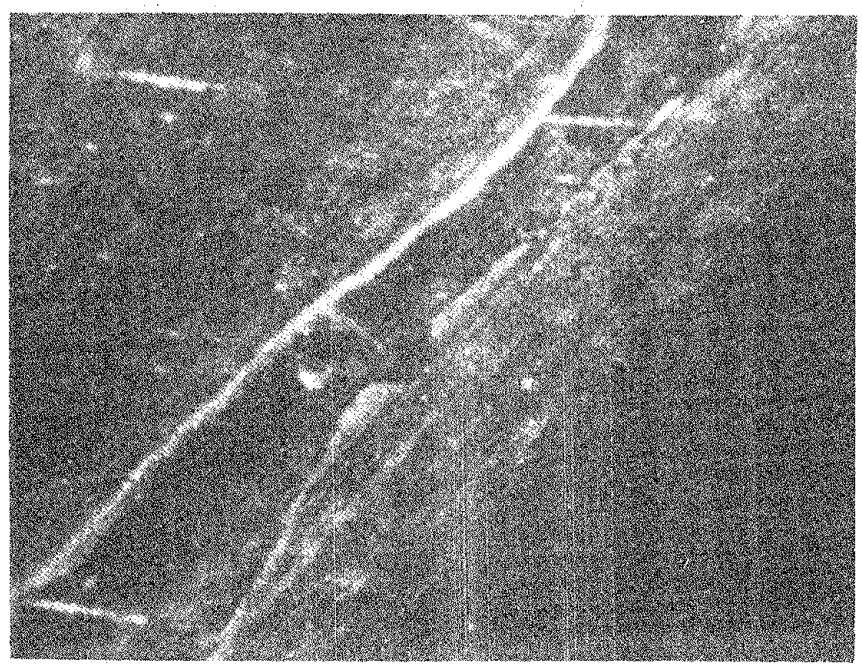

Figure 6. Apparent cracks would reduce contact pressure

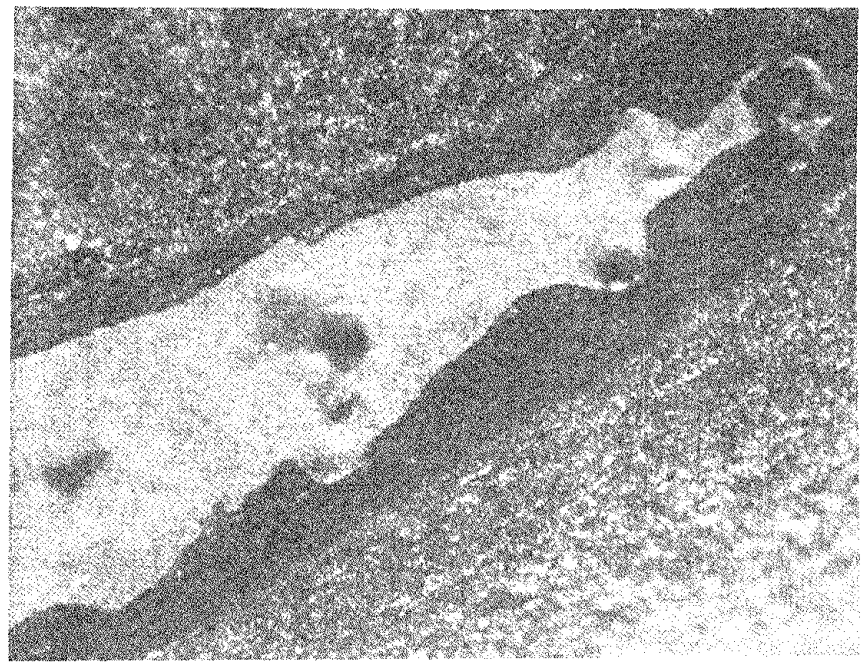

Figure 7. Cracks in Inconel indicate ultimate strain exceeded

Figure 8. Flaw in contact surface could provide a leak path

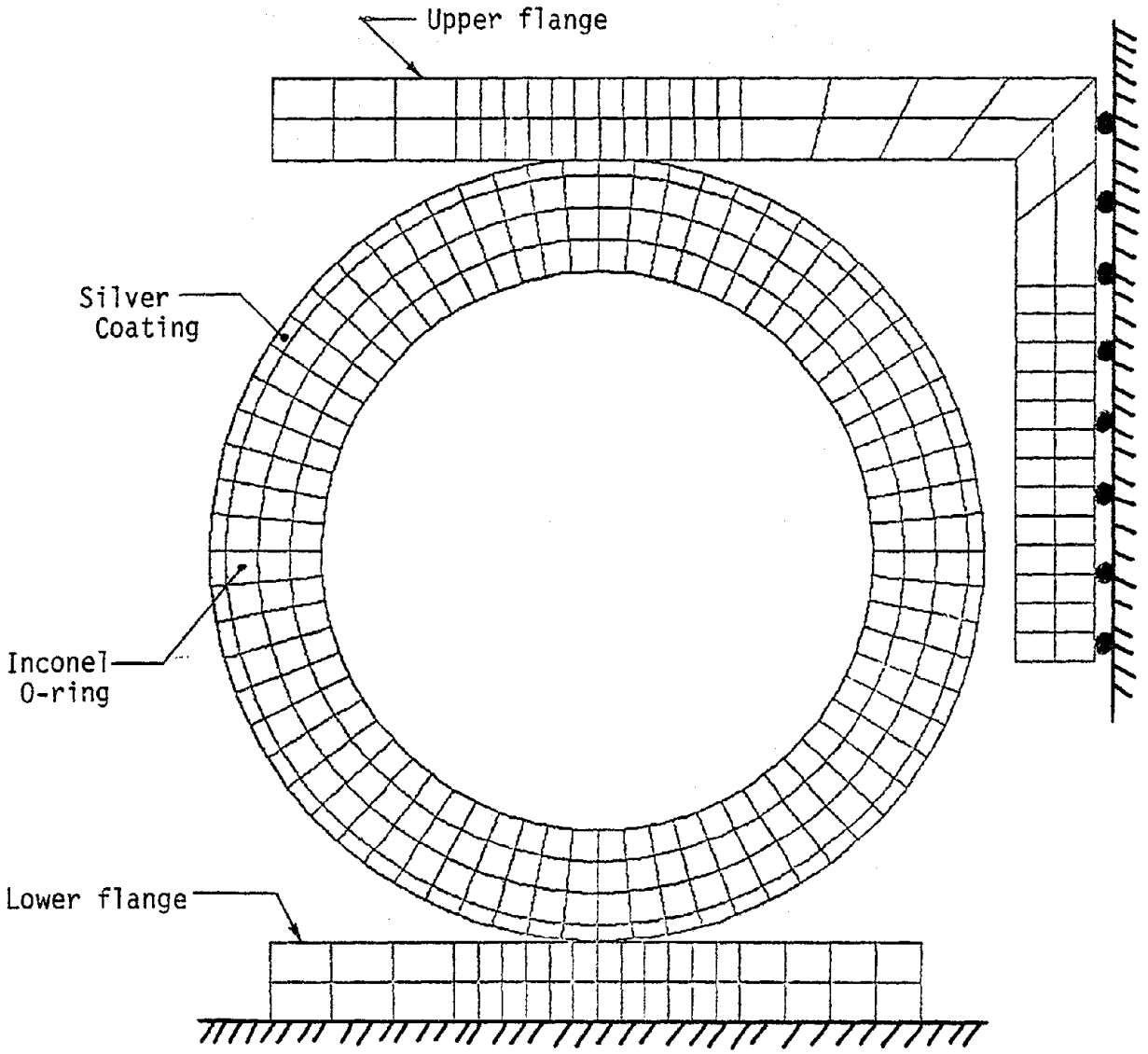

Figure 9. Detailed O-ring model used to develop load deflection curve

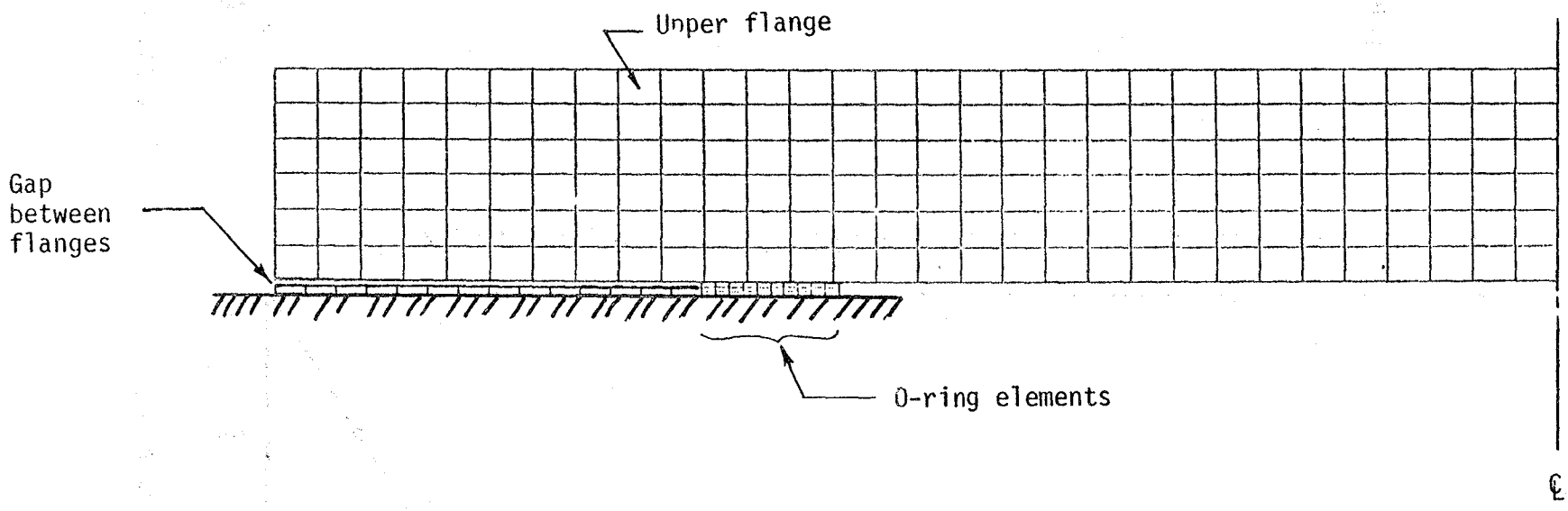

Figure 10. Flange assembly model used to develop seal deflection curve

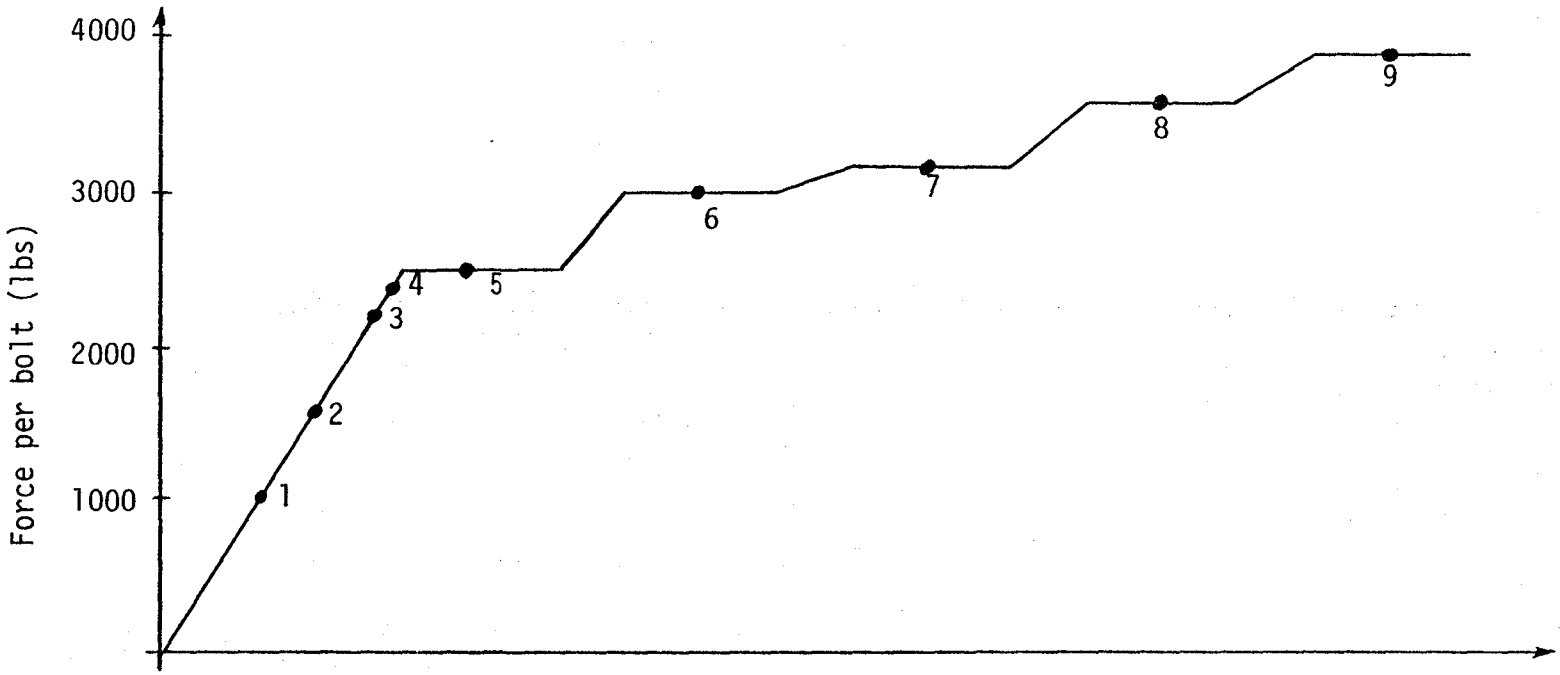

Figure 11. Bolt force load history corresponding to test sequence

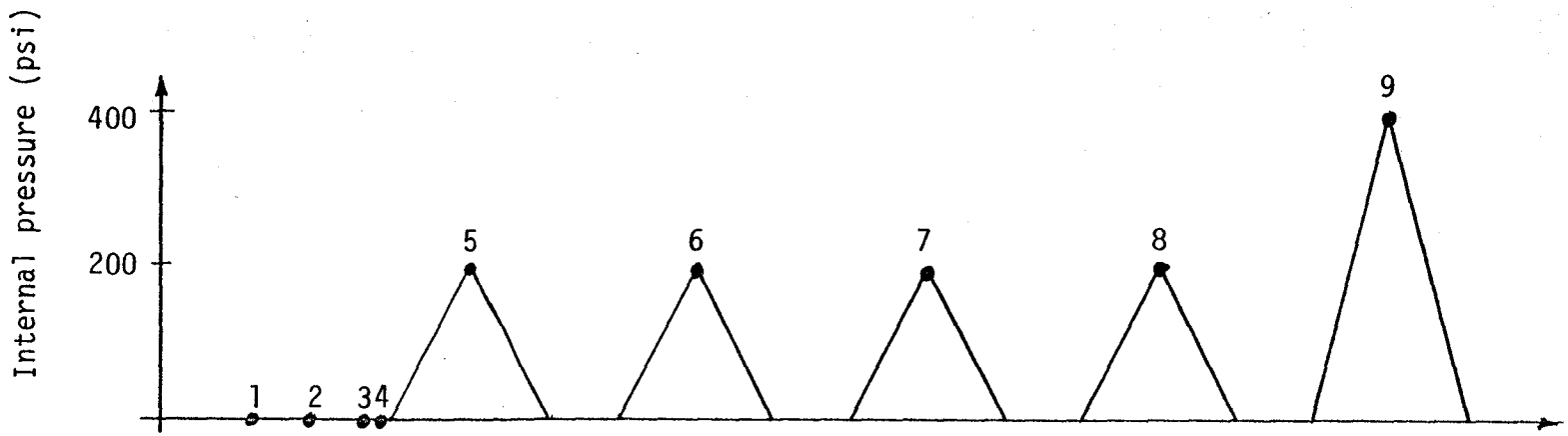

Figure 12. Pressure load history corresponding to test sequence

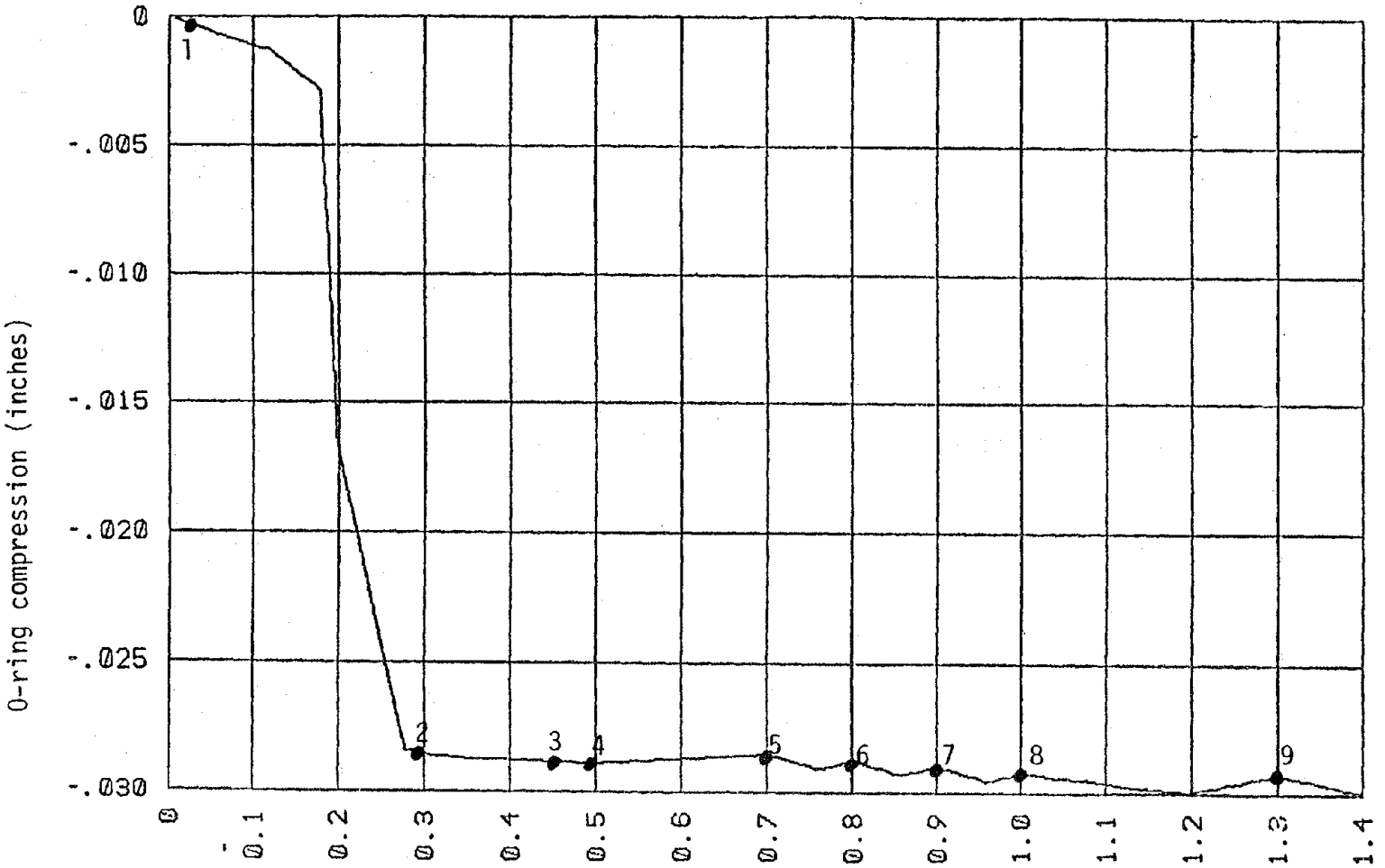

Figure 13. O-ring deflection history input to detailed model

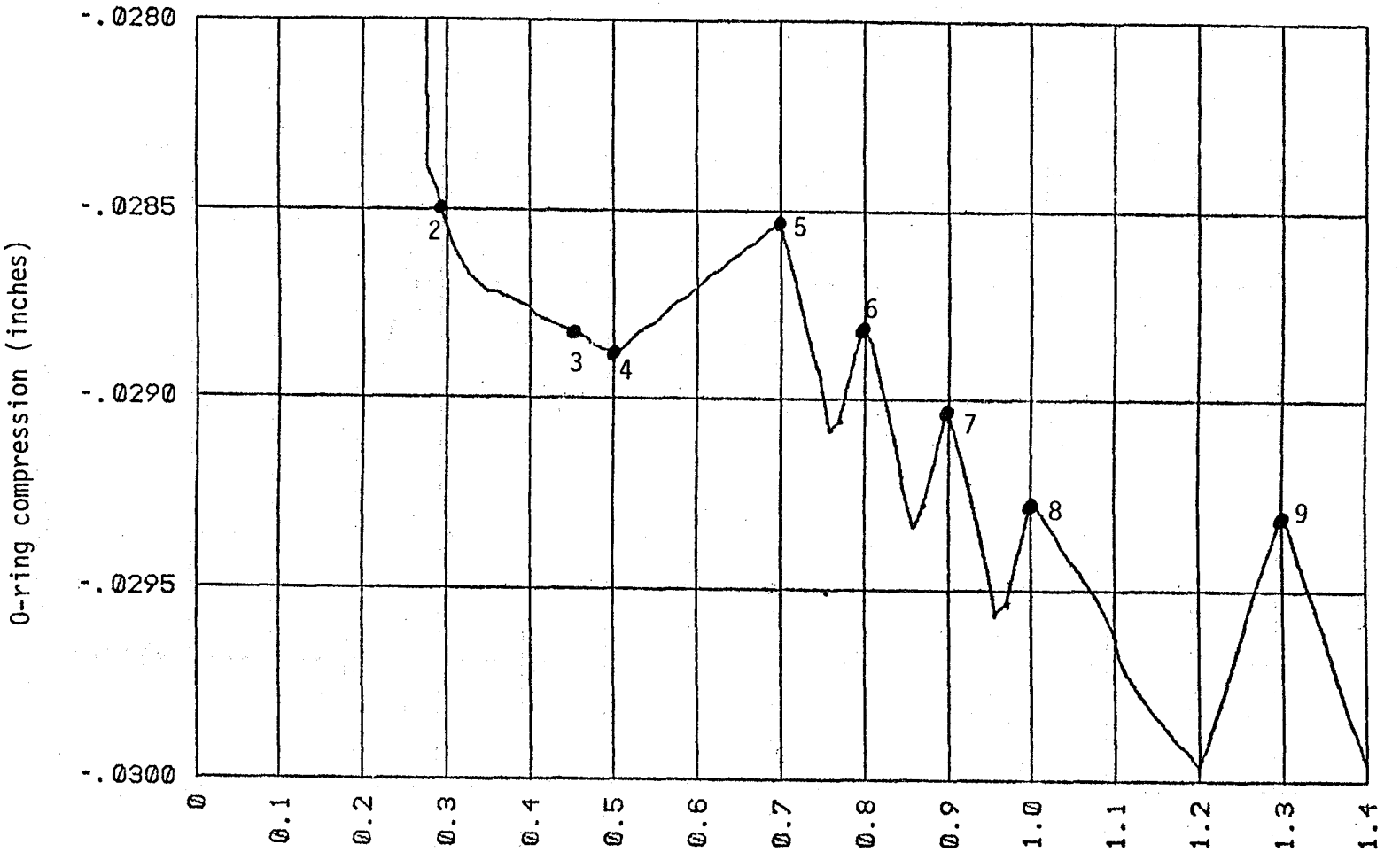

Figure 14. O-ring deflection history with expanded vertical scale

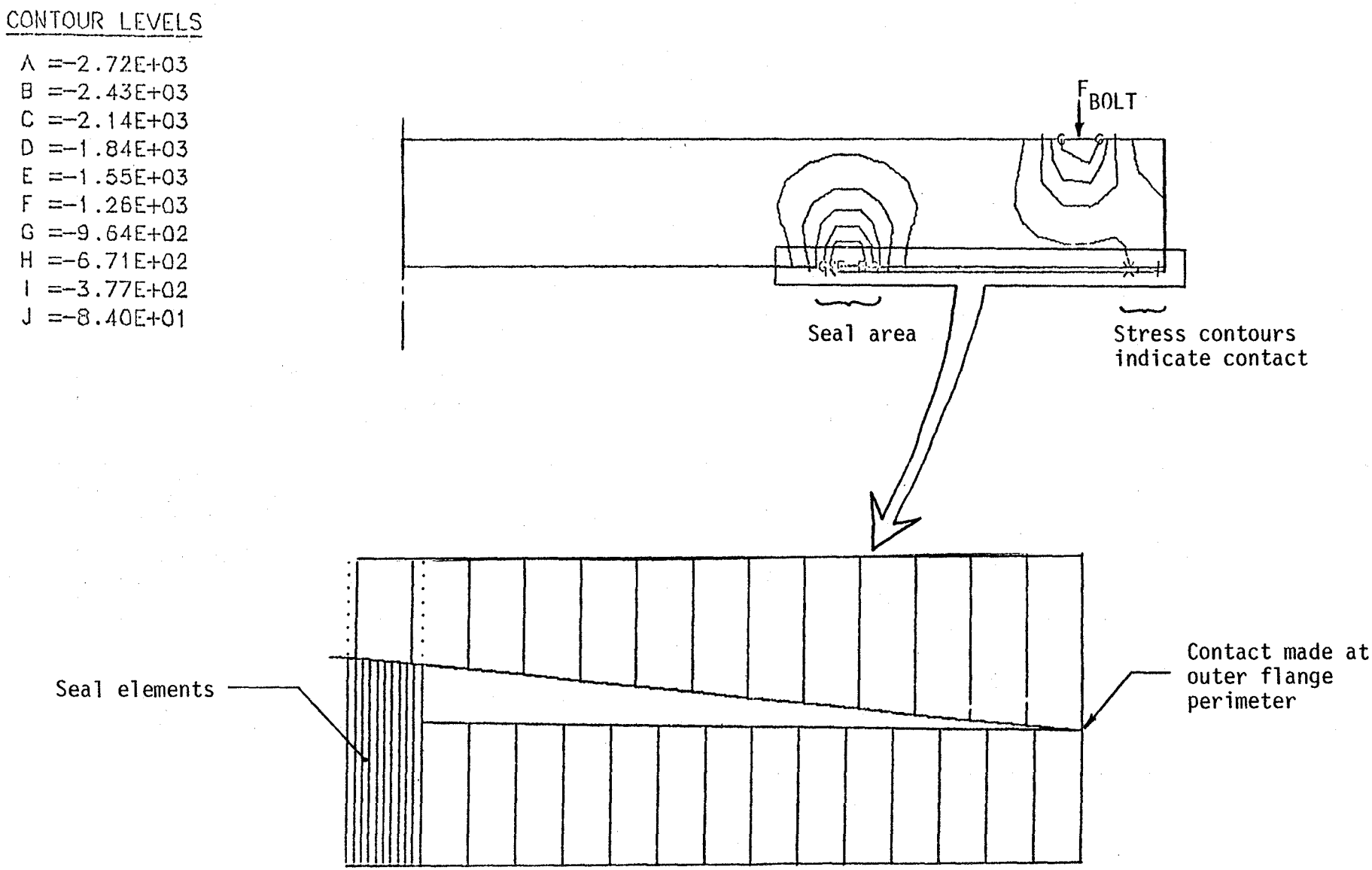

Figure 15. Deformed flange model shows contact at outer perimeter

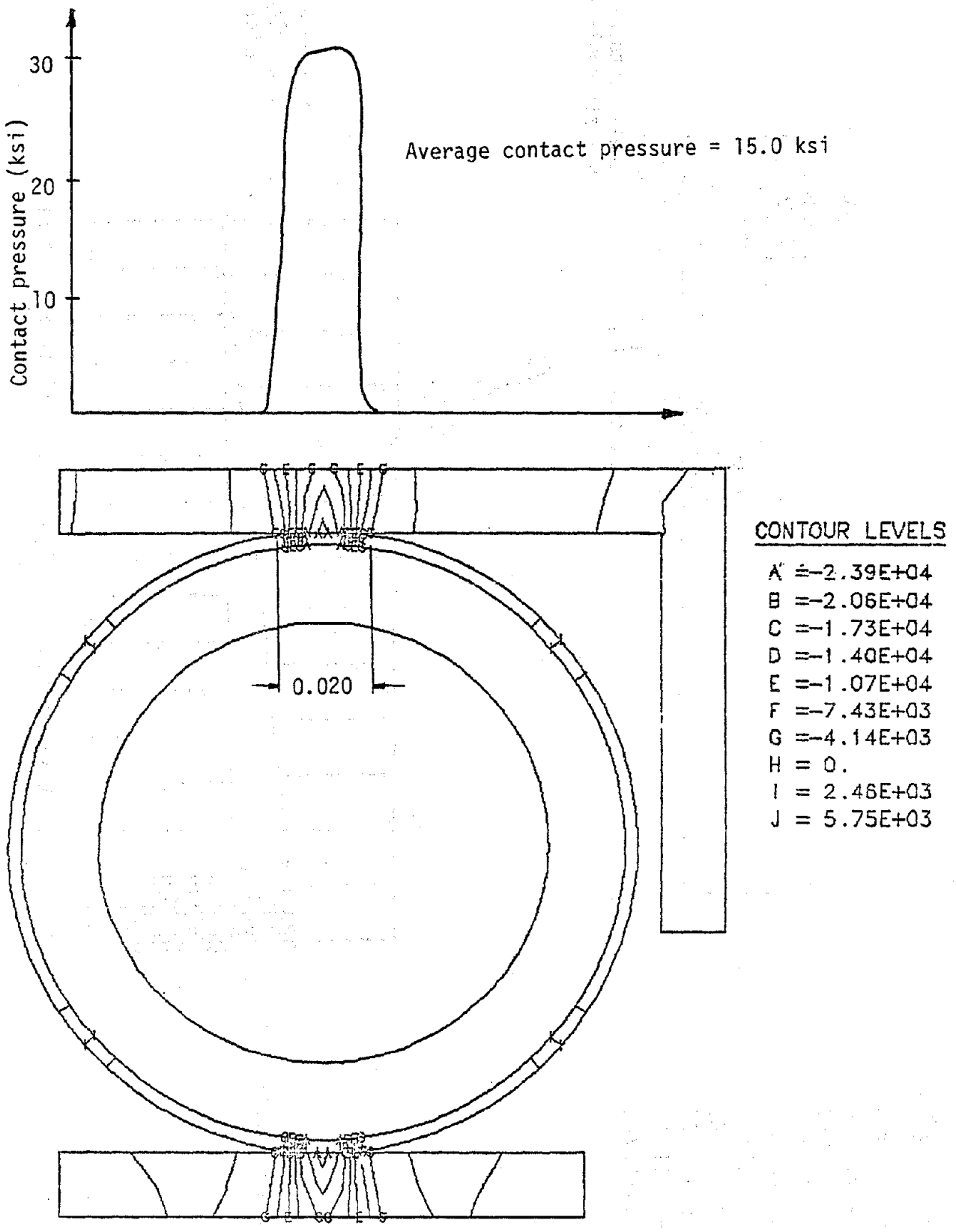

Figure 16. Contact area and pressure for test point 1

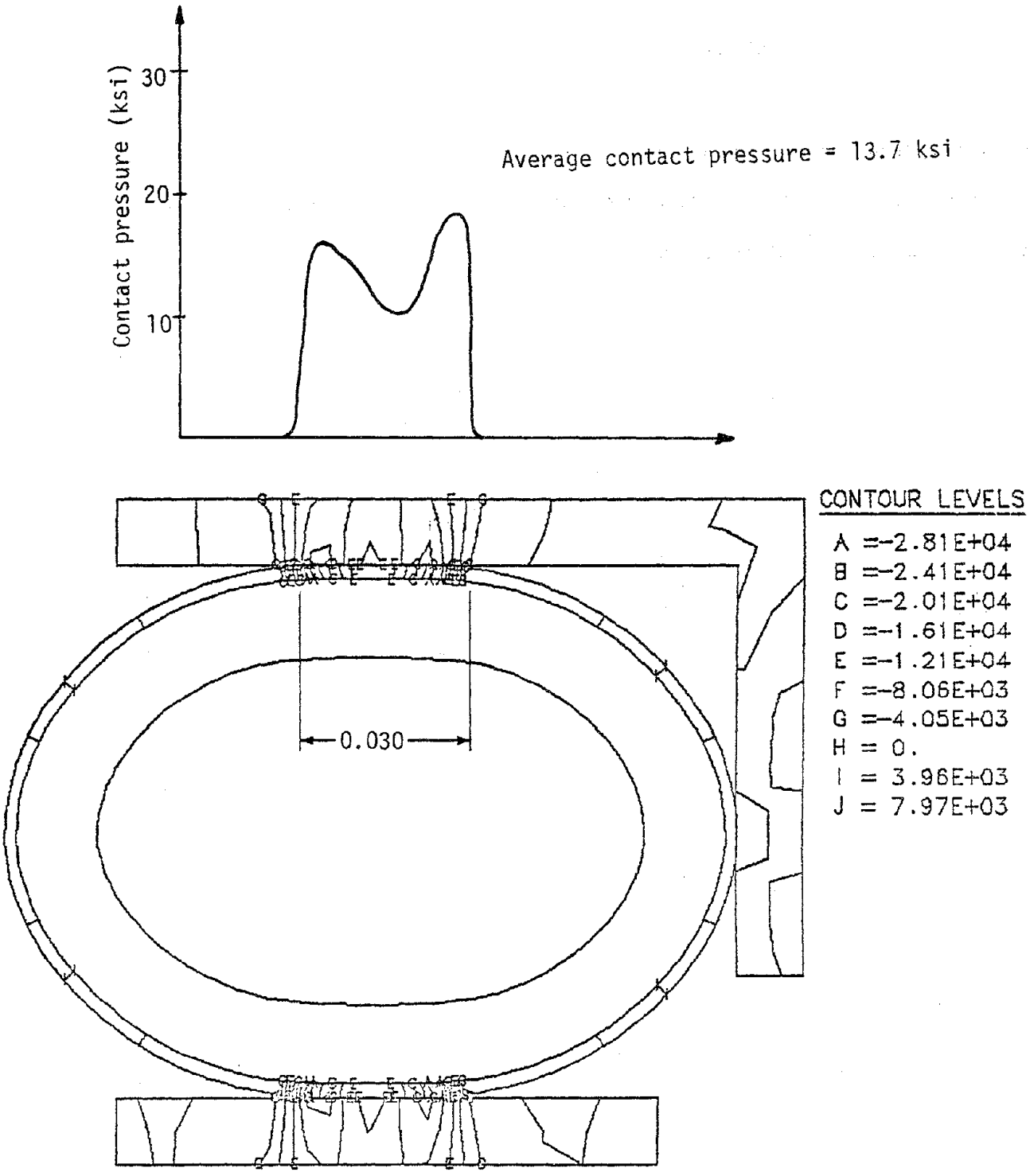

Figure 17. Contact area and pressure for test point 2

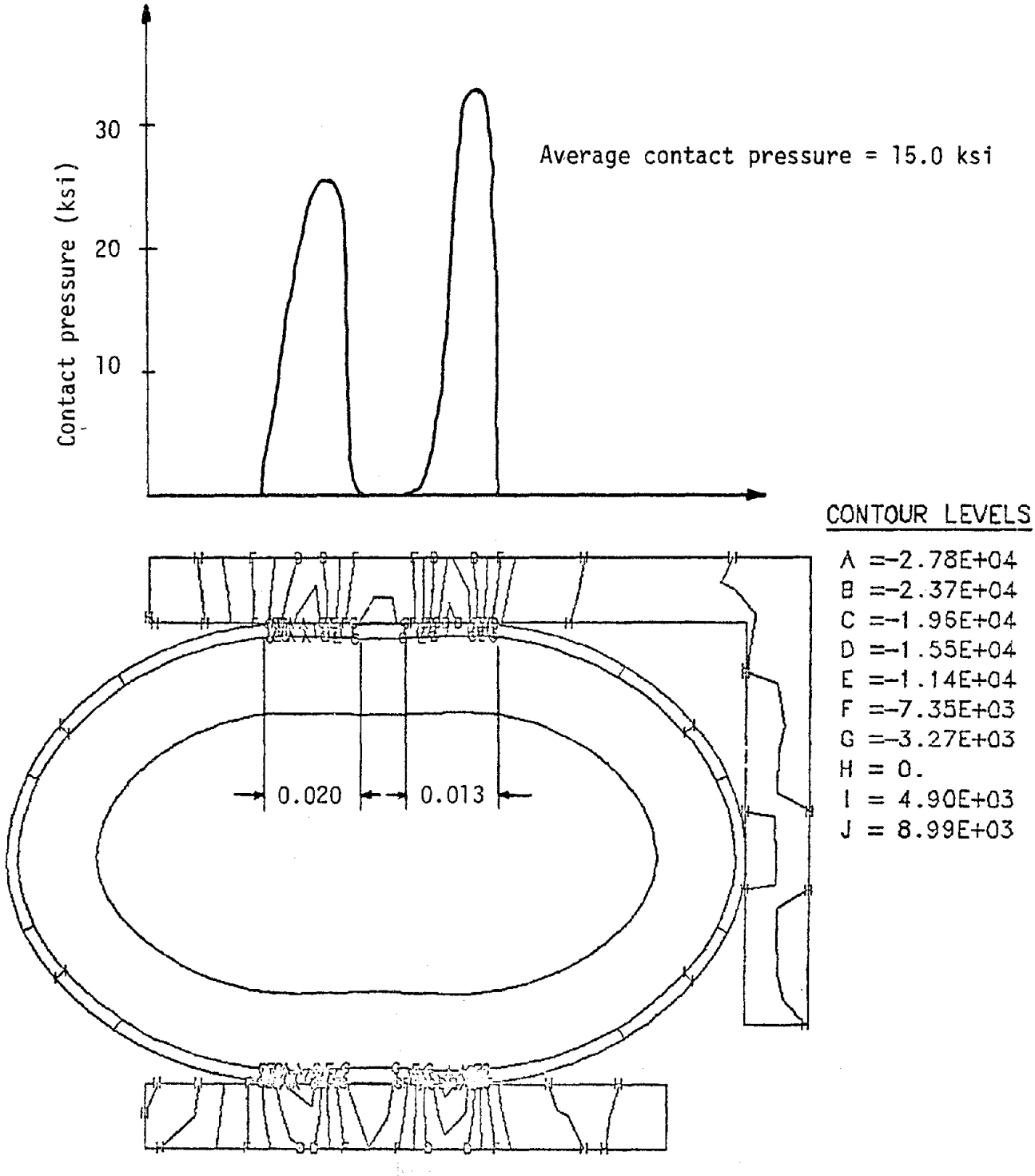

Figure 18. Contact area and pressure for test point 3

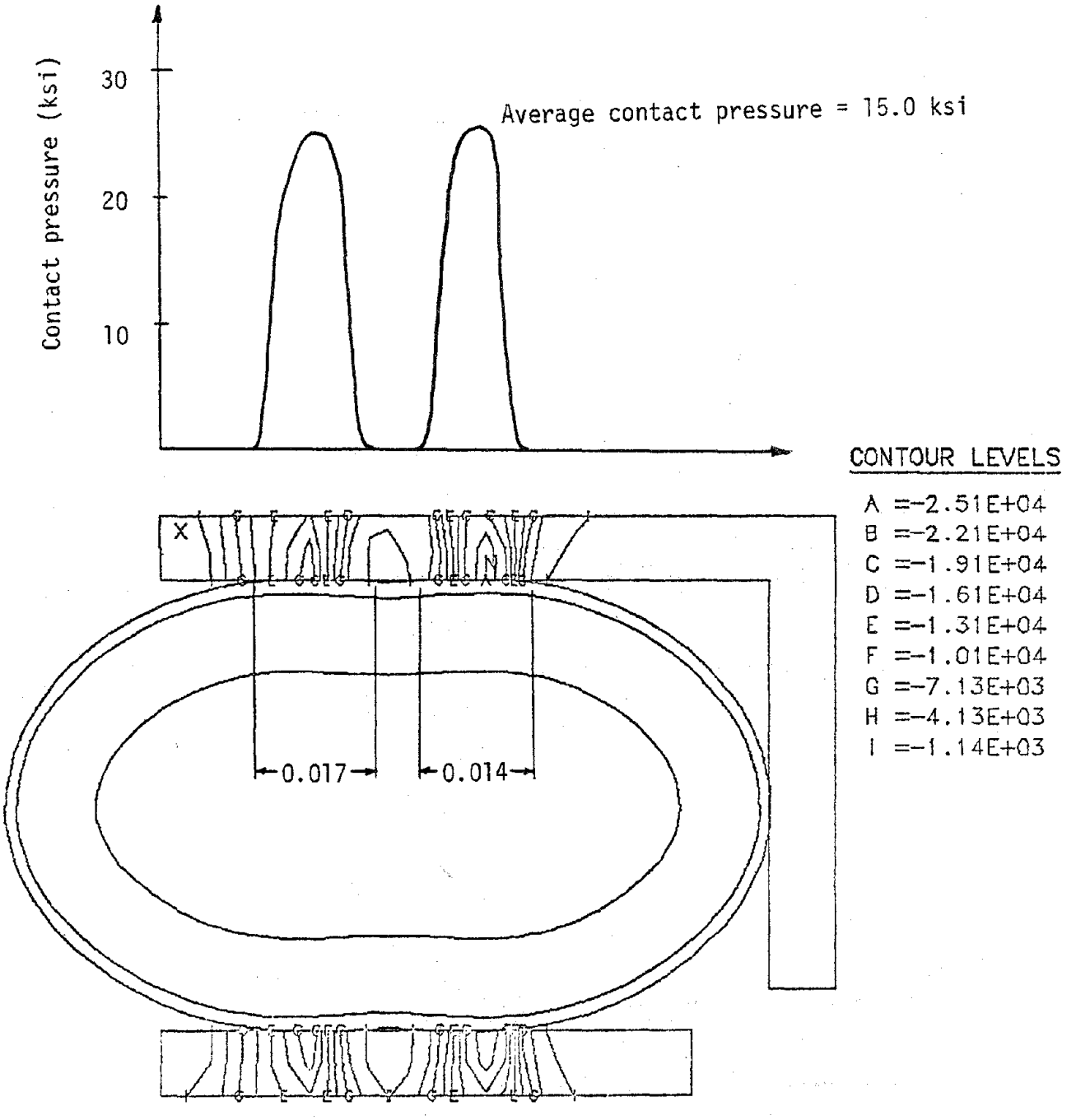

Figure 19. Contact area and pressure for test point 4

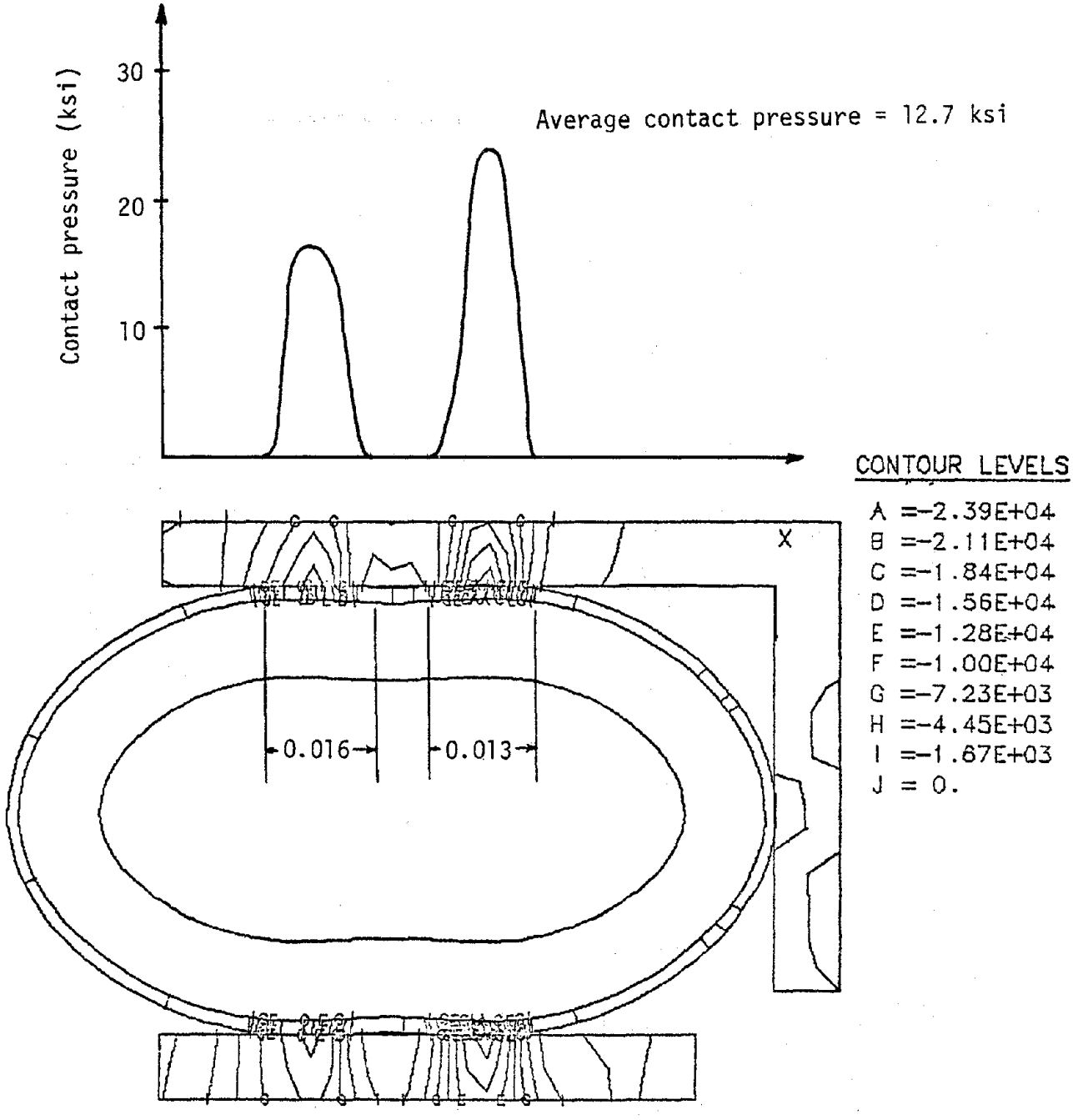

Figure 20. Contact pressure and area for test point 5

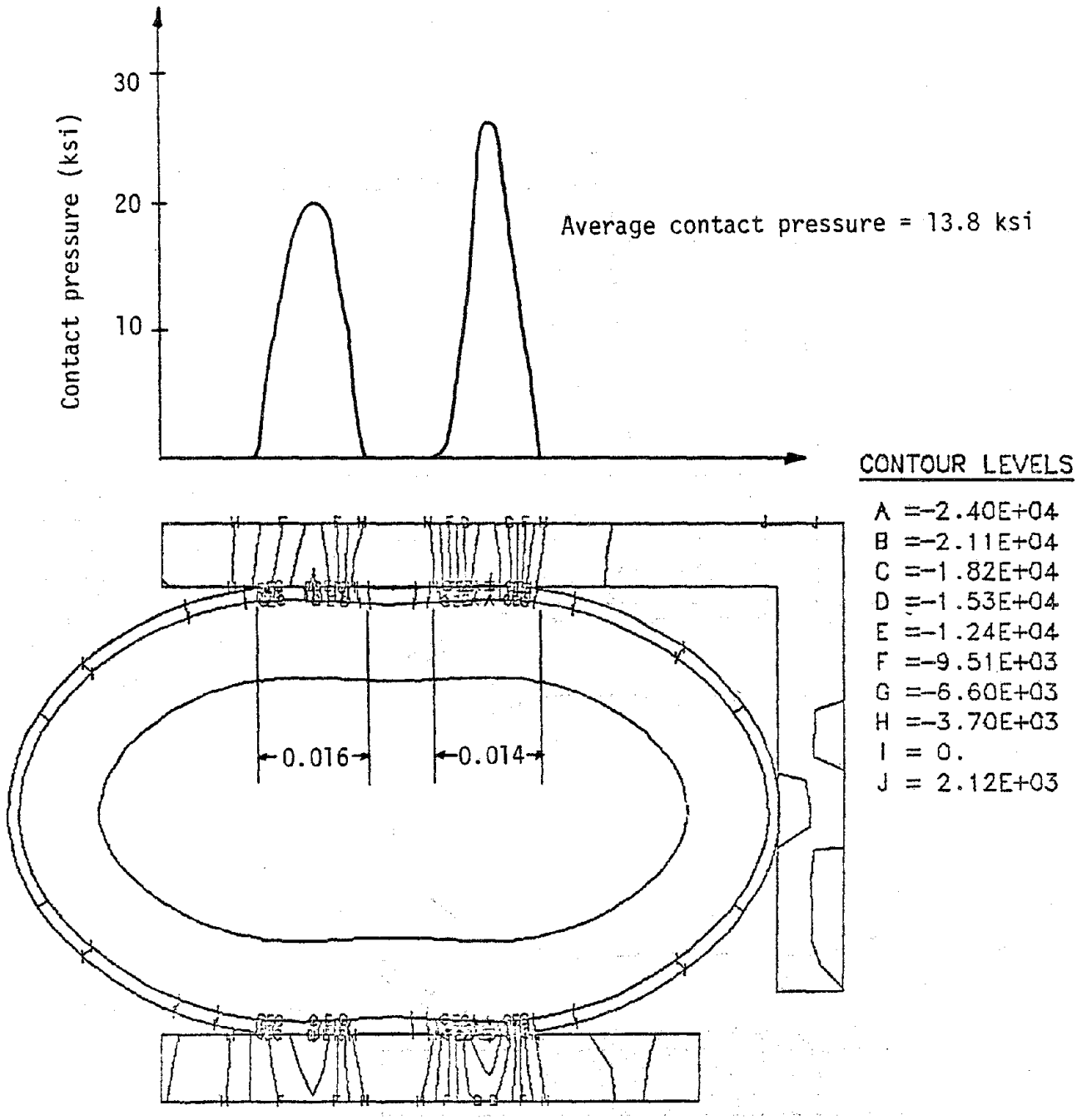

Figure 21. Contact area and pressure for test point 6

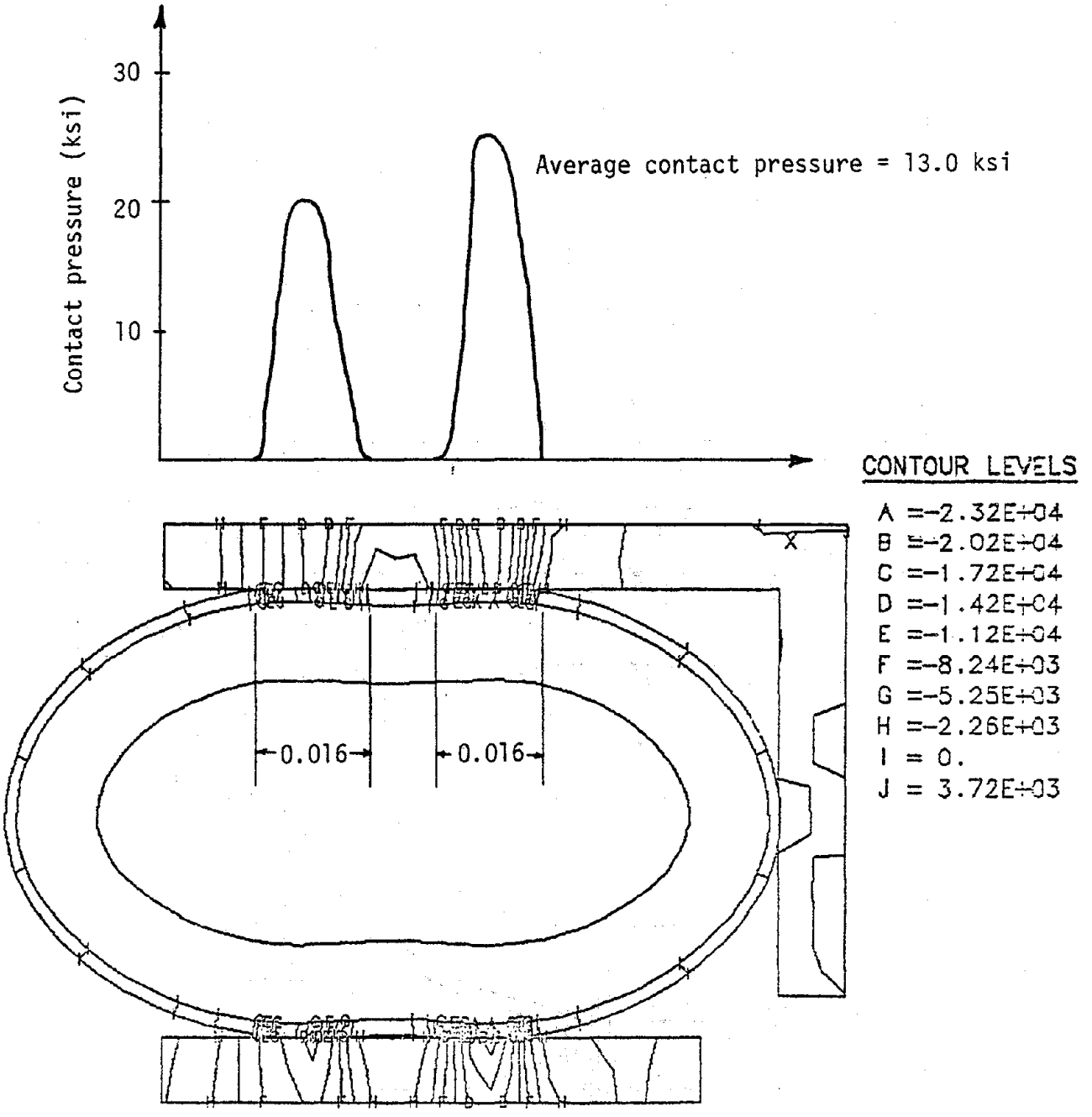

Figure 22. Contact area and pressure for test point 7

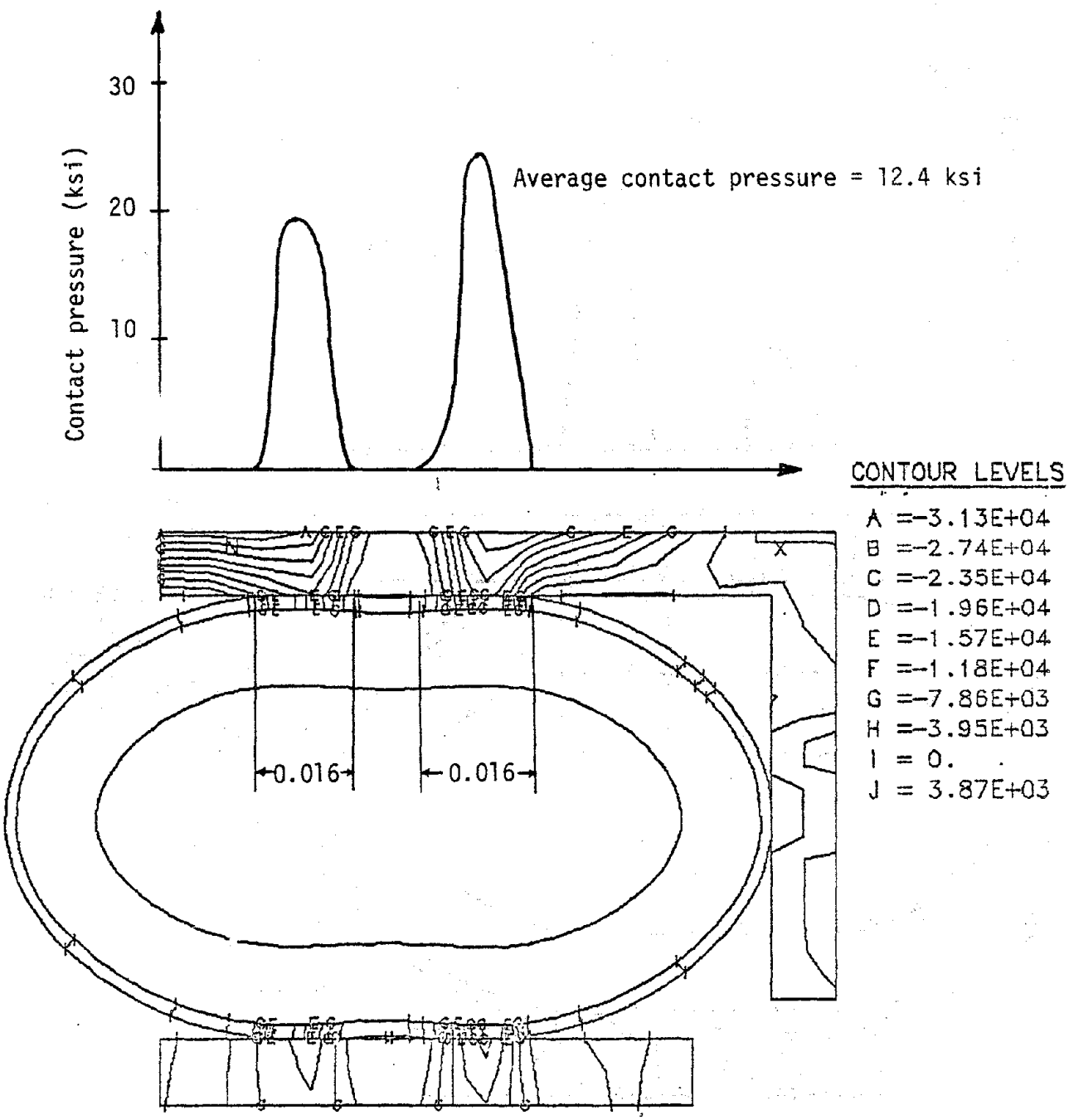

Figure 23. Contact area and pressure for test point 8

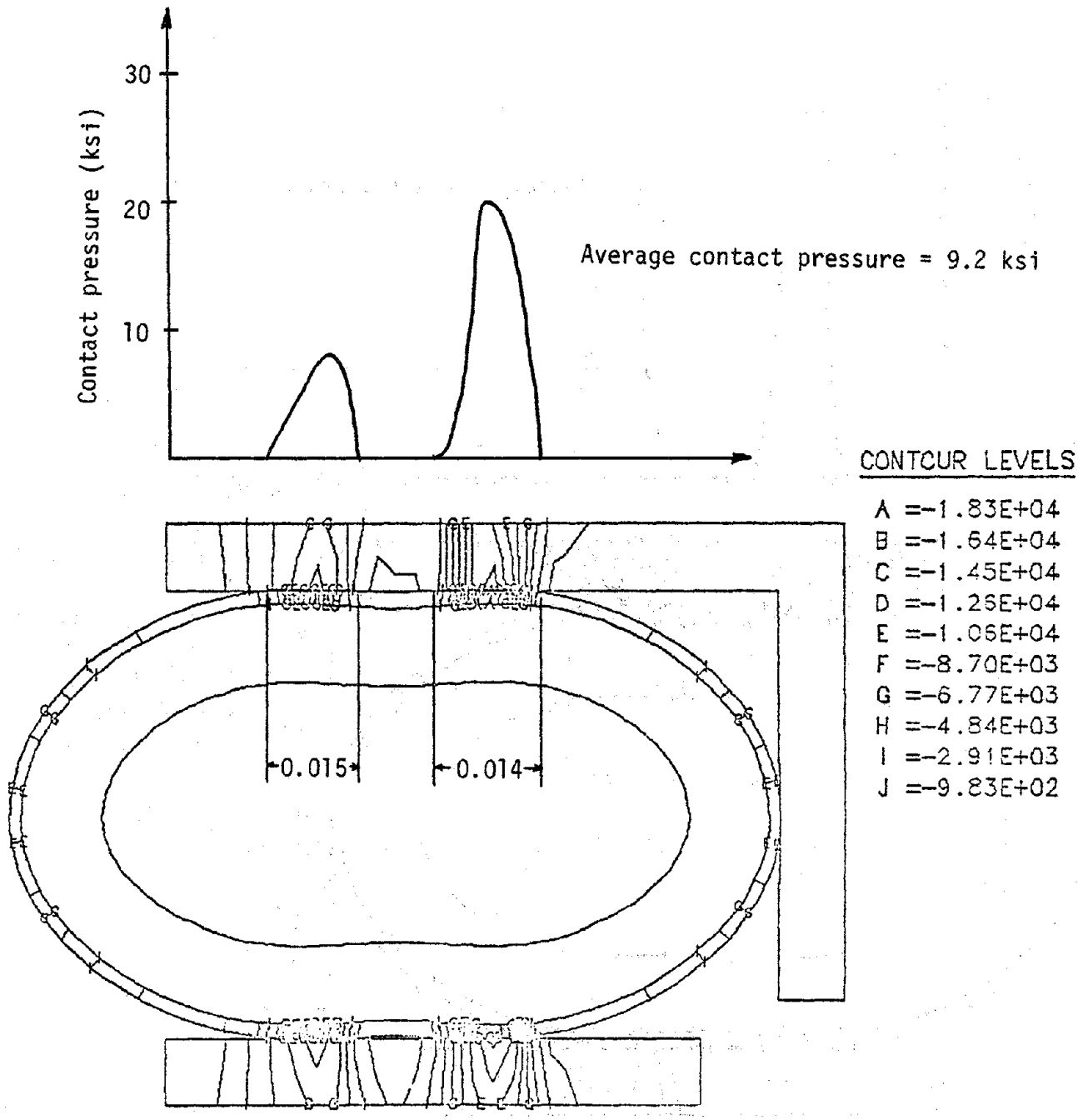

Figure 24. Contact area and pressure for test point 9

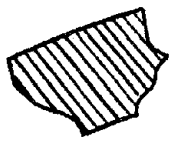

Elastic portion of O-ring

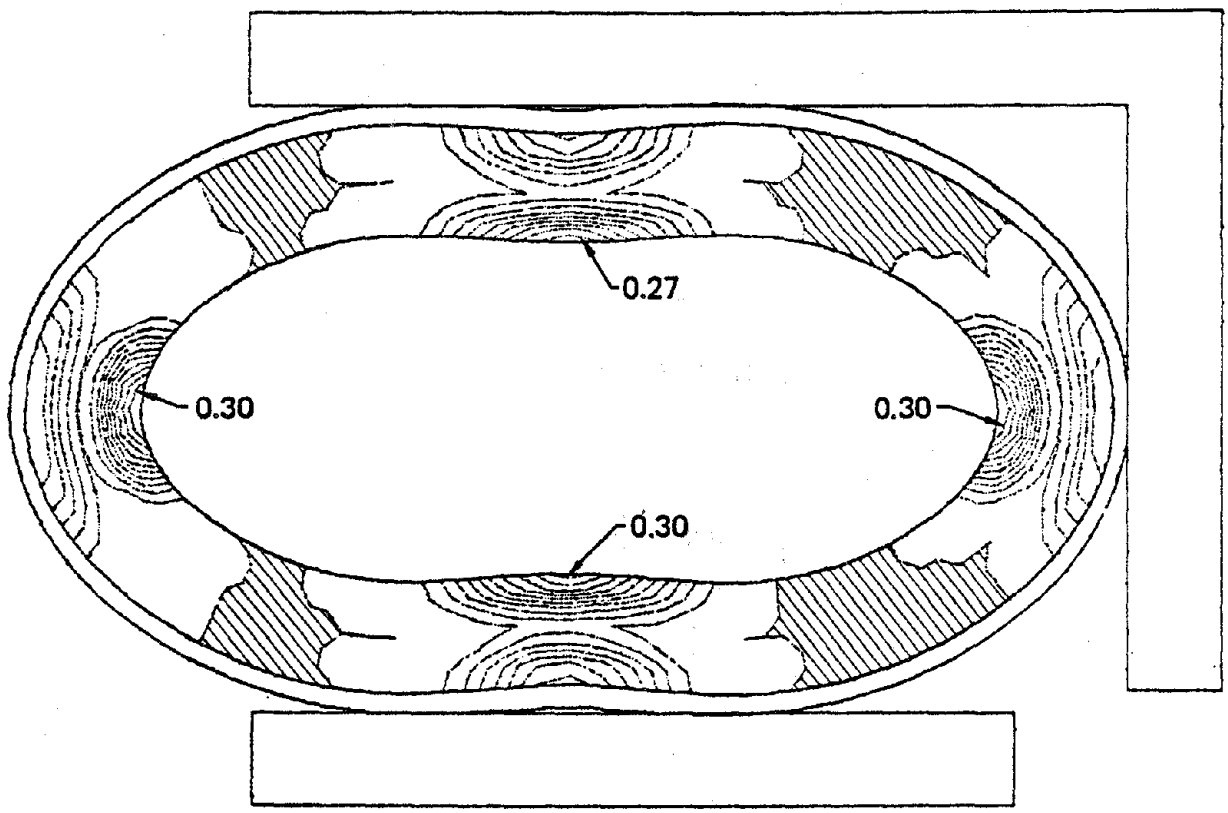

FIG. 25 Effective plastic strain in compressed O-ring

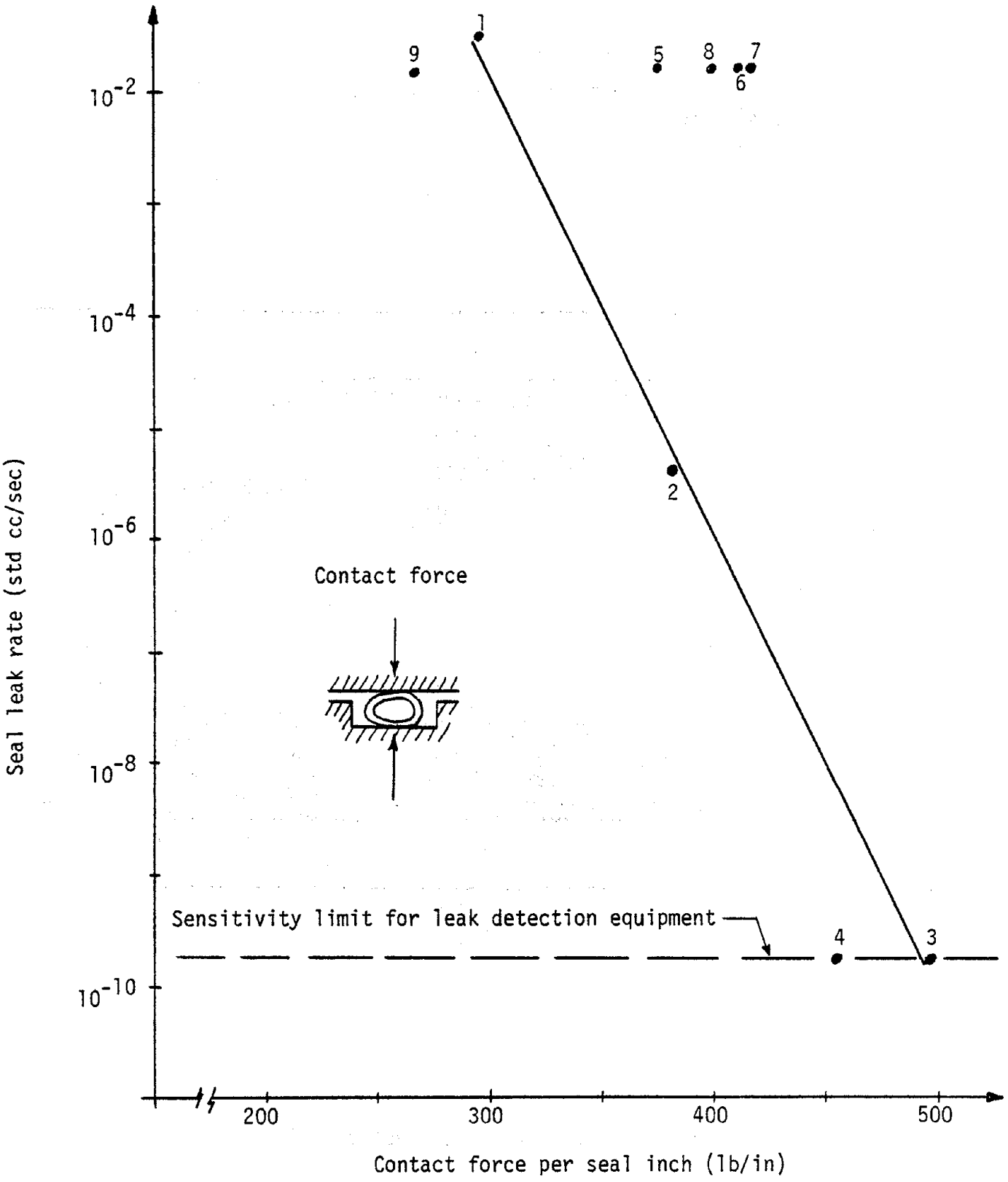

Figure 26. Seal leak rate versus contact force

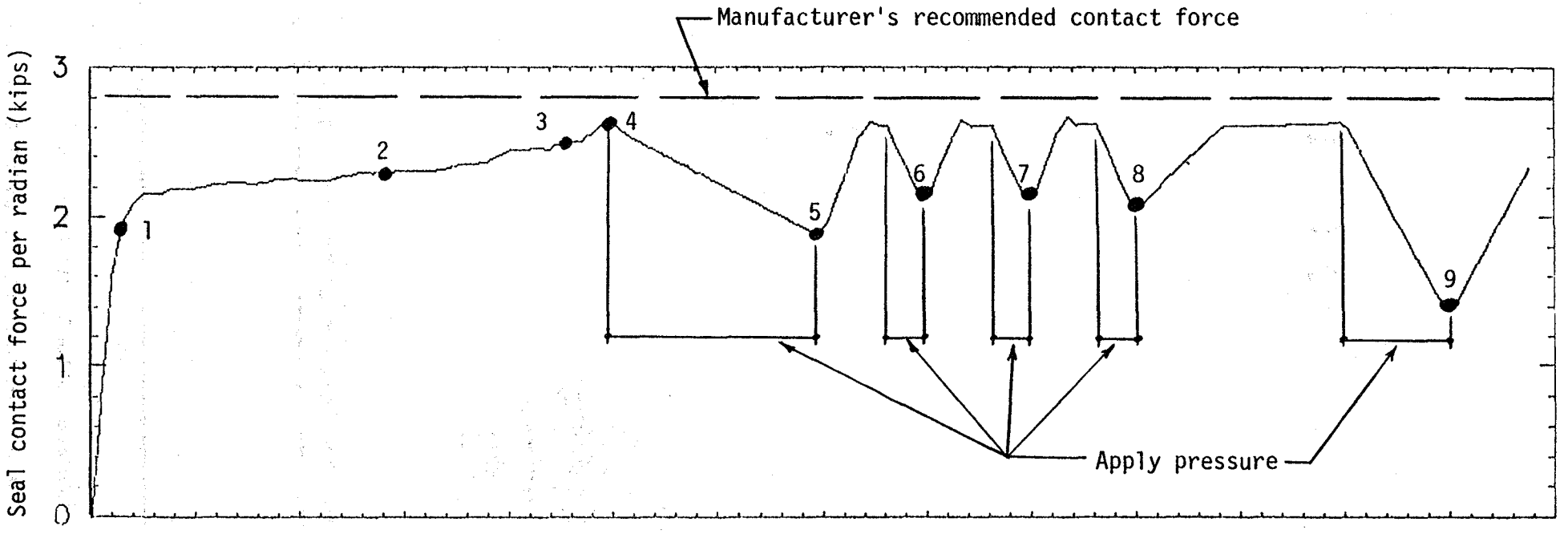

Figure 27. Contact force history illustrates effect of pressure

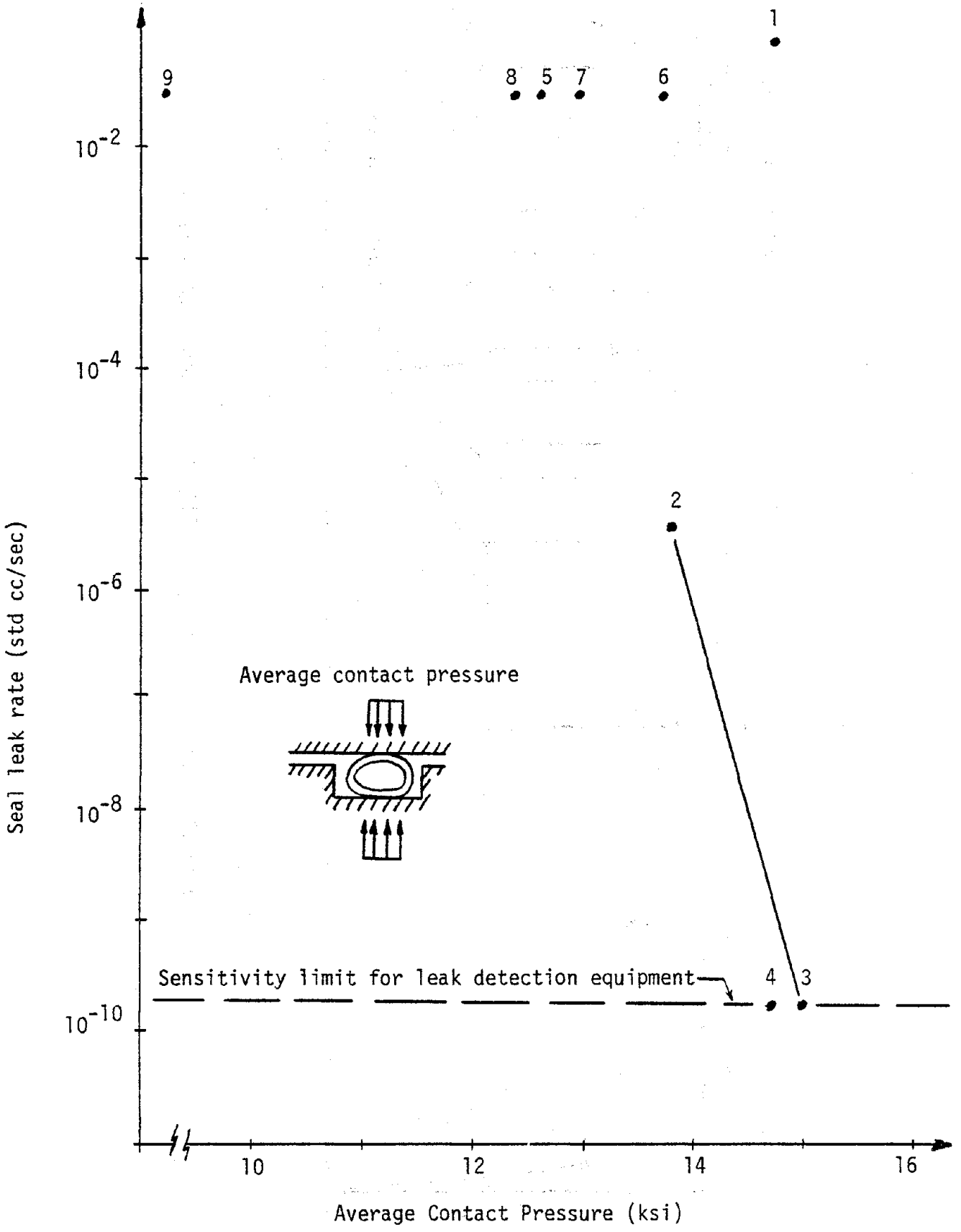

Figure 28. Seal leak rate versus average contact pressure

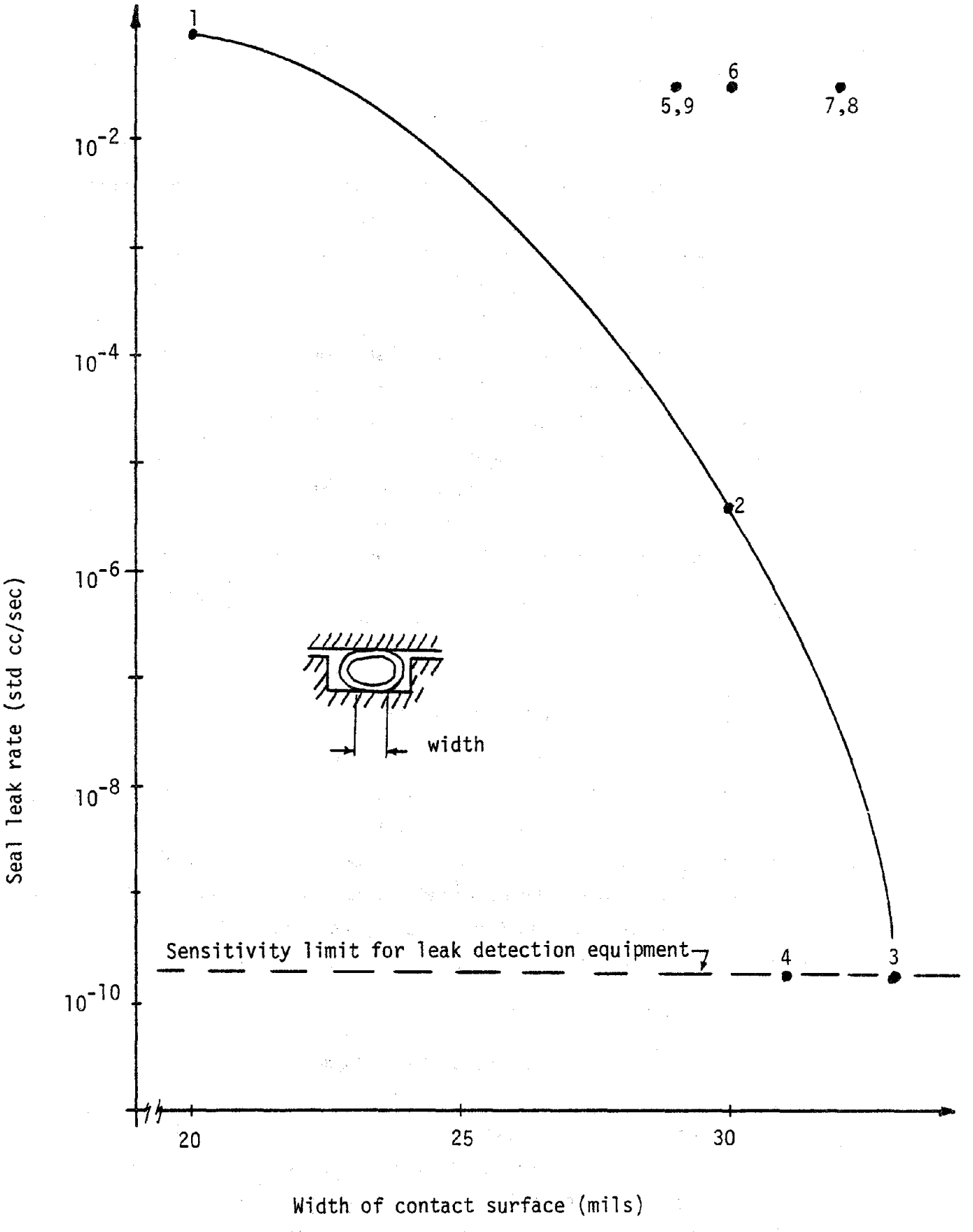

Figure 29. Seal leak rate versus contact surface width

APPENDIX D: BATZER FLANGE

INTRODUCTION

The Batzer flange was developed by Thomas Batzer at Lawrence Livermore Laboratory where its primary use has been in vacuum applications. The Batzer flange was included in this research program because of its past successful use over a broad temperature range and due to its unique manner of attaining a seal.

Figure D-1 illustrates a detailed cross-section of the flange contact region. At first appearance, the flange seems to employ a knife edge type of seal design--small, pointed contact surface in conjunction with a soft aluminum gasket. In actual use, however, applied bolt forces cause the contact surfaces to rotate. The edges undergo plastic deformation until a region of the contact point attains a state of hydrostatic compression. Increasing the applied bolt force then increases the stress in this region without additional plastic deformation. The high stress level obtained in this fashion assures a low leak rate through the seal.

SUMMARY

Once the design of the Batzer flange had been completed and fabrication had begun, a preliminary analysis was conducted to determine whether the analytical parameters could be obtained for this seal configuration. The substructuring approach that we employed with our finite element models of the flange was able to determine the magnitude of the contact stress and area for a general loading condition. No further analyses were performed as no experimental tests were conducted with this set of hardware.

ANALYSIS DESCRIPTION

As with the other seal configurations, the purpose of the finite element analysis of the Batzer flange was to determine the contact force and contact area corresponding to a given bolt load. The preliminary analysis was performed to also determine whether the substructuring approach that was used for the O-ring seals could be applied to the Batzer flange. First, a model of

the entire flange was generated (Fig. D-2). Bolt forces were applied at the appropriate locations of the model. Displacements and rotations of nodes near the contact region were determined and applied as boundary conditions to a detailed model of the contact area (Fig. D-3). From this second analysis, the contact force and area were determined.

CONCLUSION

Although all necessary hardware had been fabricated and subsequently delivered to LLL, no testing of the Batzer flange was conducted during this seal study. A preliminary analysis of the configuration was performed to establish the adequacy of the finite element models and our substructuring analytical approach. No additional work was completed.

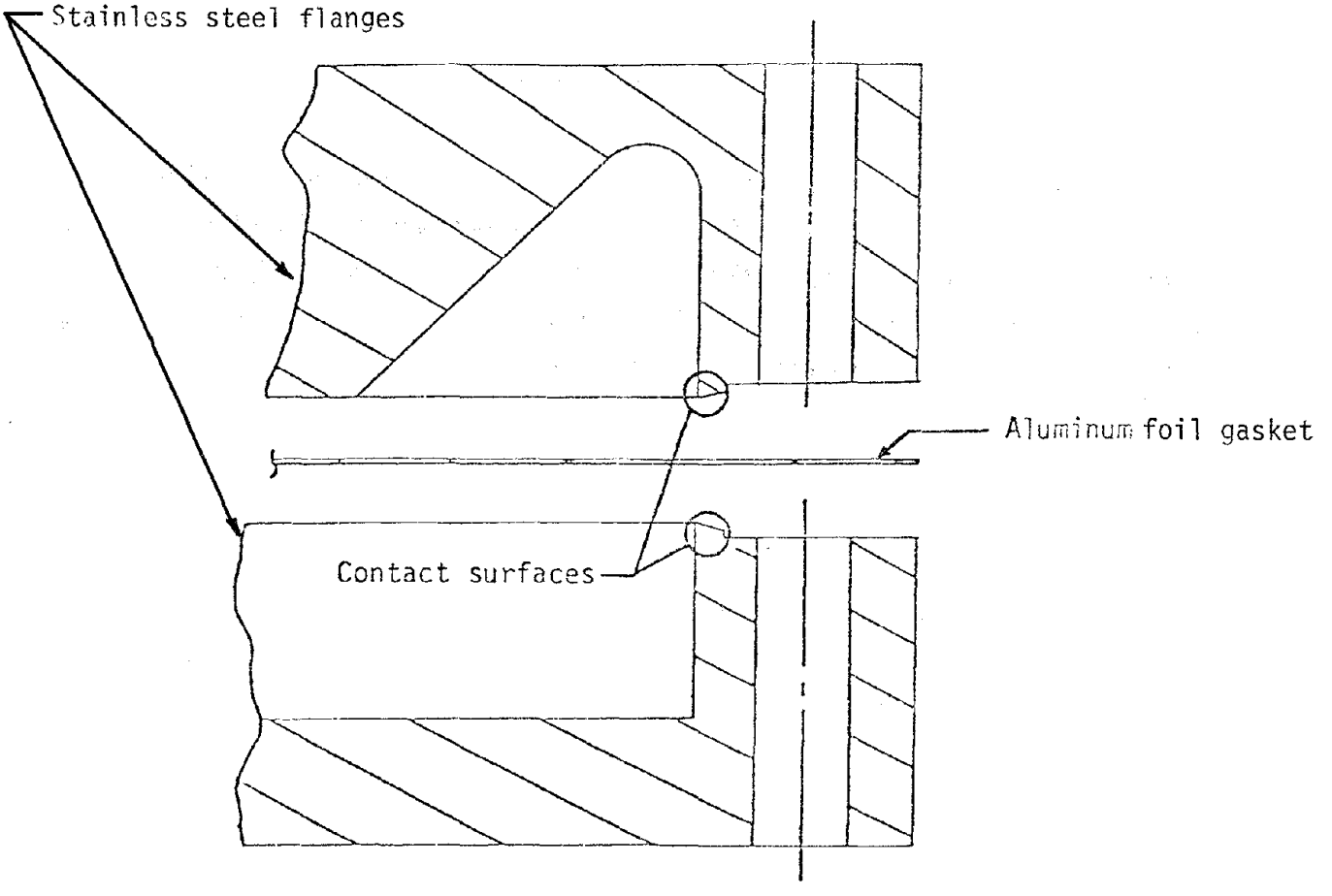

Figure D-1. Batzer flange showing contact area.

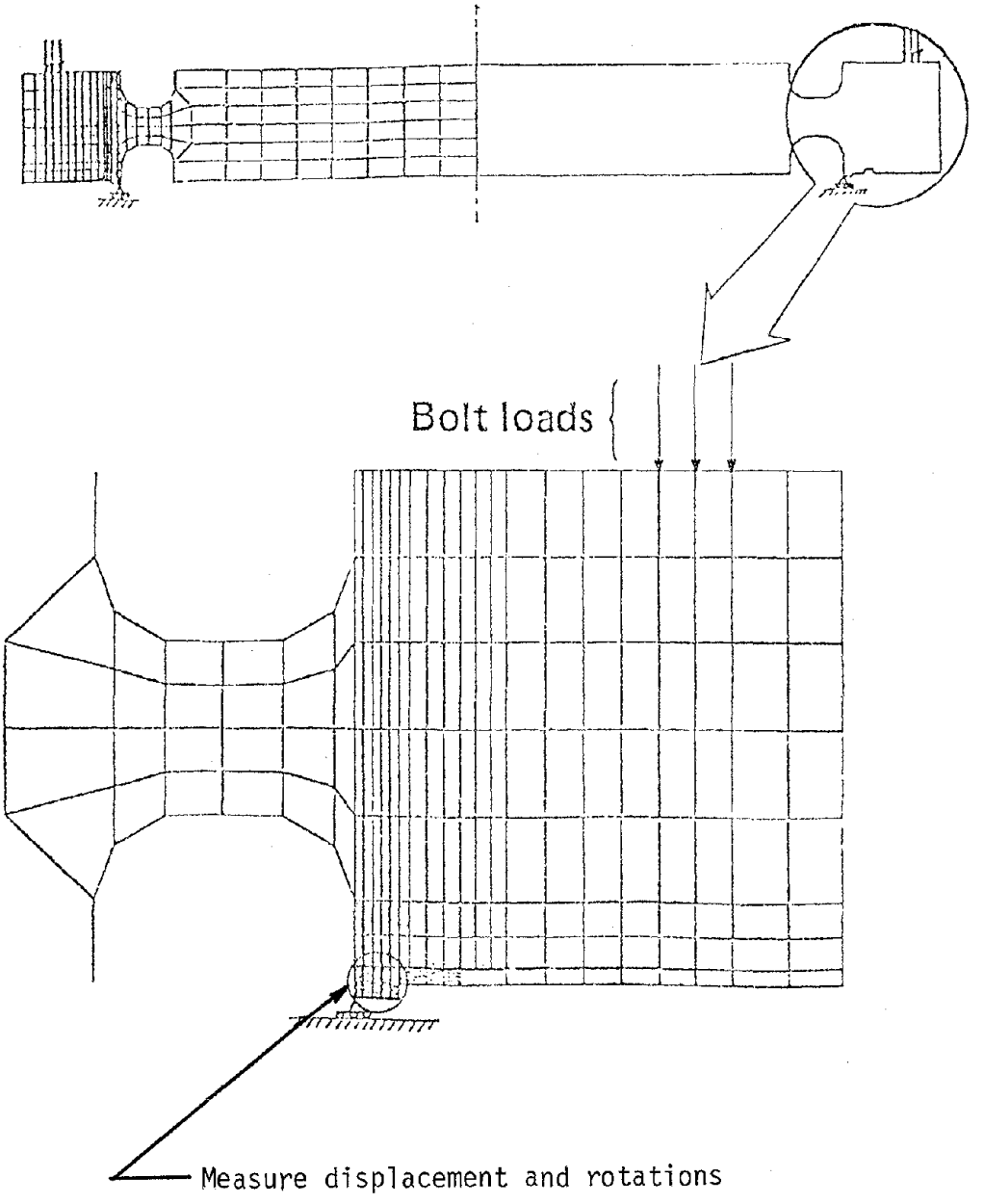

Figure D-2. Finite element model of Batzer flange with expanded view of contact area.

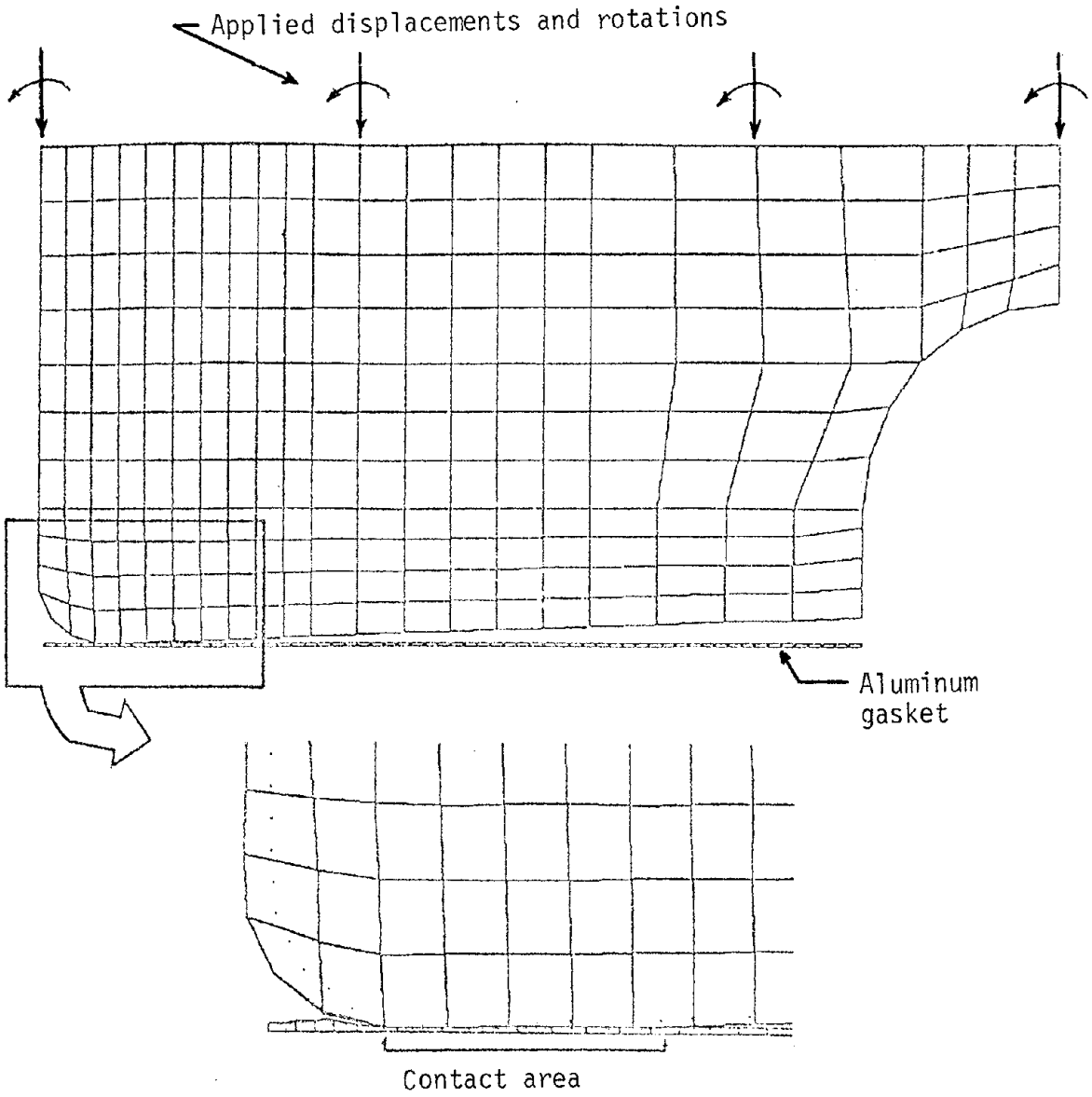

Figure D-3. Detailed model of contact surface.

APPENDIX E: TEST HARDWARE

In this appendix, all hardware associated with this seal research program and currently being stored at LLL are listed by seal configuration. In addition to a hardware list, the final drawings for several test flanges are shown. The Conoseal and Grayloc seal designs are proprietary, and their designs were not available. Finally, all miscellaneous hardware used during the tests (nuts, bolts, etc.) are listed.

POLYMER O-RINGS

All silicone O-rings were obtained from the Parker Seal Company. The numbers given with each seal below correspond to the company's numbers. The Viton O-rings were fabricated at LLL as required. Consequently, no extra Viton O-rings remain.

Quantity	Number	I.D.	Material
3	2-389	20.073	S604-70
9	2-391	22.085	S604-70
5	2-390	21.079	S604-70
5	2-378	10.538	S604-70
3	2-380	11.544	S604-70

1 pair of flanges for testing 10 inch nominal seal
Drawing number LE 108385 / AAA80-100367-OA

1 pair of flanges for testing 20 inch nominal seal
Drawing number LE 108385 / AAA80-100367-OA

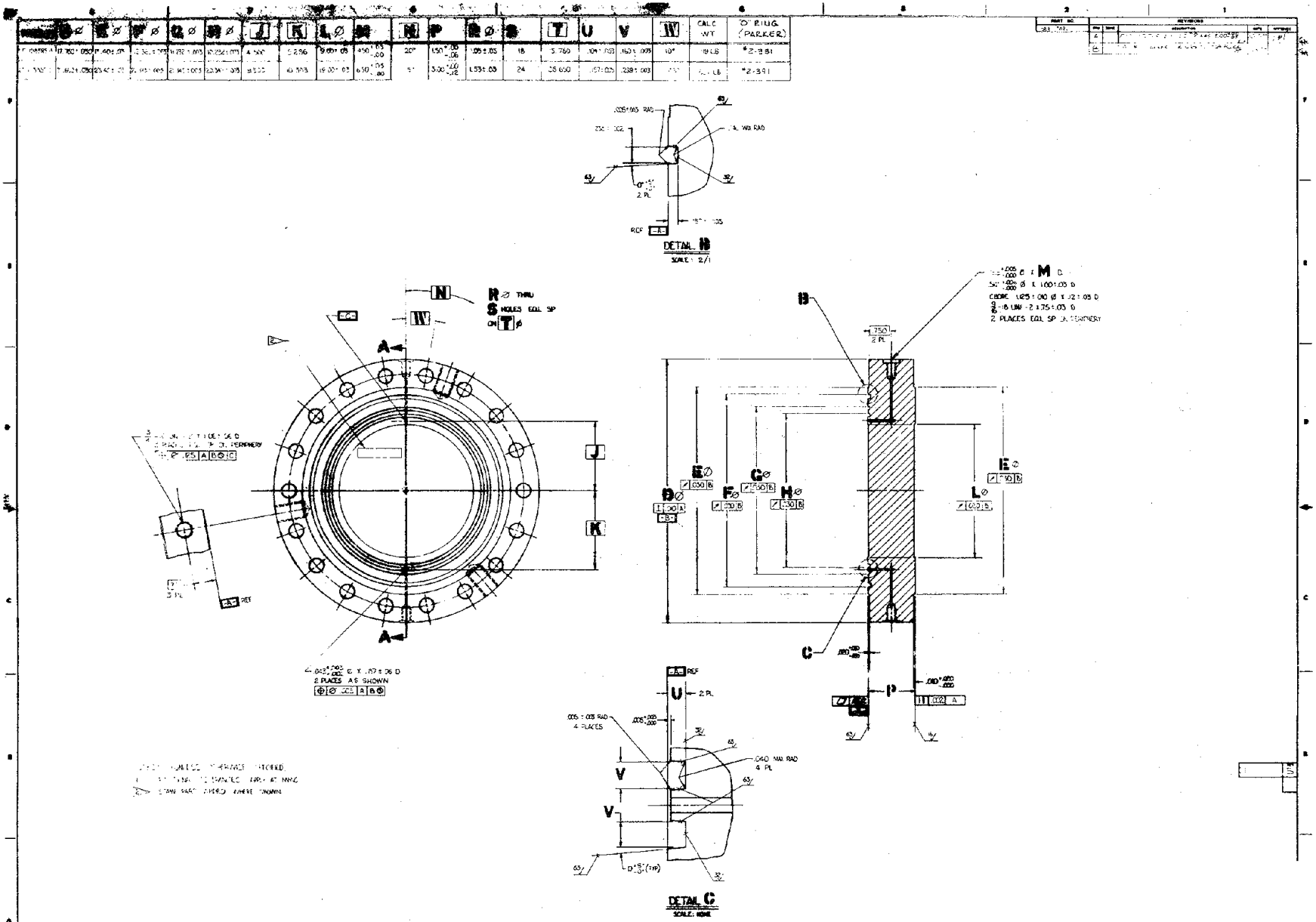

Polymer O-Rings

METALLIC O-RINGS

All metallic O-rings were purchased from UAP Components. Both the 321 stainless steel and the Inconel X-750 seals are listed.

Quantity	Number	O.D.	Material
3	U2420-20500 SEA	20.50	321 stainless steel
3	U2420-21000 SEA	21.00	321 stainless steel
1	U2312-10250 SEA	10.25	321 stainless steel
1	U2312-10750 SEB	10.75	321 stainless steel
1	U6312-10750 SEB	10.75	Inconel X-750
1	U6312-10250 SEB	10.25	Inconel X-750
3	U6420-20500 SEB	20.50	Inconel X-750
3	U6420-21000 SEB	21.00	Inconel X-750

1 pair of flanges for testing 10-in. nominal seal
Drawing number LE 108384 / AAA80-100366-OA

1 pair of flanges for testing 20-in. nominal seal
Drawing number LE 108384 / AAA80-100366-OA

PART NO	D ø	E ø	F ø	G ø	H ø	J	K	L ø	M	N	P	R ø	S	T	U	V	W	CALC WT	O RING (PARKER)
LE 430394-1	17.78 ±.03	13.00 ±.03	11.8654 .050	10.762 +.000 -.004	10.262 +.000 -.004	4.750	5.171	8.50 ±.05	.065 +.004 -.009	.159 +.005 -.000	.650 +.00 -.05	1.05 ±.05	16	15.760	10°	20°	4.25 +.05 -.00	98 LB	*2-580
LE 108364-2	21.65 ±.03	23.501 .03	22.343 .050	21.015 +.000 -.005	20.515 +.000 -.005	9.500	10.297	18.00 ±.03	.080 +.005 -.030	.170 +.002 -.000	5.00 +.00 -.12	1.53±.03	24	28.650	7.5°	15°	6.50 +.05 -.00	657 LB	*2-341

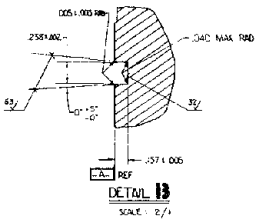

DETAIL B
SCALE : 2/1

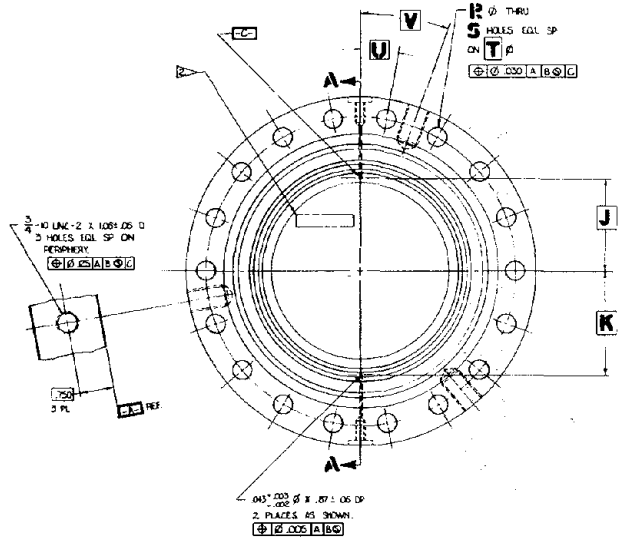

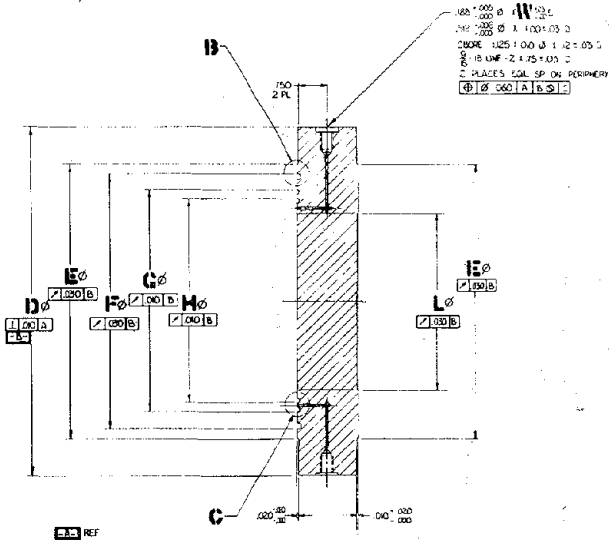

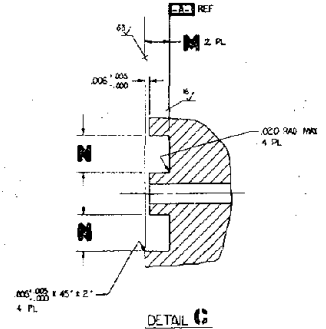

DETAIL C
SCALE : NONE

NOTES: (UNLESS OTHERWISE SPECIFIED)
1. POSITIONAL TOLERANCES APPLY AT MMC.
2. STAMP PART NO. APPROX WHERE SHOWN.

Metallic O-Rings

120

BATZER FLANGES

The contact surfaces that comprise the Batzer flange are machined into the test fixture; therefore, the fixtures are the seals themselves. Metallic O-rings are used in conjunction with the flanges. For these series of leak rate tests, shims were employed to prevent overstressing the contact area.

1 pair of test flanges -- 10-in. Batzer seal
Drawing number LE 108733 / AAA80-100368-00

1 pair of test flanges -- 20-in. Batzer seal
Drawing number LE 108742 / AAA80-100369=00

1 shim for 10-in. test flange
Drawing number LC 108746-1

1 shim for 20-in. test flange
Drawing number LC 108747-2

Quantity	Number	O.D.	Material
3	U2620-11500 SEA	11.50	321 stainless steel
3	U2620-21250 SEA	21.25	321 stainless steel

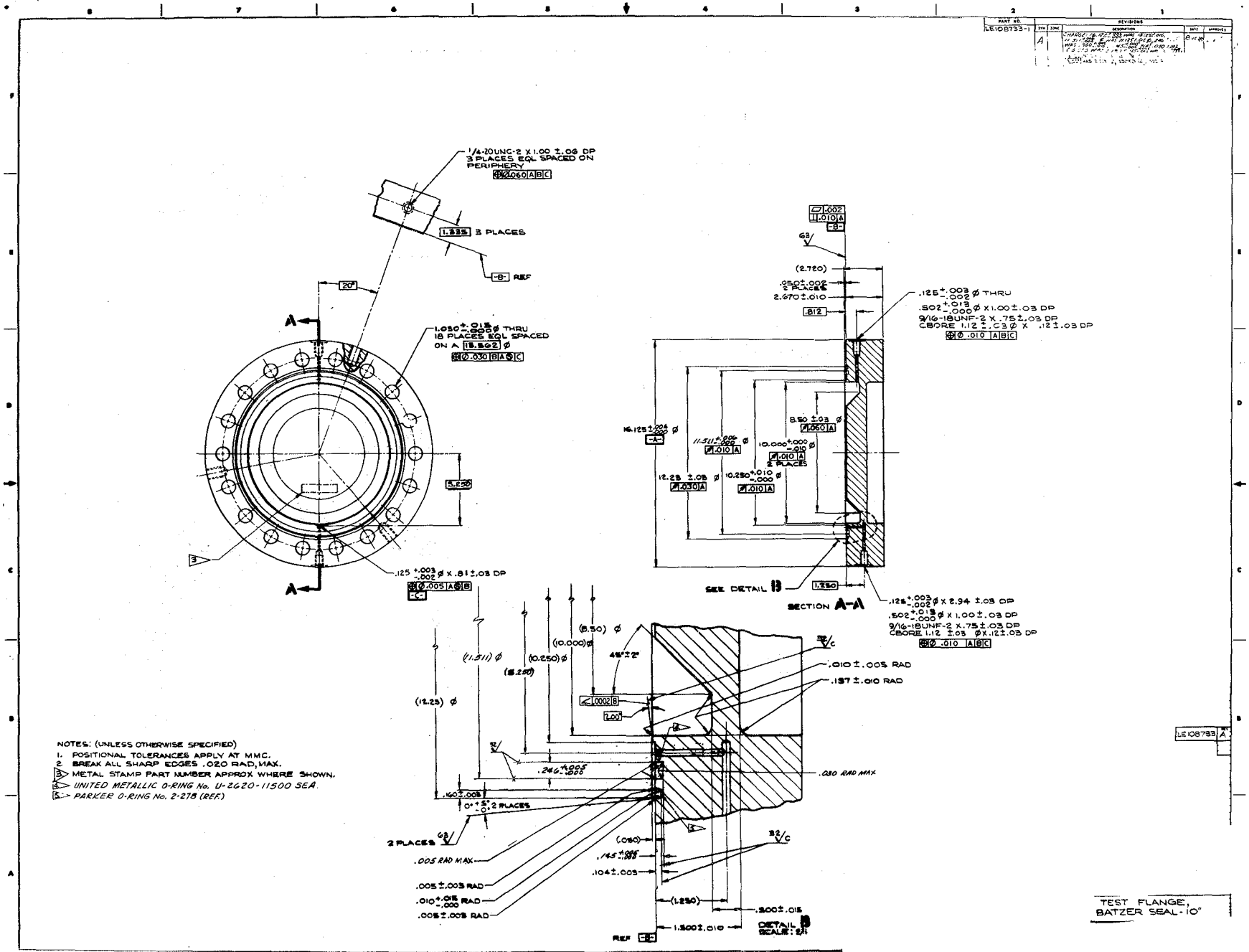

NOTES: (UNLESS OTHERWISE SPECIFIED)
1. POSITIONAL TOLERANCES APPLY AT MMC.
2. BREAK ALL SHARP EDGES .020 RAD. MAX.
3. METAL STAMP PART NUMBER APPROX WHERE SHOWN.
4. UNITED METALLIC O-RING No. U-2620-11500 SEA.
5. PARKER O-RING No. 2-278 (REF.)

LE108733 A

TEST FLANGE, BATZER SEAL-10"

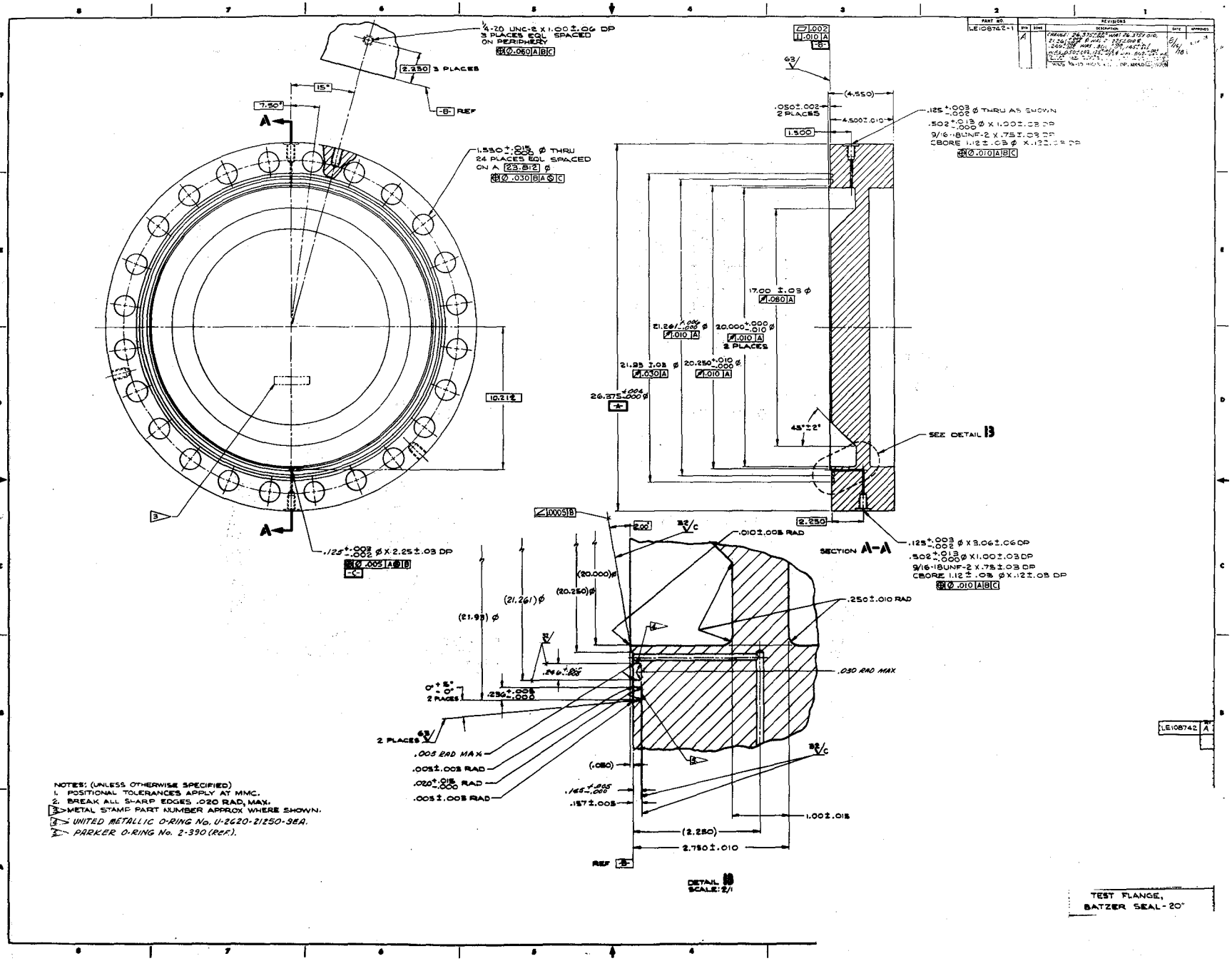

NOTES: (UNLESS OTHERWISE SPECIFIED)
1. POSITIONAL TOLERANCES APPLY AT MMC.
2. BREAK ALL SHARP EDGES .020 RAD. MAX.
3. METAL STAMP PART NUMBER APPROX WHERE SHOWN.
4. UNITED METALLIC O-RING No. U-2620-21250-SEA.
5. PARKER O-RING No. 2-390 (REF.).

CONOSEAL

The Conoseal is a proprietary seal manufactured by the Aeroquip Corporation. Drawings used to fabricate the test flanges are not intended for public release.

Quantity	Number	Nominal diameter	Material
3	50887-1000S	10 in.	321 stainless steel
3	57505-2000S	20 in.	321 stainless steel

1 male flange for 10-in. nominal gasket
Drawing number LE108787 / AAA80-100371-00

1 female flange for 10-in. nominal gasket
Drawing number LE 108771 / AA80-100370-00

1 male flange for 20-in. nominal gasket
Drawing number LE 108787 / AAA80-100271-00

1 female flange for 20-in. nominal gasket
Drawing number LE 108771 / AA80-100370-00

1 polymer O-ring 22.5-in. O.D.

GRAYLOC GASKET

The Grayloc gasket is a proprietary seal developed by the Gray Tool Company. As with the Conoseal, no drawings of the test flanges are available.

Description	Quantity
Grayloc seal test fixture flange, 16 3/8" OD x 3 1/8" thk., SA182-F316, w/three 33/64" test taps and one pressurizing tap, recessed ring seat	1
Grayloc seal test fixture flange, 16 3/8" OD x 3 1/8" thk., SA182-F316, w/three 33/64" test taps and one pressurizing tap, recessed ring seat	1
Grayloc seal ring, size 94, C.S., Cad. plt.	3
Flexitallic spinal wound gasket, 10 3/4" ID x 11 1/2" OD x 0.125" thk., with blue dye Canadian asbestos filler	2
Grayloc seal test fixture flange, 27 1/4" OD x 4 3/8" thk., SA182-F316, w/three 33/64" test taps and one pressurizing tap, recessed ring seat	1
Grayloc seal test fixture flange, 27 1/4" OD x 4 3/8" thk., SA182-F316, w/three 33/64" test taps and one pressurizing tap, recessed ring seat	1
Grayloc seal ring, size 192, C.S., Cad. plt.	3

Description	Quantity
Flexitallic spiral wound gasket, 20 3/4" ID x 21 1/2" OD x 0.125 thk., with blue dye Canadian asbestos filler	2

Miscellaneous Hardware

Item	Description	Quantity
Bolts	UNF 1-12 316 stainless steel	20
Bolts	UNF 1 1/2-12 stainless steel	26
Nuts	For above bolts, 316 stainless steel	46
Adapter	High pressure fitting that connects flanges to pressure source	2